INTERLEUKIN-15 BASED MAINTENANCE OF METABOLIC HOMEOSTASIS AND TREATMENT OF LUNG CANCER

by

HAO SUN

(Under the Direction of Dexi Liu)

ABSTRACT

IL-15 is a multifunctional cytokine and plays a key role in activating various types of cells including NK and $CD8^+$ T cells. It also serves as an endocrine involved in the regulation of metabolic homeostasis. The goals of this dissertation study are to demonstrate IL-15 activity in blocking and reversing high-fat diet-induced obesity and obesity-associated metabolic diseases, and to explore its therapeutic potential for treatment of lung cancer metastasized in the liver and kidneys. Gene transfer approach using hydrodynamic-based procedure was employed to achieve over-expression of IL-15 in the form of either IL-15, or IL-15/sIL-15Rα complexes in high-fat diet-fed mice or mice carrying Lewis lung carcinoma. The results show that the method of hydrodynamic gene transfer is effective in delivering *Il-15* gene to mouse liver, generating high levels of IL-15 in the blood. An elevated protein level of IL-15 is able to block high-fat diet-induced obesity, insulin resistance, and development of fatty liver. Similarly, transfer of the *Il-15/sIl-15Rα* gene in obese mice results in reduction of body weight and improvement of insulin sensitivity and glucose homeostasis. The beneficial effects of IL-15 obtained are associated with up-regulation of transcription of genes involving lipolysis in the adipose tissue and skeletal muscle, and decreased mRNA levels of genes responsible for lipogenesis in the liver.

Hydrodynamic transfer of the *Il-15/sIl-15Rα* gene into mice carrying the Lewis lung tumor in the lungs, liver, and kidneys prolongs the survival time of the animals. These results demonstrate the therapeutic potential of IL-15 and provide direct evidence in support of its applications to the treatment of obesity and obesity-associated metabolic diseases, and to lung metastasis in the liver and kidneys.

INDEX WORDS: Interleukin 15, Interleukin 15 receptor, Gene therapy, Hydrodynamic delivery, Cancer, Obesity, Metabolic homeostasis.

INTERLEUKIN-15 BASED MAINTENANCE OF METABOLIC HOMEOSTASIS AND TREATMENT OF LUNG CANCER

by

HAO SUN

BS Pharmaceutical Science, SUNY at Buffalo, 2011

MS Regulatory Affairs, University of Georgia, 2015

A Dissertation Submitted to the Graduate Faculty of The University of Georgia in Partial Fulfillment of the Requirements for the Degree

DOCTOR OF PHILOSOPHY

ATHENS, GEORGIA

2016

INTERLEUKIN-15 BASED MAINTENANCE OF METABOLIC HOMEOSTASIS AND TREATMENT OF LUNG CANCER

by

HAO SUN

Major Professor:	Dexi Liu
Committee:	James V. Bruckner
	Shelley B. Hooks
	Jin Xie

Electronic Version Approved:

Suzanne Barbour
Dean of the Graduate School
The University of Georgia
May 2016

DEDICATION

This dissertation is dedicated to my loving family members, my father Xueliang Sun, my mother Li Gong and my brother Zeyu Gong, for their endless love, support and encouragement. I must thank them for giving me faith, strength, and confidence to succeed, when I was facing challenges and difficulties. I would also like to dedicate this dissertation to my wife Ying Lou, for her love, company and support. At last, I would like to dedicate this dissertation to my lovely newborn twin girls, Angelbella Qianyu Sun and Angelina Qianxun Sun, for welcoming these two new members to our family.

ACKNOWLEDGEMENTS

First and foremost, I would like to express my sincere gratitude to Dr. Dexi Liu, my major advisor, for the wisdom and generous support he offered. He guided me into the field of molecular biology and provided me with great training opportunities and technical advices, which were all essential for completion of this dissertation. His patience and encouragement throughout my graduate studies fostered my growth in the path to what I want to be.

Besides my major professor, I would also like to thank the members of my dissertation committee, Dr. James V. Bruckner, Dr. Shelley B. Hooks and Dr. Jin Xie for their perpetual support and valuable suggestions. They are the keys to help me develop keen insights into academic research and to shape me into a scientist.

I must also express my sincere thanks to our lab manager, Guisheng Zhang, for her thoughtful care. Her assistance and warmhearted encouragement gave me strength and faith to face difficulties. Last but not the least, I would like to say thanks to all my fellow labmates: Mingming Gao, Yongjie Ma, Chunbo Zhang, Mohammad Al Saggar, Sary Alsanea, Parisa Darkhal, Yahya Al Hamhoom and Linna Yan for the technical supports, stimulating discussions, valuable suggestions, and joyful moments they gave me throughout my graduate studies. This dissertation would never have been done without the help and support from all these wonderful people.

TABLE OF CONTENTS

Page

LIST OF TABLES

Page

LIST OF FIGURES

Page

CHAPTER 1

INTRODUCTION AND LITERATURE REVIEW

1.1 INTERLEUKIN-15 (IL-15) BIOLOGY

1.1.1 IL- 15

Interleukin-15 (IL-15) is a cytokine that shares conserved coding sequence among different species [1, 2]. In humans, the IL-15 gene is encoded on the 34 kilo-base pair (kbp) region of chromosome 4q31 and is made of nine exons and eight introns [1, 3]. Among animal species examined, simian exhibits highest identity (97%) with human IL-15 coding sequences [4], whereas the coding sequence of porcine and mouse IL-15 shows 82% and 73% identity match with human IL-15 [1, 2]. The mature IL-15 protein (14–15 kilo-Dalton, kDa) contains 114 amino acids (AA) and is encoded by three introns and four exons (exon 5 to 8) [3]. Analysis of the IL-15 secondary structure reveals four α-helix bundle structures at positions 1 to 15, 38 to 57, 65 to 78, and 94 to 112 AAs [5]. Two disulfide links are identified in the mature IL-15 protein at positions Cys35–Cys91 and Cys42– Cys88 [4], and two N-linked glycosylation sites, Asn79, and Asn112, are found at C-terminus [6, 7].

IL-15 has two isoforms that are encoded with different length of the signal peptide (SP) (Figure 1.1). One isoform of IL-15 comprises a long signal peptide (LSP) of 48-AA and an 114-AA mature IL-15 protein [4]. It is translated from IL-15 cDNA that contains a 316 bp 5'-untranslated region (5'-UTR), a 486 bp open reading sequence, and a 400 bp 3' noncoding region [4]. This IL-15LSP mRNA is present as 1.6 kb in length and encoded by exons 3 to 5 of the human IL-15 gene [8]. In comparison, the other IL-15 isoform has a 21-AA short signal peptide

(IL-15SSP), which consists of 11-AA encoded by exon 5 and an alternative sequence encoded by exon 4a [9]. Even though both IL-15 mRNA isoforms generate an identical IL-15 mature protein, the two isoforms show distinct patterns of endosomal localization, intracellular trafficking, and protein secretion [8]. The IL-15LSP is made for the secretory pathway, where it passes through the endoplasmic reticulum (ER) and Golgi apparatus and finally leads to deposition of IL-15 out of the cell [10, 11]. Different from the secreted IL-15 isoform, IL-15SSP stays intracellularly in the cytoplasm and is not secreted to circulation [10, 11]. As such, the signal peptide may play a major role in controlling IL-15 transcription and production [12, 13].

The expression of IL-15 shows the discrepancy between its mRNA level and protein level [8]. The IL-15 mRNA is detected in various cell types, including epithelial cells, fibroblasts, macrophages, monocytes, dendritic cells (DCs), keratinocytes and nerve cells, and multiple tissues, such as the lung, heart, skeletal muscle, and kidneys [8, 14]. However, the IL-15 protein is primarily found in monocytes, dendritic cells, and macrophages [15, 16]. In fact, IL-15 has a complex expression regulation mechanism that controls the transcription and translation of IL-15 [7]. The transcription of IL-15 is mainly controlled by multiple conserved binding motifs for regulatory transcription factors, including the consensus-binding sites within the promoter regions of nuclear factor kappa-light-chain-enhancer of activated B cells (NF-κB), the gamma interferon response element (γIRE), and the interferon regulatory factor binding element (IRF-E) [7, 17, 18]. Meanwhile, the translation of IL-15 is largely regulated through three primary checkpoints. This includes the presence of multiple start codons (AUG) in the 5'-UTR (12 in humans, 5 in mice) that reduce the translational initiation at the actual translation start site; the long signal peptide (IL-15 LSP) shows low translational efficacy; and the presence of several regulatory components at C-terminus decreases the translational termination and secretion

efficiency [14]. Therefore, elimination of these translation checkpoints will significantly enhance the production and secretion of bioactive IL-15 [19].

1.1.2 IL-15 Receptor

The IL-15 receptor complex is made of three subunits: an IL-15 specific α subunit (IL-15Rα); a β chain also known as cluster of differentiation 122 (CD122, IL-2R/15Rβ) and shared with the IL-2 receptor; and a common γ subunit (γ_c), known as CD132 and shared with different cytokines, including the IL-2, IL-4, IL-7, IL-9, and IL-21 [20].

The IL-15 β subunit (IL-2R/15Rβ, CD122) consists of a signal peptide of 26-AA, a 214-AA extracellular fragment, a transmembrane domain of 25-AA, and a 286-AA cytoplasmic region [21]. The IL-15 γ subunit (γ_c, CD132) consists of a 22-AA signal peptide and a 347-AA mature protein, which includes an extracellular segment of 233-AA, a 28-AA transmembrane domain, and a 86-AA cytoplasmic domain [22].

The IL-15 specific α subunit (IL-15Rα) is a glycosylated protein and is preceded by a 32-AA signal peptide, an extracellular domain of 173-AA containing a Proline/Threonine-rich region, a 21-AA transmembrane domain, and a cytoplasmic segment of 37-AA [23]. The expression of IL-15Rα mRNA has been identified in various cell types, which include the effector T cells, nature killer (NK) cells, neutrophils, monocytes, dendritic cells, macrophages, epithelial cells, myocytes, and adipocytes [23, 24]. The IL-15Rα gene is encoded on human chromosome 10 and is made of seven exons (exons 1-7) [25]. Additionally, a common motif known as the Sushi domain, which is identified in the extracellular region and encoded on exon 2, is required for the IL-15 binding and signaling [20, 25]. To date, eight different isoforms of IL-15Rα have been identified due to the nature of splicing of IL-15Rα exons [25]. These include the

alternative usage of exon 7 or 7', alternative splicing of exon 3, and deletion of exon 2 [25]. Isoforms without exon 2 show the inability of IL-15 binding [25]. Exon 2 has a putative nuclear localization signal and is responsible for the post-translational routing of IL-15Rα [8, 25]. Deletion of exon 2 leads IL-15Rα isoforms to the non-nuclear membranes [8, 25].

Other than the membrane-bound form, IL-15Rα could be naturally cleaved from the transmembrane receptor, generating a soluble form, known as sIL-15Rα [26]. The rate of IL-15Rα proteolytic cleavage can be induced by phorbol 12-myrisrate 13-acetate (PMA) and ionomycin [26]. With an *N*-linked glycosylation, the molecular mass of human sIL-15Rα is about 42 kDa, whereas murine sIL-15Rα is about 30 kDa in size [26]. The presence of the soluble form of IL-15Rα indicates its functional importance in mediating the IL-15 response.

1.1.3 The IL-15/IL-15 Receptor System

Intracellular signaling of IL-15 is activated through its receptor system [8]. Binding of IL-15 to the IL-2R/15Rβ and γ_c subunits is essential to exert its functions and to lead a series of signaling events [8]. At the cell membrane, the IL-2R/15Rβ and γ_c subunits are presented as a heterodimeric form (IL-2/IL-15Rβγ_c) and interact with IL-15 with an intermediate affinity (Ka~10^9 M^{-1}) [27]. The major signaling event of IL-15 involves the activation of the Janus kinase (JAK) and the signal transducer, and the activation of the signal transducer and activator of the transcription (STAT) pathway [28]. For activation, IL-15 interacts with the IL-2/IL-15Rβγ_c on the cell membrane, and then recruits JAK1 and JAK3 into close proximity to activate and phosphorylate STAT3 and STAT5 [28]. The phosphorylated STAT3 and STAT5 then form either homo- or heterodimers and traffic from the cytoplasm to the nucleus, and regulate the downstream gene expression through the binding of regulatory elements on target DNA

fragments in the nucleus [28]. Other than the JAK/STAT signaling pathway, the IL-15 receptor system is also capable of inducing the B-cell lymphoma 2 (Bcl-2) and the proto-oncogene *Src*-related tyrosine-protein kinase, stimulating the RAS/mitogen-activated protein kinase (MAPK) signaling event and activating the proto-oncogenes, such as *Fos/Jun* [7, 29].

Given that low levels of IL-15 can be found in serum, IL-15 performs multiple biological functions through its cell membrane-associated form, the IL-15/IL-15Rα complex. IL-15 and IL-15Rα are co-expressed intracellularly, form the IL-15/IL-15Rα complex with a high binding affinity ($Ka \sim 10^{11}\ M^{-1}$) [20], and then translocate to the cell membrane and remain anchored [30, 31]. The exceptionally high affinity of the IL-15/IL-15Rα complex is due to the intracellular interaction between IL-15 and IL-15Rα, which leads to an ionic network interaction via the Sushi domain [32]. The cytoplasmic domain of IL-15Rα contributes to the intra-cellular signaling [33] and plays an essential role for the endosomal recycling of the IL-15/IL-15Rα complex [34]. As such, formation of the IL-15/IL-15Rα complex stabilizes the IL-15 in circulation and decreases the elimination rate of IL-15 [35].

At the cell membrane, the IL-15/IL-15Rα complex can enhance the activation and proliferation of neighboring cells that express the receptors IL-2/15Rβ and the γ_c via cell-to-cell contact ("trans-presentation") [31, 34] (Figure 1.2). Additionally, the crystal structure of IL-15Rα reveals a threonine/proline-rich region, which confers flexibility between the transmembrane domain and the IL-15 binding domain [36]. This indicates that the IL-15/IL-15Rα complex can also present IL-15 on the same cell by binding to its IL-2/15Rβ and the γ_c subunits ("cis-presentation") [37] (Figure 1.2). However, the trans-presentation system has proven to be the most important mechanism of IL-15 action and augments overall IL-15 bioactivity. IL-15Rα binding stabilizes the conformation of IL-15, resulting in an increase of binding affinity of IL-15 and IL-

2Rβ by 150-fold, and enhancing the efficiency to stimulate cells bearing the receptor of IL-2/15Rβ and the γ_c subunits [38]. Moreover, the IL-15/IL-15Rα complex could be cleaved from the cell surface by proteolytic cleavage and generates the soluble form of IL-15/IL-15Rα complex (IL-15/sIL-15Rα) (Figure 1.2). The IL-15/sIL-15Rα extends the half-life of IL-15 by increasing its molecular size over the renal filtration threshold [39]. Therefore, the complex IL-15/IL-15Rα may present the true biological form of IL-15.

1.1.4 IL-15 in Immune Cell Biology

1.1.4.1 IL-15 and T cells

IL-15 was first identified by two independent groups in 1994 as a T cell growth factor [4, 40]. Subsequent studies have expanded the knowledge of IL-15's role in the development and maintenance of different types of T cells [7]. *In vitro,* IL-15 is able to stimulate the proliferation of naïve $CD8^+$ human T cells and human memory $CD4^+$ and $CD8^+$ T lymphocytes [41]. Moreover, IL-15 supports the survival of $CD44^{hi}CD8^+$ memory T cells due to the high expression of IL-2/15Rβ [42]. In comparison, IL-15 shows minimal effect on naïve $CD4^+$ T cells [41]. *In vivo,* IL-15 transgenic mice induce the homeostatic proliferation of memory $CD44^{hi}$ $CD8^+$ T cells and support their long-term survival [43]. Conversely, a significant loss of naïve $CD8^+$ T lymphocytes and activated memory $CD44^{hi}$ $CD8^+$ T cells has been identified in mouse spleen and peripheral lymph nodes when IL-15 and IL-15Rα are genetically deleted [44, 45]. IL-15 blocks apoptosis mediated by the TNF-related apoptosis-inducing ligand (TRAIL) pathway on antigen-specific CD8+ T lymphocytes, which in turn mediates their cytotoxic activity towards pathogens and stimulates immune activity [42, 46]. Moreover, IL-15 shows minimal effects on $CD4^+CD25^+$ regulatory T cells

(T_{reg}) expressing the *FOXP3* gene, which play critical roles in suppressing immune responses by inhibiting the effector T cell subtypes [47].

IL-15 also plays a major role in inhibiting the T-cell apoptosis and activation-induced cell death (AICD) process, which results in the programmed death of activated T lymphocytes [48]. Meanwhile, IL-15 has been shown to upregulate the anti-apoptotic factors, such as the Bcl-2 family proteins, and downregulate the pro-apoptotic proteins on CD8+ memory T cells, which lead to the proliferation and long-term maintenance of this particular cell type [49, 50].

As well, the chemotactic activity of IL-15 has been identified in T cells isolated from blood [51]. Defects in T-cell homing activity to peripheral lymph nodes are observed in IL-15Rα knockout mice, which suggests the physiologic role of IL-15 in mediating the T-cell trafficking *in vivo* [45]. As the indirect mechanism to regulate T-cell trafficking, IL-15 induces the production of CC-, CXC-, and C-type chemokines in T lymphocytes, and activates human endothelial hyaluronan expression, which ultimately promotes the activated T cell extravasation [52, 53].

1.1.4.2 IL-15 and NK cells

Nature killer (NK) cells are one type of cytotoxic lymphocytes that are derived from large granular lymphocytes and engaged in the innate immune defense system [54]. IL-15 plays major roles in NK cells' differentiation, development, and survival [54]. In support of NK cell differentiation, IL-15 is constitutively expressed at transcript and protein levels in the bone marrow (BM) stromal cells [55]. In BM, IL-15 is essential to stimulate the hematopoietic precursor cell differentiation to the NK cells through the upregulation of the stem cell growth factors, such as FMS-like tyrosine kinase 3 (FLT3) [56, 57].

The signaling transduction pathways of IL-15 are critical for NK cell development [54]. Even though NK cells are not the major site for IL-15 production, the IL-15 receptors, including IL-15Rα and the IL-2/IL-15Rβγc complex are constitutively expressed on resting NK cells [58]. In experimental animals, mice with genetic deletion of IL-15, IL-2/IL-15Rβ, and IL-15Rα show reduced NK cell count or an absence of NK cells [44, 45, 59]. Therefore, the IL-15 receptor system is required for NK cells' development [54]. Upon trans-presentation, IL-15 upregulates the NK cell receptors and enhances NK cell differentiation [60]. Deletion of the IL-15 receptor downstream signals, such as JAK3 and STAT5 pathway, significantly impair the activity of NK cells [61, 62]. Conversely, animals administered or overexpressed with IL-15 show an increased number and induced proliferation and survival time of NK cells [58, 63]. Additionally, the presence of IL-15 can induce the secretion of immunoregulatory cytokines from NK cell subsets, including Granulocyte-macrophage colony-stimulating factor (GM-CSF) protein, tumor necrosis factor alpha (TNF-α), and interferon gamma (IFN-γ) [64, 65]. As such, IL-15 stimulates the cytolytic activity and antibody-dependent cellular cytotoxicity (ADCC) of NK cells through the upregulation of cell surface receptors, including the MHC class I polypeptide-related sequence A (MICA) and the killer cell lectin-like receptor subfamily K, member 1 (NKG2D); induction of cytotoxic effector molecules, granzyme B and perforin; and enhancement of signaling molecules' phosphorylation, such as extracellular-signal-regulated kinases (ERK1/2) and STAT [63, 66].

IL-15 also regulates the proliferation and survival of NK cells [67]. Upon transient stimulation, administration of IL-15/IL-15Rα complexes significantly increases the number of NK cells and their effector activities in experimental animals [68]. Similarly, sustained stimulation results in a remarkable expansion of activated NK cells in the presence of preformed IL-15/IL-15Rα complexes [68].

1.1.4.3 IL-15 and B lymphocytes

IL-15 was initially identified as having no role or at most a limited role in B cell biology, since animals with genetic disruption of IL-15 or IL-15Rα show minimal impact on B lymphocytes [44]. However, with accumulating evidence, it has become more apparent that IL-15 is essential for the B lymphocyte functions [8]. In fact, compared to the direct impact of IL-15 on T and NK cells, IL-15 shows indirect effects on B lymphocytes [8]. IL-15 combined with CpG oligonucleotides increases the proliferation rate of differentiated memory B lymphocytes [69]. In combination with anti-immunoglobulin (Ig) and CpG, IL-15 is able to enhance the proliferation of naïve B lymphocytes [69]. Another study also showed that in the presence of phorbol ester or immobilized anti-human IgM, IL-15 co-stimulated the proliferation and activity of B cells [70]. Additionally, combined with recombinant CD40 ligand, IL-15 induces the secretion and production of polyclonal immunoglobulin A (IgA), IgG1, and IgM, but does not change the level of IgE and IgG4 [70]. In studies using the follicular DCs as the specialized component of the germinal center B lymphocytes' survival and proliferation, IL-15 produced by follicular DCs went through the trans-presentation process and induced the proliferation of associated germinal center B cells [71]. It ultimately led to an enhancement of high-affinity antibody production from the B cells to fight against the invasion of pathogens [71].

1.1.4.4 IL-15 and monocytes/macrophages and dendritic cells

IL-15 is constitutively expressed by the monocytes, macrophages, and dendritic cells at the mRNA and protein levels [8]. In monocyte and macrophage cell lineages, IL-15 stimulates their phagocytic activity through promoting the secretion of monocyte chemotactic protein 1 (MCP-1) and IL-8 [72]. The membrane-associated IL-15 on monocytes also stimulates the proliferation of T lymphocytes and leads to the release of TNF-α, IL-6, and IL-8 [73, 74]. Moreover, the up-regulation of IL-15 and its receptor component, IL-15Rα, on macrophages are critical for their differentiation and proliferation [75]. Upon activation, IL-15 augments the anti-infectious immune responses in macrophages, including the induction of phagocytic activity through the induction of IL-12 [76]. Therefore, IL-15 is important in fighting against pathogens as an innate immune regulator cytokine.

In DCs, IL-15 and its receptor system are essential for their functional maturation, differentiation, and survival [8]. In the presence of IL-15, DCs show maturation with induced co-stimulatory molecules expressing on the cell surface, such as CD40, CD86, and MHC class II molecules, and increased IFN-γ production [77]. Conversely, there is a significant reduction in total numbers of DCs in animals genetically deleted with IL-15, while overexpression or administration of IL-15 can partially compensate the loss of DCs in the IL-15 knockout mice [78]. Therefore, these observations provide the evidence that IL-15 is essential for DCs' survival [78]. Moreover, DCs incubated with IL-15 demonstrate enhanced abilities to stimulate the proliferation and activation of $CD8^+$ T cell and NK cells [8]. IL-15 combined with GM-CSF stimulates the monocytes' differentiation towards DCs, where the DCs are acting as the antigen presenting cells and then induce the functional activity of $CD8^+$ T and NK cells with the increased production of type 1 (Th1) cytokines [79, 80]. Mechanistically, IL-15 and its receptor

system are able to generate an autocrine signaling loop on DCs, which can be used to stimulate the differentiation, proliferation and activation of targeting $CD8^+$ T cells and NK cells [81, 82]. IL-15 and IL-15Rα form the IL-15/IL-15Rα complexes intracellularly and translocate to the surface of DCs, where they remain anchored, and then deliver the stimulating signals to the CD8+ T cells and NK cells through the cell-cell trans-presentation [81, 83].

1.1.4.5 IL-15 and neutrophils/eosinophils

IL-15 is capable of modulating the phagocytic activity and inducing the secretory activities of neutrophils and eosinophils, as well as protecting them from apoptosis [84, 85]. In human neutrophils, IL-15 induces the release of the IL-1R antagonist and IL-8, and enhances their phagocytosis against invading pathogens [86]. Moreover, IL-15 prevents the loss of neutrophils via increasing the level of anti-apoptotic molecules, such as myeloid leukemia cell differentiation protein (Mcl-1) expression, and inhibiting the vimentin cleavage through downregulating the caspases-3 and -8 activities [87]. In human eosinophils, IL-15 upregulates the production and activity of growth factors, such as GM-CSF and NF-κB, to reduce the apoptosis rate of eosinophils [85].

1.1.5 IL-15 Functions in Non-Immune Cells

In addition to its significant impacts on immune cells, IL-15 is also widely recognized as a potent modulator on various non-immune cells. The effects of IL-15 on both immune and non-immune cells are summarized in Figure 1.3.

1.1.5.1 IL-15 and adipocytes

IL-15 exhibits an anti-adipogenic role on adipocytes. Adipocytes express IL-15 receptors, including IL-15Rα, IL-2R/15Rβ, and γ_c subunits [88]. Using murine and human adipocyte cell lines, IL-15 decreases lipid deposition in differentiating and mature adipocytes [89-91]. In experimental rodents, administration of recombinant IL-15 resulted in the reduction of white adipose tissue and cell shrinkage of adipocytes, with no change in food intake [88, 92]. Moreover, obese Zucker rats showed a reduced mRNA level of IL-2R/15Rβ and γ_c subunits in adipose tissue, suggesting that IL-15 has direct impacts on adipose tissue [88].

IL-15 is a key regulator of lipid metabolism in adipose tissue. In cultures of primary pig adipocytes, IL-15 dose-dependently stimulated lipolysis and showed more potent lipolytic activity than TNF-α, IL-6, or lipopolysaccharides (LPS) [93]. Additionally, this study revealed an inhibitory effect on lipogenesis after IL-15 administration. In rat white adipose tissue, IL-15 administration induced significant reduction in lipoprotein lipase activity (LPL) and the rate of lipogenesis [92]. Moreover, a recent study demonstrated that the effects of IL-15 on adipose tissue were associated with the alteration of mitochondrial function [89]. Using mature 3T3-L1 cells and IL-15 transgenic mice, IL-15 significantly increased the mitochondrial membrane potential and induced the activity of mitochondria in adipocytes, suggesting the role of IL-15 in regulating the lipolysis and fatty acids oxidation in adipose tissues [89]. As such, IL-15 is acting as a potential anti-obese agent in regulating body composition.

1.1.5.2 IL-15 and myocytes

IL-15 mRNA and protein is constitutively expressed in skeletal muscle and have been identified in primary human myogenic cultures [94], rat clonal myogenic cell line [95], and mouse C2 skeletal myogenic cell line [96]. At the mRNA level, IL-15 is the most expressed of all measured cytokines in human skeletal muscle [97]. At the protein level, IL-15 is released from human muscle fibers following whole-body resistance exercise, indicating that release of IL-15 may regulate the beneficial events of physical activity [98].

IL-15 is considered as an anabolic factor for myocytes [99]. In primary bovine skeletal myogenic cell lines, IL-15 is able to accumulate contractile proteins in differentiated muscle fibers and myocytes and increase the muscle-specific myosin heavy chain [100]. In mouse C2C12 cell lines, overexpression of IL-15 leads to muscle fiber hypertrophy and induced muscle mass, indicating that IL-15 is important for muscle fiber development [96]. However, it is important to differentiate the anabolic activity of IL-15 on myocytes from the well-recognized hypertrophic action of muscle cells, where the proliferation and differentiation of skeletal myoblasts are mainly stimulated by insulin-like growth factor-I (IGF-I) [101]. Instead, IL-15 acts directly on differentiated myotubes by increasing protein synthesis, decreasing protein degradation and inducing myofibrillar protein accumulation, and ultimately leads to the hypertrophic morphology [96]. Furthermore, IL-15 could decrease the proteolytic rate in skeletal myogenic cells, indicating that IL-15 may also play roles in the alleviation of muscle wasting [102]. In fact, in tumor-bearing rats, IL-15 administration partially suppressed the process of cancer-related progressive muscle loss and protein degradation [103]. This process is seen in cancer patients where tissue proteins, particularly in the skeletal muscles, are over-catabolized, resulting in a clear muscle wasting condition known as cachexia [103].

In addition to the anabolic effect, IL-15 also plays a catabolic role in skeletal muscle. Evidence suggests that IL-15 may activate the transcription factor peroxisome proliferator-activated receptors delta (PPAR-δ), resulting in the regulation of various gene expression for protein metabolism in C2C12 cells, and may also enhance the rate of palmitate oxidation [104]. In line with cell cultures, recombinant IL-15 administration induces a significant elevation in the PPAR-δ mRNA level and enhances oxidation of fatty acid in skeletal muscle, followed by the administration of triglyceride in the form of [^{14}C]-triolein in experimental animals [105]. This indicates the significant role of IL-15 in lipid metabolism.

Further evidence suggests that IL-15 modulates glucose uptake in muscle cell cultures, indicating an anti-diabetic effect of this cytokine since skeletal muscle is the most significant glucose-utilizing organ [106]. In animal studies, administration of IL-15 increased glucose transporter 4 (GLUT-4) in muscle cells, resulting in an induced uptake of 2-deoxyglucose in skeletal muscle [106]. Furthermore, overexpression of IL-15 showed improved glucose metabolism in high-fat diet-induced obese animals, suggesting a role of IL-15 in inhibiting diabetic development [107]. Taken together, these studies establish the potential of IL-15 to prevent muscle waste and mediate metabolic homeostasis.

1.1.5.3 IL-15 and endothelial cells

IL-15 has a direct impact on endothelial cell biology [99]. Endothelial cells sustainably express the IL-15 receptor complexes, including IL-15Rα, IL-2R/15Rβ and γc subunits, and bind to IL-15 with high affinity [108]. Stimulating the endothelial cells with IL-15 induces the expression of endothelial hyaluronan, which binds to effector T cells through the T-cell surface glycoprotein CD44 [53]. In fact, interactions between hyaluronan and CD44 are important to

recruit activated T cells to the blood vessel and to promote T cells' extravasation [53]. Additionally, IL-15 mRNA and protein are identified in human umbilical vein endothelial cells, indicating another direct impact of IL-15 on endothelial cell biology [109]. IL-15 derived from endothelial cells is able to increase T-cell motility and transendothelial migration activity via the induction of integrin adhesion molecules' binding capacity, such as lymphocyte function-associated antigen 1 (LFA-1) (CD11a/CD18) [109]. These studies signify the importance of IL-15 on endothelial cells in mediating the extravasation and immune activity of effector T cells.

1.2 INTERLEUKIN-15 AS A DRUG

1.2.1 IL-15 in cancer immunotherapy

The ability of IL-15 to activate antitumor immune responses makes IL-15 a promising candidate for cancer immunotherapy. Both cytotoxic NK and $CD8^+$ T cells are engaged in eliminating tumor cells through granule- or FAS-mediated pathways [110]. In multiple tumor animal models with different experimental designs, IL-15 shows significant therapeutic activity on various tumor types [111]. Many strategies have been employed to induce the anti-tumor activity of IL-15.

One of those strategies is to improve the biological activity of IL-15. By introducing an aspartic acid substitution of asparagine at the amino acid residue 72 of the mature protein, the modified IL-15 improves its binding affinity to the human IL-2/15Rβ receptor and induces its biological activity by 4- to 5-fold compared with the wild-type IL-15, including enhanced anti-apoptotic activity and increased JAK1 and STAT5 phosphorylation [112]. According to the trans-presentation mechanism, the biological activity of IL-15 can be significantly induced by pre-forming the IL-15 with its IL-15Rα as IL-15/IL-15Rα [39, 113] or IL-15/IL-15Rα-IgG1-Fc complex

[114]. Both forms demonstrate enhancement of activation and proliferation of cytotoxic NK and $CD8^+$ T cells to promote the destruction of established tumors.

The combination of IL-15 with other cytokine-based immunotherapy, such as IL-7, IL-12, and IL-21, is another strategy to strengthen its antitumor activity [115]. In animals bearing 4T1 mammary carcinoma, IL-15 combined with IL-7 inhibited the tumor development and lung metastasis by inducing the specific immune response against breast cancer [116]. Using a methylcholanthrene-induced fibrosarcoma mouse model, the IL-15 and IL-12 combination augmented cytotoxic NK and $CD8^+$ T cells activity, resulting in a synergistic anti-tumor effect [117]. Similarly, this combination induced the cytolytic activity of NK cells and was accompanied by an increase of IFN-γ production in a mouse melanoma model [118]. Combined administration of plasmids carrying the IL-15 and IL-21 genes separately into animals bearing lymphomas resulted in synergistic antitumor activity with 80% complete response [119]. The synergistic effects are mainly caused by the expansion of cytotoxic $CD8^+$ T lymphocytes in tumor-bearing animals and do so without changing the number of T_{reg} cells [120, 121]. Additionally, the IL-15 and IL-21 combination induced the production of IFN-γ and augmented cytolytic activity of NK and T cells on tumor cells [119, 122].

IL-15 has also been shown to induce an anti-tumor effect as a chemotherapy agent [115]. In mice bearing rhabdomyosarcoma, IL-15 induced the anti-tumor activity of cyclophosphamide by stimulating the effector T and NK cells against tumors, leading to a prolonged survival rate and a complete cure of 32% of the tumor-bearing animals [123, 124]. In colorectal cancer-bearing rats, the IL-15 administration potentiated the anti-tumor activity of 5-fluorouracil and diminished the gastrointestinal side effects induced by the chemotherapy agent [125]. In comparison,

administration of IL-2 with 5-fluorouracil showed only minimal enhancement of anti-tumor activity associated with chemotherapy-related toxicities [125].

Moreover, IL-15-based anti-tumor activity can be significantly induced by utilizing the agents to stimulate antigen presentation cells and to reactivate the effector NK and $CD8^+$ T cells from the "helpless state" [115]. The agonistic anti-CD40 antibody is one agent used to trigger CD40-mediated signaling events and recruit cytotoxic immune effector cells into the tumor microenvironment [126, 127]. IL-15 combined with agonistic anti-CD40 demonstrates stronger therapeutic effects in mice bearing renal adenocarcinoma or colorectal cancer compared to the anti-CD40 antibody or IL-15 monotherapy [126, 127]. Mechanistically, the IL-15 and anti-CD40 agonistic antibody combination increases the IL-15Rα expression on NK cells and enhances the antigen presentation ability of dendritic cells, leading to the potentiated cytolytic activity of NK cells and improved antitumor activity [127]. Similarly, combination of IL-15 and CpG-A oligonucleotides to activate DCs shows stronger cytolytic activity of effector $CD8^+$ T and NK cells than using either agent alone [128].

Efforts have also been made to induce the anti-tumor effect of IL-15 by relieving the inhibitory checkpoints on the immune system. When the cytotoxic T-lymphocyte antigen 4 (CTLA-4) and programmed death ligand 1 (PD-L1) antibody were used to diminish the negative T-cell signaling pathways, tumor-bearing mice receiving IL-15 and the combination of both PD-L1 and CTLA-4 antibodies demonstrated a remarkably prolonged survival rate [129]. Together, these observations support further investigations into combination therapy of IL-15 with multiple immune checkpoint inhibitors or other agents to enhance anti-tumor activity.

1.2.2 IL-15 as a vaccine adjuvant

Vaccination is a process that occurs by introducing an immune booster to enhance a long-lived immune response against invasion pathogens [130]. To date, various strategies have been developed or are under development to fend off infectious agents, such as the hepatitis virus, malaria, influenza and human immunodeficiency virus (HIV) [130]. During vaccination, cytokines are usually used as adjuvants to help to induce the immune response in humans and animals with diverse genetic backgrounds [130, 131]. Multiple techniques have been utilized to deliver IL-15 as an adjuvant to enhance immune response [131]. In mice bearing *Brucella abortus*, co-administration of plasmid DNA encoding IL-15 (DNA-IL-15) and *Brucella abortus* S19 vaccine predominantly stimulated the $CD8^+$ T cell activity and partially enhanced the $CD4^+$ T cell response [132]. Similarly, a combination of DNA-IL-15 and *Trypanosoma cruzi trans-sialidase* DNA vaccine prolonged the duration of the protective effect against the infectious challenge, mainly through the induction of memory $CD8^+$ T cells' production and activity [133]. Furthermore, with co-administration of IL-15 and two vaccines against smallpox and anthrax, the treated mice showed enhanced immune activities of effector T cells against malaria, tuberculosis, and influenza [134].

IL-15 also demonstrates advantages over other cytokines in effectively inducing immune activity against infectious pathogens [131]. Compared to IL-2, the combination of IL-15 with the HIV gp160 vaccine shows a predominant effect in prolonging the survival time of effector $CD8^+$ T cells, whereas IL-2 adjuvant only demonstrates short-term immune response [135]. Similarly, IL-15 demonstrates superior effects over IL-2 in stimulating the long-lived memory effector $CD8^+$ and $CD4^+$ T lymphocytes in animals injected with influenza and tetanus toxoid vaccines [136]. Compared to IL-12, IL-15 combined with the simian immunodeficiency virus (SIV) vaccine stimulates the proliferation of antigen-specific memory $CD8^+$ and $CD4^+$ T lymphocytes

in rhesus macaques, whereas IL-12 as a molecular adjuvant only induced CD8+ effector memory T cells [137]. Taken together, these studies demonstrate the great potential of IL-15 as a vaccine adjuvant against infectious diseases.

1.2.3 IL-15 as an anti-obesity agent

Considering the impacts of IL-15 on skeletal muscle and adipose tissue, IL-15 shows potential for the treatment of obesity. Clinical investigations provide direct evidence supporting the activity of IL-15 in mediating fat deposition. One study demonstrated that the plasma level of IL-15 is negatively associated with body mass indices (BMI), and the mass of total, limb, and trunk fat in human subjects [138]. Additionally, the level of IL-15 mRNA expression in skeletal muscle is negatively associated with obesity markers [138]. A similar finding was reported in another study, in which obese patients had lower circulating levels of IL-15 than normal subjects [90].

The potential of IL-15 in mediating metabolic homeostasis has been evaluated in animals as well. Administration of recombinant IL-15 (rIL-15) protein into lean rats led to a 33% reduction in white adipose tissue (WAT) and a 20% reduction in circulating triacylglycerols without changing the rats' food consumption [92]. These observations were also accompanied by a 47% decrease in the hepatic lipogenic rate and a 36% reduction of very-low-density lipoprotein (VLDL) in plasma [92]. Using an electroporation technique to overexpress IL-15 in murine muscle resulted in reduced trunk fat mass in IL-15-transfected mice, compared to controls in both the normally fed group and the high-fat fed group [138]. Similarly, administration of an adenoviral vector expressing the IL-15 gene resulted in ~10% body weight loss was in obese mice without altering food consumption [138]. The body weight reduction is correlated with decreased fat pad

size and smaller adipocytes. Furthermore, administration of IL-15 into obese or lean mice showed an improvement in insulin sensitivity and glucose homeostasis [107]. Together, these studies provide compelling evidence for the utilization of IL-15 in the treatment of obesity and obesity-associated metabolic complications.

1.2.4 IL-15 toxicology

The safety profile of IL-15 has been assessed in animal studies, including experimental mouse and non-human primate studies. The major dose-limiting side effect of cytokine-based immunotherapy is vascular leak syndrome (VLS), which is defined by the induction of vascular permeability and increased extravasation of fluids and proteins into tissues. The VLS causes an increase in body weight and fluid retention, and can even lead to peripheral/pulmonary edema, as well as pleural and cardiovascular failure [139]. In comparison, IL-15 treatment shows fewer VLS effects than IL-2 based therapies. Using radiolabeled bovine serum albumin, pulmonary VLS levels were evaluated in C57BL/6 mice receiving the same amounts of rIL-2 or rIL-15 [140]. In this study, the minimal dose of IL-2 required to induce VLS was 1200 μg/kg. In contrast, the mice administered with 7200 μg/kg IL-15 showed only a minimal level of VLS effects, indicating that VLS is not a dose-limiting factor for IL-15 treatment.

Following studies further assessed the toxicity of IL-15 in non-human primates with different dosing and administration strategies [14]. Using SIV-infected rhesus macaques, recombinant rhesus macaque IL-15 (rMamu IL-15) was given at doses of 10 or 100 μg/kg via twice weekly subcutaneous injections for four weeks [141]. The study animals demonstrated a significant induction of $CD8^{+}CD3^{-}$ NK cells by nearly 3-fold and a 2-fold increase in $CD8^{+}$ T cells [141]. Importantly, animals injected with IL-15 did not show any sign of adverse events [141].

These include no body weight changes, no observed abnormalities, and no changes in most clinical laboratory tests, such as serum chemistries, white/red cell counts, leukocyte counts, and liver function in study animals [141]. The only exception was a non-statistically significant increase of platelets in animals treated with high dose IL-15 [141]. In another study, recombinant human IL-15 (rhIL-15) was administered to macaques at a daily dose of 15 μg/kg for 14 days and led to a sustained IL-15 plasma level [47]. However, transient toxicities were identified, including weight loss, skin rash, anemia, and reversible neutropenia, although discontinuing the IL-15 injections causes rapid recovery from these events [47]. In comparison, a daily low-dose IL-15 administration (<5 μg/kg) or intermittent IL-15 administration (<10 μg/kg for every three days) was found safe with minimal adverse events, including skin rash and low-grade fever [47]. Two more studies conducted in rhesus macaques from U.S. National Cancer Institute (NCI) showed similar effects after IL-15 administration [142, 143]. Overall, daily intravenous injection of recombinant human IL-15 for 12 days did not induce severe adverse events at doses of 10, 20, or 50 μg/kg [142, 143]. The most severe side effect was transient neutropenia (grade 3/4), which was identified in three out of six rhesus macaques that were administered with either 20 μg/kg or 50 μg/kg IL-15. However, discontinuing the IL-15 administration restored the neutrophils back to normal range within 72 hours [142, 143]. Additionally, no animals were identified as developing antibodies against IL-15, positive autoimmune markers, renal failure, or VLS [142, 143]. Together, IL-15 administration shows minimal toxicities in preclinical studies, and it warrants further investigations in human clinical trials.

1.2.5 Clinical Trials of IL-15

IL-15 has been extensively studied in the clinic as an immunotherapeutic agent to treat cancer and HIV infections. To date, a total of fourteen clinical trials are either under investigation or completed, all of which have focused on the safety and therapeutic efficacy of IL-15 (Table 1). Eleven trials are focused on cancer therapy, and three trials are for HIV treatment. In four of the cancer trials, the recombinant human IL-15 is either administered to the patients alone (ClinicalTrials: NCT01727076 and NCT01021059) or combined with the engineered haploidentical NK cells (ClinicalTrials: NCT01385423 and NCT01385423). The primary objective of these trials is to evaluate the toxicity profile of IL-15, including the dose-limiting side effects and the maximum tolerable dose of intravenous or subcutaneous rhIL-15 administration. The secondary objectives are focused on the evaluation of the pharmacokinetics/pharmacodynamics (PK/PD) profiles after rhIL-15 administration and to assess the biological activity, immunogenicity, and anti-tumor effects of rhIL-15 in humans. In another trial, rhIL-15 is introduced *ex vivo* and used as an anticancer vaccine to stimulate the antigen presentation activities of DCs against tumor development (ClinicalTrials: NCT01189383). Other than using the rhIL-15, six trials have been conducted to assess the anti-tumor effect of IL-15/IL-15Rα by pre-forming the IL-15 and IL-15Rα or IL-15Rα-IgG1-Fc complexes (ClinicalTrials: NCT01946789, NCT02452268, NCT02099539, NCT02138734, NCT02384954 and NCT01885897). Altor BioScience Corporation has launched several clinical trials in patients with different cancer types using ALT-803. ALT-803 is the super-agonist form of IL-15 with N-to-D substitution at position 72 in IL-15Rα Sushi domain. The primary objectives of these trials are to determine the minimum efficacious and maximum tolerated dose (MED/MTD) and to study the anti-tumor efficacy of IL-15/sIL-15Rα complexes in cancer

patients. In HIV trials (ClinicalTrials: NCT00775424, NCT00528489, and NCT00115960), DNA-rIL-15 is used as an adjuvant and co-administered with genetic HIV vaccine expressing HIV antigens against HIV infection. In these trials, the objectives are to determine the impact of IL-15 on the enhancement of HIV vaccine immunogenicity since the vaccine showed limited immunogenicity when used alone.

To date, only one clinical trial using rIL-15 as an immunotherapeutic agent for various metastatic cancers has been published [144]. In this trial, patients were divided into three dosing groups (3.0 μg/kg: five patients; 1.0 μg/kg: four patients; 0.3 μg/kg: nine patients), and received daily intravenous administration of rIL-15 for 12 days. Unexpectedly, a transient reduction in circulating NK and memory $CD8^+$ T cells was observed within 20 minutes after rhIL-15 administration. However, the circulating NK cell numbers were slowly normalized within 24 hours and ultimately increased by 10-fold in two days. In comparison, the memory $CD8^+$ T cells finally showed an 8-fold expansion. The pharmacokinetic results demonstrated that rhIL-15 had an average half-life of ~2.5 hours in three dosing regimens, and the IL-15 plasma level rapidly declined after reaching the maximum plasma concentration. The toxicity data reveals that rhIL-15 is safe to be given at a low dosage. Only patients receiving 1.0 or 3.0 μg/kg of rhIL-15 showed dose-limiting side effects, including thrombocytopenia, hypotension, and liver enzyme elevations. In comparison, patients receiving 0.3 μg/kg of rhIL-15 showed only minimal toxicity, and four patients even completed the second round of treatment. Importantly, patients administered with rhIL-15 had only limited VLS and showed no sign of development of rhIL-15 antibodies. Additionally, the anti-tumor activity of rIL-15 was determined according to computed-based radiographic scans and the Response Evaluation Criteria in Solid Tumors (RECIST) criteria. Even though a stable form of the disease is considered as the best response

after IL-15 treatment, five patients revealed a reduction of tumor size by 10% to 30%, and two patients have experienced clearing of their lung lesions. In summary, this first set of clinical trial demonstrates that administration of rhIL-15 is safe at a low dose. IL-15 treatment induces the proliferation and activation of cytolytic NK and $CD8^+$ T lymphocytes, which results in a modest anti-tumor activity.

1.3 RESEARCH OBJECTIVES

The overall goal of this dissertation research was to investigate the potential of IL-15 in the maintenance of metabolic homeostasis and the suppression of tumor growth. The study is designed to achieve the following specific objectives:

1) Determine the preventive effect of IL-15 against high-fat diet-induced obesity, fatty liver, and diabetes.
2) Assess the anti-obese activity of IL-15/sIL-15Rα.
3) Investigate the anti-tumor activity of IL-15/sIL-15Rα against Lewis lung carcinoma growing in the lungs, liver, and kidneys.

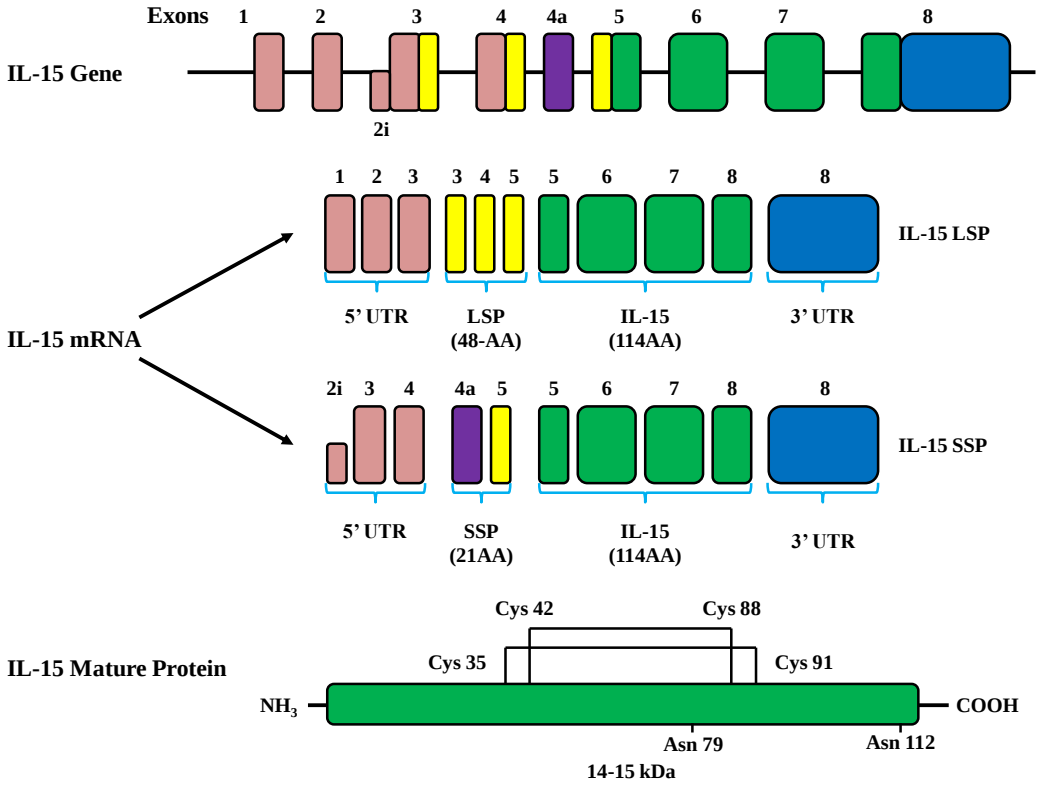

Figure 1.1 IL-15 gene, mRNA, and protein structure. The human IL-15 is located on chromosome 4q31 and is comprised of nine exons. There are two isoforms of IL-15 mRNA: the classical IL-15LSP and alternative IL-15SSP, which are differentiated by the signal peptide length. Both isoforms produce the same mature protein of 114 AAs, which contains two disulfide bonds and two N-linked glycosylation sites. However, the two isoforms have distinct intracellular trafficking (see text for details). 2i indicates intron 2. [Modified based on Figure 1 from *Fehniger TA, et al.* ***(Blood 2001; 97(1): 14-32)*** and Figure 1 from *Bamford R.N, e*t al. **(*J. Leukoc. Biol. 1996; 59(4): 476-480*)**]

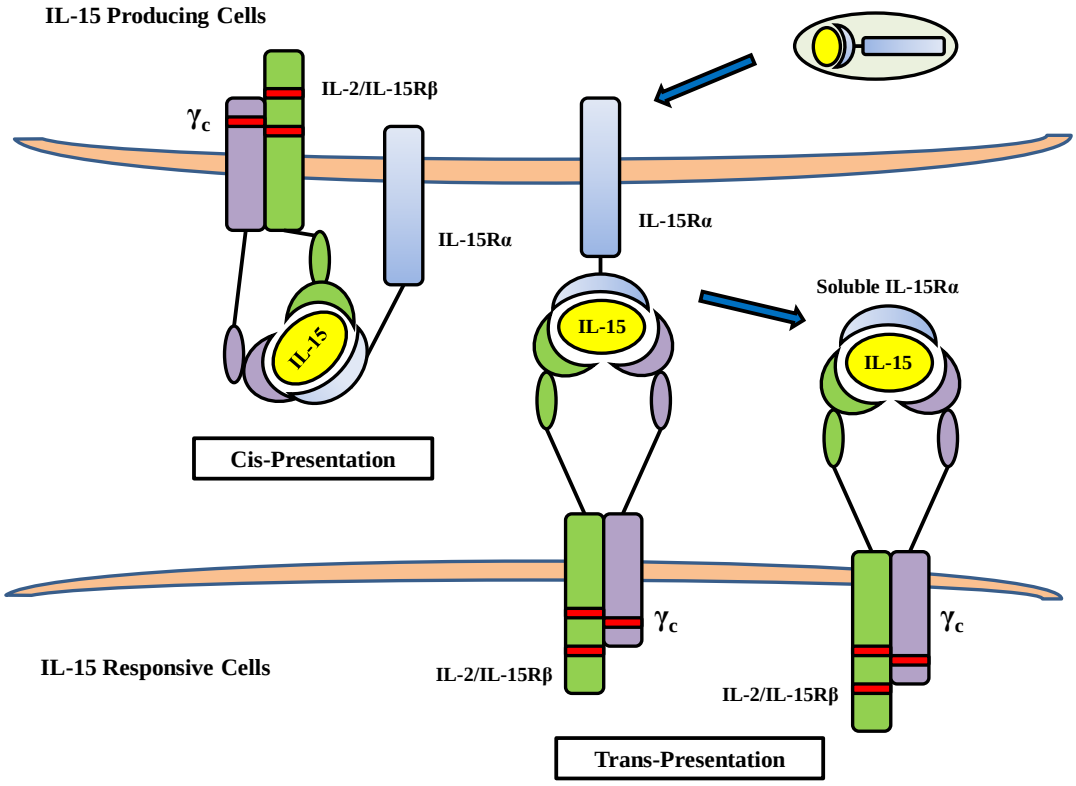

Figure 1.2 Interaction of IL-15 and its receptor (IL-15R). The IL-15 receptor (IL-15R) composed of the common cytokine receptor γ subunit (γ_c), a β subunit (IL-2R/IL-15Rβ), and a private α subunit (IL-15Rα). Receptor specificity is conferred by α subunit (IL-15Rα) and signal transduction is mediated through IL-2R/IL-15Rβ and γ_c. Little IL-15 appears to be expressed in a free soluble state. Instead, IL-15 is secreted in the form of soluble IL-15/IL-15Rα complex. The IL-15/IL-15Rα complex interacts with IL-2R/IL-15Rβ and γ_c by two presentation types. 1) Trans-presentation: IL-15Rα and IL-15 are synthesized in the same cell and transported to the cell surface where the membrane bound IL-15/IL-15Rα complex or soluble form of IL-15/IL-15Rα complex can stimulate neighboring cells through the IL-15Rβγc; 2) Cis-presentation: IL-15 is presented by IL-15Rα on the same cell. [Modified based on Figure 2 from *Steel JC, et al.* ***(Trends Pharmacol. Sci. 2012; 33(1): 35-41.)***]

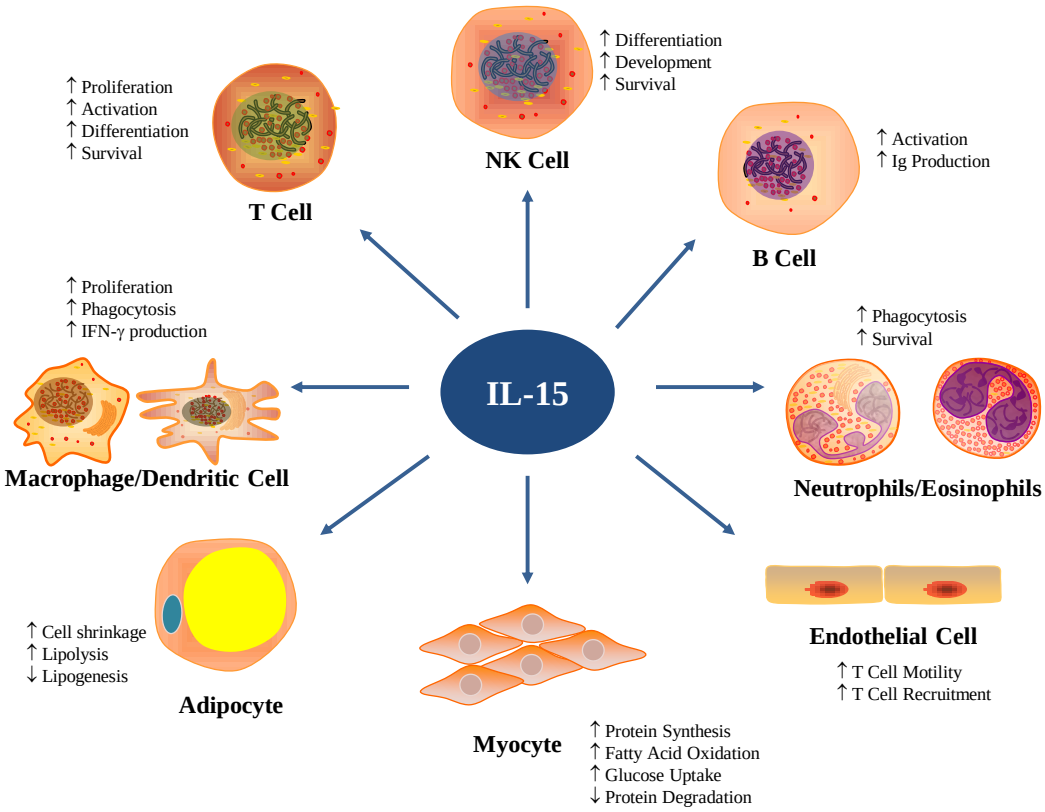

Figure 1.3 Functional properties of IL-15. Schematic diagram demonstrated the IL-15-mediated effects in different cell types**.** [Modified based on Figure 2 from *Jakobisiak M et al.* ***(Cytokine Growth Factor. Rev. 2011; 22(2): 99-108.)***. The cell images are generated using the ScienceSlides Software]

Table 1.1. Clinical trials with IL-15 (Assembled from data available at *clinicaltrials.gov*)*

Trial Name/ID Number	Study Objectives	Disease	Agents	Study Design	Sponsor	Number of Centers Involved	Status
Haploidentical Donor NK Cell Infusion With IL-15 in AML **(NCT01385423)**	**Primary:** MTD/MED for rhIL-15 (*i.v.*) **Secondary:** 1) Treatment related mortality 2) NK cell expansion	AML	rhIL-15	**Purpose**: Treatment **Endpoint**: Safety/Efficacy Study **Model**: Single Group Assignment **Masking**: Open Label	Masonic Cancer Center	Single clinical center (US)	Phase 1 (Completed)
MT2014-25: Haplo NK With SQ IL-15 in Adult Relapsed or Refractory AML Patients **(NCT02395822)**	**Primary:** Potential efficacy of NK cells and IL-15 to achieve complete remission of AML while maintaining safety	Refractory or Relapsed AML	rhIL-15	**Purpose**: Treatment **Endpoint**: Efficacy Study **Model**: Single Group Assignment **Masking**: Open Label	Masonic Cancer Center	Single clinical center (US)	Phase 2 (Recruiting)
Recombinant Interleukin-15 in Treating Patients With Advanced Melanoma, Kidney Cancer, Non-small Cell Lung Cancer, or Squamous Cell Head and Neck Cancer **(NCT01727076)**	**Primary:** MTD of rhIL15 (*s.c.*) **Secondary:** 3) Effect on the PBMCs 4) Tumor response rate 5) PK/PD	Advanced Solid Tumors	rhIL-15	**Purpose**: Treatment **Endpoint**: Safety Study **Model**: Single Group Assignment **Masking**: Open Label	NCI	Four clinical centers (US)	Phase 1 (Recruiting)
A Phase I Study of Intravenous Recombinant Human IL-15 in Adults With Refractory Metastatic Malignant Melanoma and Metastatic Renal Cell Cancer **(NCT01021059)**	**Primary:** DLT and MTD of rhIL15 (*i.v.*) **Secondary:** 1) Effect on the NK and T cells 2) Antitumor effects 3) PK/PD	Metastatic Melanoma or Renal Cell Carcinoma	rhIL-15	**Purpose**: Treatment **Endpoint**: Safety Study **Model**: Single Group Assignment **Masking**: Open Label **Allocation**: Non-Randomized	NCI	Single clinical center (US)	Phase 1 (Completed)
IL15 DCs Vaccine for Patients With Resected Stage III (A, B or C) or Stage IV Melanoma **(NCT01189383)**	**Primary:** Evaluate the immune and clinical efficacy of DC-IL-15 vaccine using in melanoma patients	High Risk Melanoma	IL15-DCs Vaccine	**Purpose**: Treatment **Endpoint**: Safety/ Efficacy Study **Model**: Single Group Assignment **Masking**: Open Label	Baylor Research Institute, NIH and NCI	Single clinical center (US)	Phase 1/Phase 2 (Initialed)
A Phase 1 Study of the Clinical and Immunologic Effects of ALT-803 in Patients With Advanced Solid Tumors **(NCT01946789)**	**Primary:** Assess the effect of ALT-803 (*i.v.)* 1) Safety 2) Immunogenicity, 3) Immunomodulatory properties, 4) Clinical benefits	Advanced Solid Tumors	ALT-803 (IL-15/sIL-15Rα-Fc)	**Purpose**: Treatment **Endpoint**: Safety/ Efficacy Study **Model**: Single Group Assignment **Masking**: Open Label	Altor - Bioscience Corp. and NCI	Six clinical centers (US)	Phase 1 (Recruiting)

A Study of ALT-803 in Patients With Relapsed or Refractory Multiple Myeloma **(NCT02099539)**	**Primary:** MTD and MED of ALT-803 (*i.v.*) **Secondary:** 1) Effect on the NK and T cells 2) Immunogenicity 3) PK/PD	Relapsed or Refractory Multiple Myeloma	ALT-803	**Purpose**: Treatment **Endpoint**: Safety/ Efficacy Study **Model**: Single Group Assignment **Masking**: Open Label	Altor - Bioscience Corp. and NCI	Four clinical centers (US)	Phase 1/Phase 2 (Recruiting)
A Study of Intravesical BCG in Combination With ALT-803 in Patients With Non-Muscle Invasive Bladder Cancer **(NCT02138734)**	**Primary:** MTD of ALT-803 and RD of ALT-803+BCG (Intravesical instillation.) **Secondary:** 1) Immunogenicity 2) PK/PD	Non-Muscle Invasive Bladder Cancer	ALT-803+BCG (Bacillus Calmette-Guerin)	**Purpose**: Treatment **Endpoint**: Safety/ Efficacy Study **Model**: Factorial Assignment **Masking**: Open Label **Allocation**: Non-Randomized	Altor - Bioscience Corp.	Six clinical centers (US)	Phase 1/Phase 2 (Recruiting)
ALT-803 in Patients With Relapse/Refractory iNHL in Conjunction With Rituximab **(NCT02384954)**	**Primary:** MTD and MED of ALT-803 (*i.v/s.c*) and Rituximab (*i.v)* **Secondary:** 1) Immunogenicity 2) PK/PD 3) Immune cells and biomarkers	Relapse or Refractory iNHL	ALT-803 + Rituximab	**Purpose**: Treatment **Endpoint**: Safety/ Efficacy Study **Model**: Single Group Assignment **Masking**: Open Label	Altor - Bioscience Corp.	Single clinical center (US)	Phase 1/Phase 2 (Recruiting)
IL-15 Super Agonist ALT-803 to Treat Relapse of Hematologic Malignancy after Allogeneic Stem Cell Transplant **(NCT01885897)**	**Primary:** MTD and MED of ALT-803 (*i.v)* **Secondary:** Antitumor activity	Relapse of Hemato-logic Malignancy	ALT-803	**Purpose**: Treatment **Endpoint**: Safety/ Efficacy Study **Model**: Single Group Assignment **Masking**: Open Label	Masonic Cancer Center	Three clinical centers (US)	Phase 1/Phase 2 (Recruiting)
A Study of Subcutaneous Recombinant Human hetIL-15 in Adults With Metastatic Cancers **(NCT02452268)**	**Primary:** DLT and MTD of hetIL-15 (s.c.)	Metastatic Cancers	hetIL-15	**Purpose**: Treatment **Endpoint**: Safety Study **Model**: Single Group Assignment **Masking**: Open Label	Admune Therapeutics LLC. and NCI	Single clinical center (US)	Phase 1 (Recruiting)
Safety and Effectiveness of PENNVAX-B Vaccine Alone, With IL-12, or IL-15 in Healthy Adults **(NCT00528489)**	**Primary:** Assess safety, tolerability, and immune response to the DNA HIV vaccines (DNA-IL-15 and PENNVAX-B	HIV/AIDS	IL-15 Plasmid DNA+PENNVAX-B	**Purpose**: Prevention **Endpoint**: Safety/ Efficacy Study **Model**: Parallel Assignment **Masking**: Double Blind **Allocation**: Randomized	NIAID	Six clinical centers (US)	Phase 1 (Completed)
PENNVAX-B With or Without IL-12 or IL-15 as a DNA Vaccine for HIV Infection **(NCT00775424)**	**Primary:** Safety and optimal doses of DNA-IL-15+ PENNVAX-B **Secondary:** 1) Immunological responses 2) Antibody response 3) CD8 cell	HIV/AIDS	IL-15 Plasmid DNA+PENNVAX-B	**Purpose**: Treatment **Endpoint**: Safety Study **Model**: Parallel Assignment **Masking**: Double Blind **Allocation**: Randomized	University of Pennsylvania and Drexel University	Single clinical center (US)	Phase 1 (Completed)

Safety of and Immune Response to an HIV Preventive Vaccine (HIV-1 Gag DNA Alone or With IL-15 DNA) Given With or Without 2 Different Booster Vaccinations in HIV Uninfected Adults **(NCT00115960)**	**Primary:** Assess the safety and immune response to HIV vaccine with and without an IL-15 DNA adjuvant **Secondary:** 1) Safety 2) Immune response	HIV/AIDS	HIV Vaccine, IL-15 Plasmid DNA	**Endpoint**: Safety Study **Model**: Parallel Assignment **Masking**: Double Blind **Allocation**: Randomized	NIAID	Six clinical centers in US and one clinical center in Brazil	Phase 1 (Completed)

***Abbreviations:** NK, Natural Killer; AML, Acute Myelogenous Leukemia; MTD, Maximum Tolerated Dose; MED, Minimum Efficacious Dose; *i.v*, Intravenous Injection; PK/PD, Pharmacokinetic/Pharmacodynamic, rhIL-15, Recombinant Human Interleukin-15; SQ/*s.c*, Subcutaneous Injection; PBMCs, Peripheral Blood Mononuclear Cells; NCI, National Cancer Institute; DLT, Dose Limiting Toxicity; DCs, Dendritic Cells; NIH, National Institutes of Health; Corp., Corporation; RD, Recommended Dose; BCG, Bacillus Calmette-Guerin; iNHL, Indolent B Cell Non-Hodgkin Lymphoma; hetIL-15, IL-15/sIL-15Rα; LLC., Limited Liability Company; HIV/AIDS, Human Immunodeficiency Virus and Acquired Immune Deficiency Syndrome; NIAID, National Institute of Allergy and Infectious Diseases.

CHAPTER 2

HYDRODYNAMIC DELIVERY OF INTERLEUKIN 15 GENE PROMOTES RESISTANCE TO HIGH FAT DIET-INDUCED OBESITY, FATTY LIVER AND IMPROVES GLUCOSE HOMEOSTASIS

Hao Sun and Dexi Liu. (2015).

Gene Therapy; **22**: 341-347.

2.1. ABSTRACT

The objective of this study is to examine the effect of hydrodynamic delivery of plasmid containing *Il-15* gene on high fat dietinduced obesity and obesity-associated metabolic disorders. We demonstrate that *Il-15* gene transfer results in multiple beneficial effects, including blockade of weight gain, alleviation of fatty liver and improvement in glucose homeostasis in mice. These effects are accompanied by suppressed expression of genes involved in lipogenesis and gluconeogenesis including *Scd-1*, *Fas*, *Pdk4*, *Pepck* and *G6p*, and enhanced expression of genes responsible for lipolysis and glucose metabolism such as *Cpt1-α*, *Cpt1-β*, *Acadm*, *Acadl* and *Glut-4*. Collectively, our results suggest that *Il-15* gene transfer is an effective approach in preventing diet-induced obesity and obesity-associated complications.

2.2. INTRODUCTION

Obesity is a major risk factor in the development of several diseases including diabetes, cardiovascular diseases, metabolic disorders and cancer [145, 146]. With an increasing prevalence of obesity, physical exercise is often recommended as a means of effectively preventing weight gain or losing weight for people who are obese [147]. At the molecular level, muscle contraction is associated with release of cytokines such as interleukin 6 (IL-6), IL-8 and IL-15 that work to send signals to the liver and adipose tissue for glycolysis and lipolysis, generating glucose to support muscle activities. While the detailed mechanism on how these cytokines work remains illusive and controversial, exercise-induced IL-6 is believed to suppress inflammation by increasing cytokine inhibitors such as IL-1 receptor antagonist and soluble tumor necrosis factor-α receptors, and triggering the release of the major anti-inflammatory cytokine IL-10 [148]. Exercise induced IL-8, on the other hand, serves as a potent angiogenic factor that signals the

need for building more blood vessels in muscle [149]. Different from IL-6 and IL-8, muscle-released IL-15 works by interacting with transcription factor such as peroxisome proliferator activated receptor to enhance lipolysis and reduce the adipose tissue size [150].

In the past, IL-15 has been considered an anti-obesity cytokine although its therapeutic potential has not been demonstrated [151]. Evidence supporting the role of IL-15 in lipid metabolism and obesity is accumulating. Yang *et al.* have shown that IL-15 level is markedly lower in obese than control rats [152]. Studies of *Il-15* knockout mice showed a higher fat mass than wild-type animals [90]. Similarly, *Il-15* transgenic mice exhibit lower body weight and resistance to high fat diet (HFD)-induced obesity [150]. In addition, *Il-15* transgenic mice ran twice as long as littermate control in a run-to-exhaustion trial and preferentially used fat for energy metabolism [153].

In this study, we assessed the activity of IL-15 in blocking HFD-induced obesity, insulin resistance and fatty liver development. Using a well-established gene transfer technique to overexpress *Il-15* gene in mice fed a HFD, we demonstrate that *Il-15* gene transfer results in sustained *Il-15* expression and blocked HFDinduced obesity and obesity-associated metabolic diseases. Our results suggest that *Il-15* gene transfer is an effective approach in blocking HFD-induced obesity, and development of insulin resistance and liver steatosis.

2.3. MATERIALS AND METHODS

2.3.1. Plasmid vectors

The pLIVE plasmid vector was purchased from Mirus Bio (Madison, WI), and either mouse IL-15 *(mIl-15*) or secreted embryonic alkaline phosphatase (*SEAP)* gene was cloned into the pLIVE vector. *Il-15* gene fragment was inserted into multi-cloning sites of the pLIVE vector

created by restriction digestion of *Sac I* and *Xho I*. Plasmid constructs were confirmed by DNA sequencing (University of Georgia Genomics Facility). The plasmids were isolated using the method of cesium chloride density gradient centrifugation (spun twice) and kept in saline at − 80 ℃ until use. Lack of endotoxin in plasmid preparation was confirmed by enzyme-linked immuno sorbent assay (ELISA) using the ELISA kit from eBioscience, Inc. (San Diego, CA, USA). Optical density determination (260 and 280 nm) and 1% agarose gel electrophoresis were conducted to verify the purity of the plasmid preparations.

2.3.2. Animals and animal procedure

Male C57BL/6 mice (9 weeks old, 24~26 g) were purchased from Charles River Laboratories (Wilmington, MA) and housed under standard conditions with a 12 h-12 h light-dark cycle. The HFD (60% kcal from fats, 20% from carbohydrates and 20% from proteins) was purchased from Bio-Serv (Frenchtown, NJ; #F3282). Mice were fed continuously for 9 weeks and body weight, body composition, and food intake were measured weekly. Blood and various tissue samples were collected after sacrificing the mice for biochemical and histological examinations. All animal experiments were approved by the Institutional Animal Care and Use Committee at the University of Georgia, Athens, Georgia (protocol number, A2011 07-Y2-A3).

Hydrodynamic gene delivery of either pLIVE-SEAP plasmid (control) or pLIVE-IL-15 plasmids was performed on days 1 and 31 when animals were fed a selected diet. Briefly, 9% body weight of saline solution containing 10 μg of plasmid DNA was injected into mouse tail vein within 5-8 seconds [154]. Mouse IL-15 levels in serum were quantified using IL-15 Duoset ELISA kit (R&D Systems, Minneapolis, MN, USA).

2.3.3. Gene expression analysis by real time PCR

Total RNA was isolated from the mouse liver and muscle using TRIzol reagents from Invitrogen (Carlsbad, CA). Reverse transcription polymerase chain reaction (RT-PCR) was conducted using commercial kits from OriGene (Rockville, MD). Real time PCR (qPCR) was performed using SYBR Green as detection reagent on the ABI StepOne Plus Real-Time PCR system[155]. GAPDH mRNA was used as an internal control, and all primers (Table 2.1) were ordered from Sigma (St. Louis, MO, USA). A melting curve analysis of all quantitative PCR products was performed and showed a single DNA duplex.

2.3.4. Determination of plasma concentration of alanine transaminase (ALT) and aspartate transaminase (AST)

Blood samples were collected from heart cavities immediately after euthanizing mice. Serum was isolated by centrifugation at 5,000 r.p.m for 5 min. ALT and AST concentrations were determined using commercial kits from Thermo Scientific (Middletown, VA, USA), following the manufacture's instruction.

2.3.5. Determination of liver TG level

The procedure was performed according to the Folch method [156]. Briefly, liver samples (~ 150 mg) were homogenized in a mixture of chloroform and methanol (2:1, volume ratio). Tissue homogenates were incubated at 4 ℃ overnight and centrifuged at 12,000 r.p.m for 20 min. The supernatants were air dried and re-dissolved in 3% Triton-isopropanol. The amounts of liver TG were determined using a commercial kit from Thermo-Scientific.

2.3.6. Evaluation of glucose homeostasis

Intraperitoneal glucose tolerance test (IPGTT) and insulin tolerance test (ITT) were carried out 1 week before the end of the experiments. For IPGTT, mice were fasted for 6 h and glucose in 0.9% saline was injected (*i.p.*) at 2 g kg^{-1}, with the time point was set as 0 min. Blood glucose levels were measured at 0, 30, 60, and 120 min using glucose test strips and glucose meters. The same group of animals was allowed to rest for 2 days after IPGTT. For ITT, animals were fasted for 4 h and insulin (Humulin) from Eli Lilly (Indianapolis, IN, USA) was injected (*i.p.*) at a dose of 0.75 U kg^{-1}, and blood glucose was measured in a time course identical to IPGTT. Insulin levels in the blood were measured using a commercial ELISA kit (Mercodia Developing Diagnostics, Winston Salem, NC, USA). Insulin resistance (HOMA-IR) was calculated using the following formula: HOMAIR = (fasting insulin (ng ml− 1) × fasting plasma glucose (mg dl − 1)/405).

2.3.7. H&E staining

The samples from livers, WATs and BATs, were fixed in 10% neutral buffered formalin and then underwent gradient dehydration, paraffin embedding and tissues sectioning (5 μm). The sections were dried at 37 ℃ for at least one hour and stained with hematoxylin and eosin (H&E) with a commercial kit (BBC Biochemical, Atlanta, GA). The diameters of adipocytes in WATs were measured using the NIS-Elements imaging platform (Nikon Instruments Inc, Melville, NY).

2.3.8. Oil-red O staining

Fresh liver samples were immediately harvested from killed animals and frozen in liquid nitrogen. Frozen sections were made at eight μm using a cryostat, fixed in 10% neutral buffered formalin for 30 min and rinsed with phosphate-buffered saline solutions. The tissue sections were then stained with the freshly prepared Oil-red O working solution (Electron Microscopy Sciences, Hatfield, PA, USA) for 30 min and hematoxylin for 1 min, accompanied by a washing step (60% isopropanol for 5 min) before each staining. Microscopic examination (Nikon Instrument Inc.) was performed on tissue slides, and selected structures were photographed.

2.3.9. Statistical Analysis

All statistical analyses were performed using GraphPad Prism (GraphPad Software, La Jolla, CA, USA). Data were expressed as mean ± s.d. (n = 5). Results were analyzed using one-way analysis of variance, with a P-value of below 0.05 ($P<0.05$) considered as statistically different.

2.4. RESULTS

2.4.1. Hydrodynamic gene transfer resulted in elevated mRNA levels of Il-15 in the liver and increased serum concentrations of IL-15 protein in HFD feeding mice

Two hydrodynamic tail vein injections of pLIVE-mIL-15 or pLIVE SEAP plasmids were performed on days 1 and 31, respectively, on C57BL/6 mice on a HFD. Relative mRNA levels at the end of the 9-week feeding period were examined and showed ~ 54-fold higher in the liver, but not in the muscle (Figure 2.1a), confirming the liver specificity of the hydrodynamic

procedure of gene delivery [154, 157]. The IL-15 protein level was ~ 420 pg ml− 1 in the blood (Figure 2.1b). No significant increase in serum concentrations of liver-specific enzymes either ALT (Figure 2.1c) or AST (Figure 2.1d) was observed, indicating absence of liver damage.

2.4.2. Il-15 gene transfer blocked HFD-induced obesity in mice

The effect of *Il-15* gene delivery on diet-induced obesity was examined. Mice that received secreted *SEAP* gene transfer showed a significant increase in body weight as early as 3 weeks when fed a HFD, compared with animals fed a HFD and injected with the *Il-15* gene (Figure 2.2a). At the end of the 9-week HFD feeding, the *SEAP* gene injected control mice showed an average body weight of 39.8 ± 2.0 g, about 10 g higher than mice injected with *Il-15* gene (29.0 ± 2.4 g), almost identical to mice fed a regular chow (29.4 ± 1.8 g). The size difference among the three groups of mice is visually differentiable (Figure 2.2b). Body composition analysis using the EchoMRI-100 system (EchoMRI, Houston, TX, USA) showed that *Il-15* gene transfer, compared with chow-fed regular mice, blocked the fat mass gain without changing lean mass (Figures 2.2c and d). No significant difference was seen in average energy intake among the animals (Figure 2.2e). Together, these results demonstrate that hydrodynamic delivery of *Il-15* gene completely blocked HFD-induced obesity.

2.4.3. Il-15 gene transfer suppressed hypertrophy in adipocytes

To explore the impact of *Il-15* gene transfer on morphological change in adipocytes, we collected adipose tissue from the control and IL-15-treated mice. The average size of adipocytes (Figure 2.3a) and weight of fat pads (Figure 2.3b) were measured and showed a significant difference in epididymal, inguinal, and perirenal white adipose tissues, and brown adipose tissue

(BAT) between HFD-fed control and IL-15-treated mice. Compared to control mice injected with pLIVE-SEAP plasmid, hematoxylin and eosin (H&E) staining of white adipose tissue shows *Il-15* gene transfer significantly suppressed HFD-induced enlargement of adipocytes in epididymal, perirenal, and inguinal white adipose tissues, and fat accumulation, judging by size and number of vacuoles in BAT (Figure 2.3c). The average diameter of adipocytes in HFD-fed control mice is 89.8 ± 9.9 μm, compared to 52.5 ± 8.6 μm in IL-15-treated mice and 44.7 ± 6.3 μm in mice fed a regular chow (Figure 2.3d). No significant difference was observed between animals fed a regular chow and HFD with *Il-15* gene transfer.

2.4.4. Il-15 gene transfer prevented HFD-induced fatty liver

Excessive fat deposition in the liver is one of the major physiological changes associated with obesity. Therefore, we examined the effect of *Il-15* gene delivery on lipid accumulation in the liver. Mice transferred with the *Il-15* gene showed lower liver weights compared with those of HFD-fed control (Figure 2.4a). Histological images showed more vacuoles in liver sections of HFD-fed control mice (Figure 2.4b). Oil-red O staining confirmed a significant presence of lipid droplets (Figure 2.4b) in HFD-fed control mouse liver and *Il-15* gene transfer blocked HFD-induced lipid accumulation in the liver. Biochemical quantitation showed lower levels of TG in the liver of IL-15-treated mice (Figure 2.4c). Again, there is no statistical difference between IL-15-treated mice and those fed a regular chow.

2.4.5. Il-15 gene transfer modulates transcription of genes involved in lipid metabolism

To investigate how *Il-15* gene transfer reduced excessive lipid accumulation in HFD-fed animals, we measured mRNA levels of genes in the liver and the muscle involved in *de novo*

lipogenesis and lipolysis. We first compared mRNA levels of genes with known functions for lipogenesis including *Scd-1, Fas* and *Acc-1*. HFD feeding increased the expression of *Scd-1* and *Fas* in muscle by ~ 8.6- and ~ 3.1-folds, respectively (Figure 2.5a). *Il-15* gene transfer significantly reduced mRNA levels of the same set of genes in the muscle by ~ 58.6% and ~ 51.1%, as well as ~ 63.7% and ~ 49.4% in the liver (Figures 2.5a and b). mRNA levels of *Acc-1* did not change in the muscle or liver. Next, we evaluated mRNA levels of critical genes for fatty acid β oxidation in both muscle and liver. HFD-fed mice received *Il-15* gene transfer showed a slight, but significant increase in mRNA levels of *Cpt1-α* (~2.2-fold), *Cpt1-β* (~2.1-fold), *Acadm* (liver: ~ 1.7-fold; muscle: ~ 1.4-fold) and *Acadl* (liver: ~ 1.8- fold; muscle: ~ 1.4-fold) compared with HFD-fed control mice received control plasmid (Figures 2.5c and d).

2.4.6. Il-15 gene transfer protected mice from HFD-induced hyperinsulinemia and hyperglycemia

Obesity is a known risk factor in developing insulin resistance, one characteristic of type-2 diabetes. We then conducted an IPGTT and ITT to investigate whether mice transferred with the *Il-15* gene show an improvement in glucose metabolism. *Il-15* gene transfer decreased fasting glucose (~148mg dl− 1) levels compared with HFD-fed control mice (~222 mg dl− 1) (Figure 2.6a). Mice fed a HFD for 8 weeks become glucose intolerant judging by IPGTT (Figure 2.6b). The calculated area under the curve (AUC) of IPGTT showed that HFD fed mice transferred with the *Il-15* gene exhibited normal glucose sensitivity comparable to that of control animals fed a regular diet (Figure 2.6c). Blood insulin levels in mice fed a chow diet, HFD with injection of control plasmids, and those fed a HFD with *Il-15* gene transfer were ~ 2.2, ~ 6.2 and ~ 1.6 ng ml− 1, respectively (Figure 2.6d). Similarly, results from ITT showed HFD-fed control

mice developed insulin resistance (Figure 2.6e) and in contrast, ITT and calculated homeostasis model assessment of insulin resistance (HOMA-IR) suggested that IL-15-treated mice have normal insulin sensitivity comparable to animas fed a regular chow (Figures 2.6e and f).

2.4.7. Il-15 gene transfer affects the expression of critical genes involved in glucose metabolism

To investigate how *Il-15* gene transfer maintained glucose homeostasis, we measured the mRNA levels of genes involved in glucose metabolism in the liver and the muscle. Expression of *Pdk4*, a key gene involved in repressing glucose oxidation, was increased in HFD-fed control mice in the liver, while *Il-15 gene* transfer significantly reduced its mRNA levels by ~ 33.5% (Figure 2.7a). Expressions of genes involved in gluconeogenesis, such as *Pepck* and *G6p*, were decreased in IL-15-treated mice by ~ 29.8% and 41.8%, respectively (Figure 2.7a). Expression of *Glut-4*, a critical gene involved in glucose transportation, was reduced in HFD fed control mice in muscle. However, mice transferred with the *Il-15* gene slightly, but significantly enhance the mRNA levels of *Glut-4* by ~ 1.8 folds (Figure 2.7b).

2.5. DISCUSSION

Exercise associated factors, including IL-15, have remarkable roles in glucose and lipid metabolism and energy expenditure [151, 158]. Our group has previously shown that hydrodynamic injection of the *FGF-21* gene alleviated obesity and fatty liver in mice fed a HFD [159]. In the present work, we demonstrate that *Il-15* gene transfer generates a higher serum concentration of IL-15 during the 9-week experimental time period (Figure 2.1), resulting in a blockade of HFD-induced obesity and alleviation of obesity-related hepatic fat accumulation and glucose

intolerance (Figures 2.2-2.4 and 2.6). Mechanistically, these beneficial effects were accompanied with suppressed expression of genes involved in de novo lipogenesis and gluconeogenesis, as well as increased expression of genes involved in lipolysis and glucose transport (Figures 2.5 and 2.7).

Accumulating evidence suggests IL-15 has direct effect on adipose tissue. A previous study by Carbo *et al.*15 demonstrates that 7 days administering IL-15 to adult rats led to a 33% decrease in white adipose tissue, suggesting an anti-adipogenic role of the IL-15 [92]. These observations were confirmed using different types of mammalian adipogenic cell lines, including human derived cells [90, 91, 93]. Moreover, IL-15 administration was able to inhibit pre-adipocyte differentiation and lipid deposition[91, 160-162]. In agreement with previous reports, we observed that *Il-15* gene transfer blocked HFD-induced weight (Figure 2.2a) and fat mass gain (Figure 2.2c). Meanwhile, results from a histological analysis revealed a smaller diameter of adipocytes in the white adipose tissue and less lipid accumulation in the liver (Figures 2.3c and 2.4b). These results suggest that the function of IL-15 involves a blockade of adipogenesis.

Previous studies identified IL-15 as a key regulator for enhancing lipid oxidation and suppressing *de novo* lipogenesis. Using a primary pig model, Ajuwon *et al.* have shown that IL-15 directly targeted adipocytes through lipolysis and lipogenesis [93]. Similarly, Lopez-Soriano *et al.* demonstrated that daily injections of IL-15 reduced activity of lipogenic enzyme, such as ACC and FAS, leading to decreased lipogenic rate and carcass fat [163]. Consistent with these findings, we observed *Il-15* gene transfer repressed expression of *Scd-1* and *Fas* genes in the liver and the muscle, which are involved in *de novo* lipogenesis (Figures 2.5a and b). However, we did not observe a significant change in *Acc* gene expression. Moreover, *Il-15* gene transfer in mice fed a HFD increased transcription of several key genes for lipid oxidation, including *Cpt1-*

α, Cpt1-β, Acadm, Acadl (Figures 2.5c and d), leading to a corresponding alleviation of adipocyte deposition and fatty liver (Figures 2.3 and 2.4).

IL-15 also plays important roles in maintaining glucose homeostasis by facilitating glucose uptake in skeletal muscle. Previous studies by Busquets *et al*. demonstrate that IL-15 stimulates glucose uptake in skeletal muscle by increasing *Glut-4* expression both *in vivo* and *in vitro* [106]. Barra *et al.* provided compelling evidence showing IL-15 treatment is able to improve glucose homeostasis and insulin sensitivity in diet-induced obese mice [107]. Consistent with these previous reports, our data clearly show that *Il-15* gene transfer markedly reduced insulin resistance and improved glucose tolerance in mice fed an HFD (Figure 2.6). In addition, expression of the genes involved in glucose metabolism including *Pdk4, Pepck,* and *G6p* was decreased in the liver of mice with over expression of *Il-15* (Figure 2.7a). *Glut-4*, a critical gene involved in glucose transportation was upregulated in muscle (Figure 2.7b).

In summary, in this study, we demonstrate that hydrodynamic delivery of *Il-15* gene brought a variety of beneficial effects in diet-induced obesity and its complications, including suppression of adiposity, alleviation of fatty liver and improvement of insulin resistance. Our findings indicate that *Il-15* gene transfer could be an effective approach in preventing HFD-induced obesity and obesity-associated fatty liver and insulin resistance.

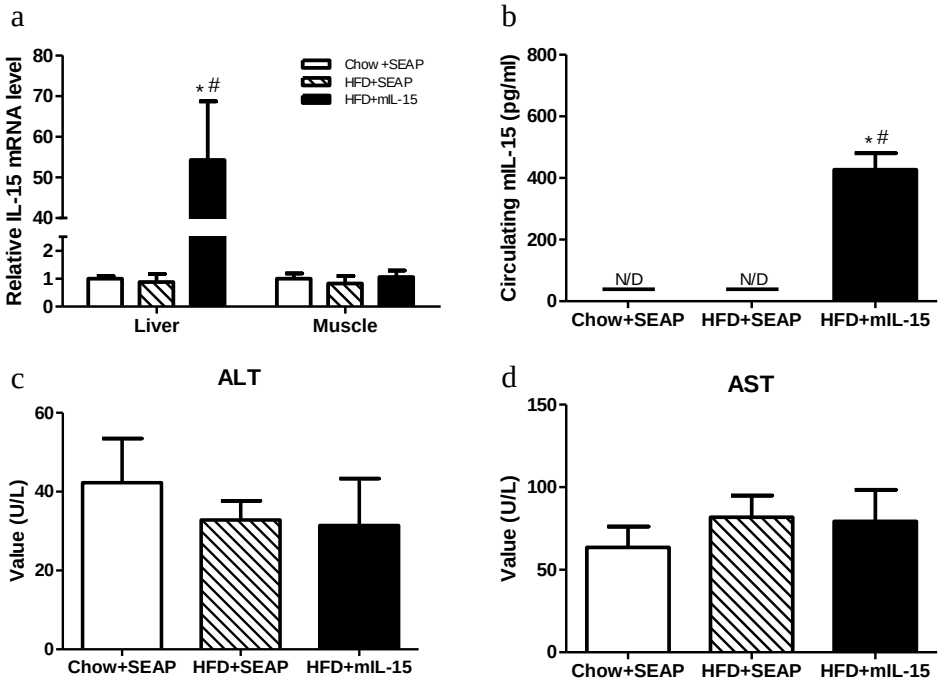

Figure 2.1. Assessment of *Il-15* gene expression after hydrodynamic delivery. Mice were hydrodynamically injected with pLIVE-IL-15 or pLIVE-SEAP plasmids and fed with selected diet for 9 weeks and IL-15 mRNA level in different organs and blood concentration of IL-15 protein were determined. (**a**) mRNA levels of IL-15 in the liver and muscle; (**b**) blood concentration of IL-15 protein; (**c**) blood concentration of alanine aminotransferase (ALT); and (**d**) blood concentration of aspartate aminotransferase (AST). (□) Mice fed a chow diet injected with pLIVE-SEAP; (▩) Mice fed a HFD and injected with pLIVE-SEAP; (■) Mice fed a HFD and injected with pLIVE-IL-15. Data represent mean ± SD (n=5). * $P<0.05$ compared with chow diet group, # $P<0.05$ compared with HFD-fed mice injected with pLIVE-SEAP plasmids.

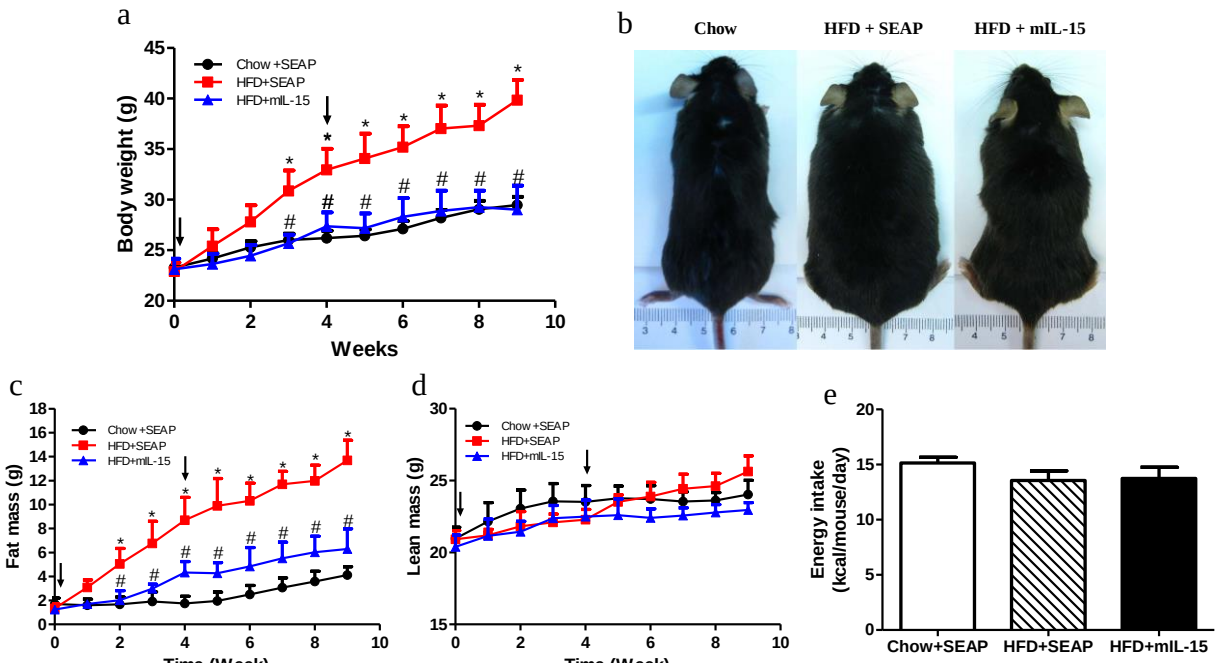

Figure 2.2. *Il-15* gene transfer blocked HFD-induced weight gain in mice. (**a**) Time dependent growth curve; (**b**) Representative images of regular diet-fed animals injected with pLIVE-SEAP (left), HFD-fed animals injected with pLIVE-SEAP (middle), and HFD-fed animals injected with pLIVE-IL-15; (**c**) Time dependent fat mass; (**d**) Time dependent lean mass; and (**e**) Time dependent energy intake. (●) Animals fed a regular chow injected with pLIVE-SEAP plasmid. (■) Animals fed a HFD and injected with pLIVE-SEAP plasmid; (▲) Animals fed a HFD and injected with pLIVE-IL-15. Data represent mean ± SD (n=5). * P<0.05 compared with animals fed a chow diet; # P <0.05 compared with mice fed a HFD and injected with pLIVE-SEAP.

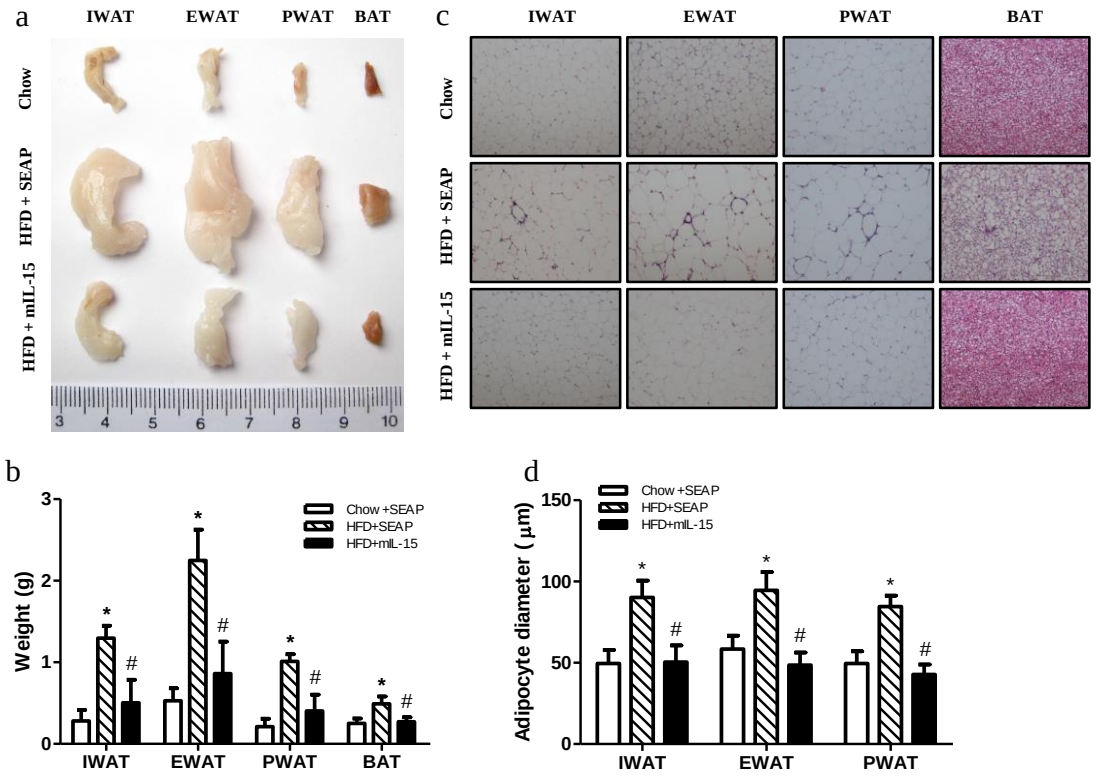

Figure 2.3. *Il-15* gene transfer suppressed hypertrophy in adipose tissue. (**a**) A representative image of different adipose tissues; (**b**) Weight of fat pads; (**c**) Images of H&E staining of IWAT, EWAT, PWAT and BAT; (**d**) Average diameter of adipocytes in WAT calculated from 500 randomly selected cells from 5 tissue slides. IWAT: inguinal white adipose tissue; EWAT: epididymal white adipose tissue; PWAT: perirenal white adipose tissue; BAT: brown adipose tissue. (□) Mice fed a chow diet and injected with pLIVE-SEAP; (▩) Mice fed a HFD and injected with pLIVE-SEAP; (■) Mice fed a HFD and injected with pLIVE-IL-15. Data represent mean ± SD (n=5). * $P<0.05$ compared with animas fed a chow diet, # $P<0.05$ compared with mice fed a HFD and injected with pLIVE-SEAP plasmids.

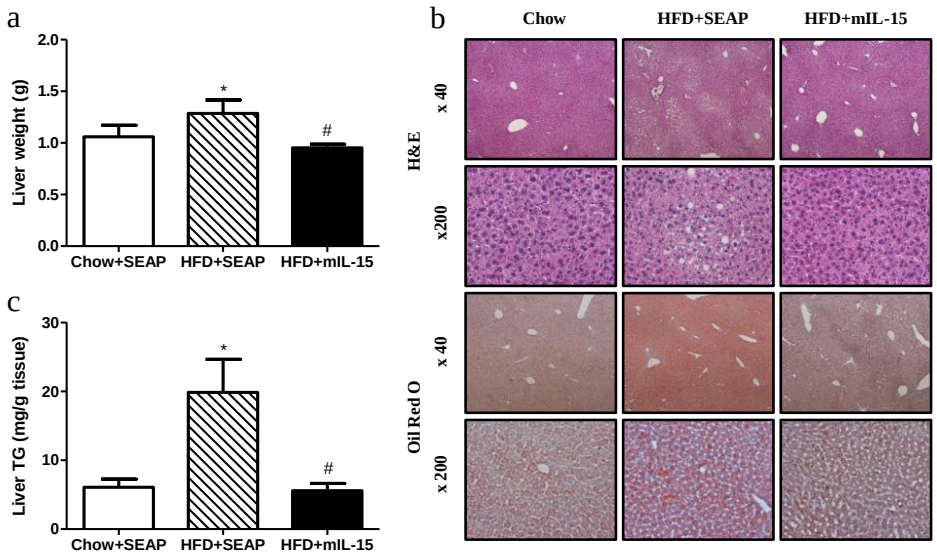

Figure 2.4. *Il-15* gene transfer prevented HFD-induced fatty liver. (**a**) Liver weight; (**b**) Representative images of H&E and oil-red O staining of the liver sections; (**c**) Relative triglyceride level in the liver. TG: triglyceride. (□) Mice fed a chow diet and injected with pLIVE-SEAP; (▩) Mice fed a HFD and injected with pLIVE-SEAP; (■) Mice fed a HFD and injected with pLIVE-IL-15. Data represent mean ± SD (n=5). * $P<0.05$ compared with animals fed a chow diet group, # $P<0.05$ compared with mice fed a HFD and injected with pLIVE-SEAP plasmid.

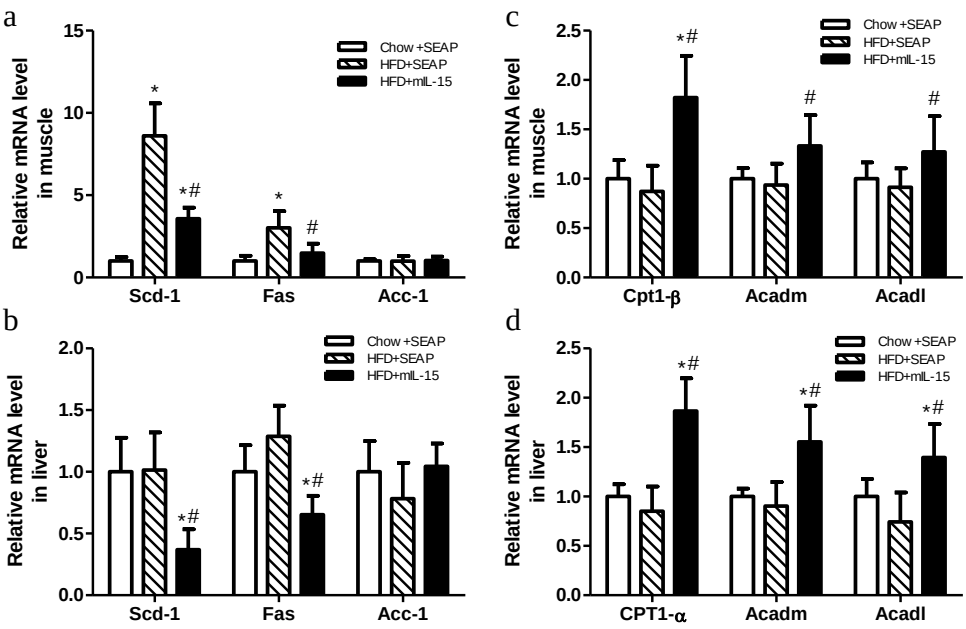

Figure 2.5. ***Il-15*** **gene transfer modulates transcription of genes involved in lipid metabolism.** (**a**) Relative mRNA levels of genes involved in *de novo* lipogenesis in muscle; (**b**) Relative mRNA levels of genes involved in *de novo* lipogenesis in liver; (**c**) Relative mRNA levels of genes involved in fatty acid β oxidation in the muscle; (**d**) Relative mRNA levels of genes involved in fatty acid β oxidation in the liver. (□) Mice fed a chow diet injected with pLIVE-SEAP plasmids; (▩) Mice fed a HFD injected with pLIVE-SEAP plasmids; (■) Mice fed a HFD and injected with pLIVE-IL-15. Data represent mean ± SD (n=5). * P <0.05 compared with animals fed a chow diet group, # P <0.05 compared with mice fed a HFD and injected with pLIVE-SEAP plasmids.

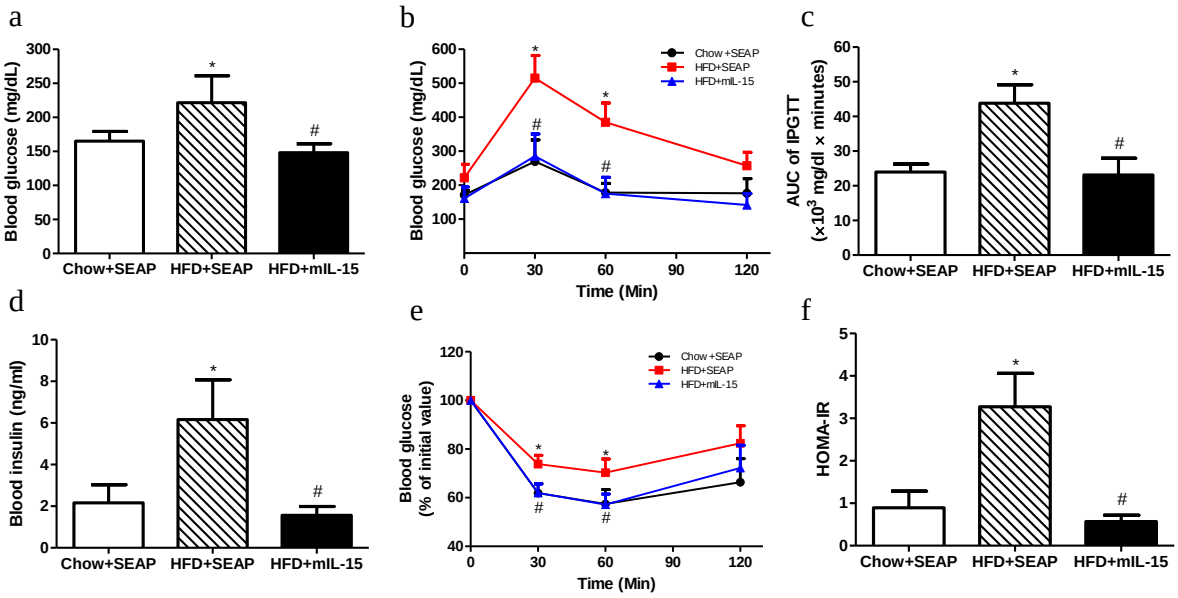

Figure 2.6. ***Il-15*** **gene transfer protected mice from HFD-induced hyperinsulinemia and hyperglycemia.** (**a**) Fasting blood glucose level; (**b**) Time dependent change of blood glucose concentration in IPGTT; (**c**) AUC of IPGTT; (**c**) Fasting blood insulin level; (**d**) Time dependent change of blood glucose concentration in ITT; (**e**) Results of HOMA-IR analysis for insulin resistance. IPGTT: intraperitoneal glucose tolerance test, AUC: area under curve, ITT: insulin tolerance test, HOMA-IR: Homeostasis model assessment of insulin resistance. (●) Animals fed a regular chow and injected with pLIVE-SEAP plasmid. (■) Animals fed a HFD and injected with pLIVE-SEAP plasmids; (▲) Animals fed a HFD and injected with pLIVE-IL-15 plasmids. (□) Mice fed a chow diet and injected with pLIVE-SEAP; (▩) Mice fed a HFD and injected with pLIVE-SEAP; (■) Mice fed a HFD and injected with pLIVE-IL-15. Data represent mean ± SD (n=5). * P<0.05 compared with animals fed a chow diet, # P<0.05 compared to mice fed a HFD and injected with pLIVE-SEAP plasmids.

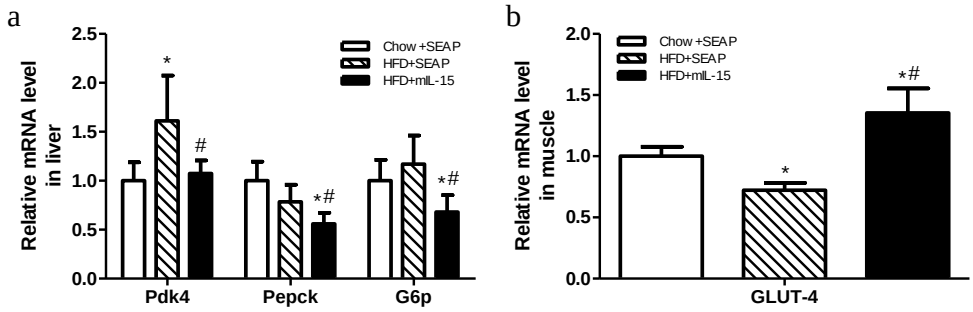

Figure 2.7. ***Il-15*** **gene transfer affects the expression of critical genes involved in glucose metabolism** (**a**) Relative mRNA levels of genes involved in glucose metabolism in liver; (**b**) Relative mRNA levels of *Glut-4* gene in muscle. (□) Mice fed a chow diet and injected with pLIVE-SEAP plasmids; (▩) Mice fed a HFD and injected with pLIVE-SEAP; (■) Mice fed a HFD and injected with pLIVE-IL-15 plasmids. Data represent mean ± SD (n=5). * $P<0.05$ compared with animals fed a chow diet, # $P<0.05$ compared with animals fed a HFD and injected with pLIVE-SEAP plasmids.

Table 2.1. Primer sequences for real time PCR analysis of gene expression

Gene	Forward primer sequence	Reverse primer sequence
Acadm	GGGTTTAGTTTTGAGTTGACGG	CCCCGCTTTTGTCATATTCCG
Acadl	TCTTTTCCTCGGAGCATGACA	GACCTCTCTACTCACTTCTCCAG
Acc-1	ATGGGCGGAATGGTCTCTTTC	TGGGGACCTTGTCTTCATCAT
Cpt1α	CTCCGCCTGAGCCATGAAG	CACCAGTGATGATGCCATTCT
Cpt1β	GCACACCAGGCAGTAGCTTT	CAGGAGTTGATTCCAGACAGGT
Fas	GGAGGTGGTG ATAGCCGGTAT	TGGGTAATCCATAGAGCCCAG
G6p	CGACTCGCTATCTCCAAGTGA	GTTGAACCAGTCTCCGACCA
Glut4	GTGACTGGAACACTGGTCCTA	CCAGCCACGTTGCATTGTAG
IL-15	AAAGCTTTATACGCATTGTCCAAAT	CATGCAGTCAGGACGTGTTGAT
Pdk4	AGGGAGGTCGAGCTGTTCTC	GGAGTGTTCACTAAGCGGTCA
Pepck	CTGCATAACGGTCTGGACTTC	CAGCAACTGCCCGTACTCC
Scd1	TTCTTGCGATACACTCTGGTGC	CGGGATTGAATGTTCTTGTCGT

CHAPTER 3

IL-15/sIL-15Rα GENE TRANSFER INDUCES WEIGHT LOSS AND IMPROVES GLUCOSE HOMEOSTASIS IN OBESE MICE

Hao Sun, Yongjie Ma, Mingming Gao and Dexi Liu. (2016).

Gene Therapy, **23**: 349-356.

3.1. ABSTRACT

Obesity and its associated metabolic problems are a major public health issue. The objective of the current study is to investigate the therapeutic effect of IL-15/sIL-15Rα on high fat diet induced obesity and obesity-associated metabolic disorders. We demonstrate that the multiple hydrodynamic delivery of 2 μg IL-15/sIL-15Rα plasmid results in numerous beneficial effects, including a reduction of body weight and fat mass, an alleviation of fatty liver, an improvement in glucose homeostasis, and insulin sensitivity in obese mice. These effects are accompanied by a suppressed mRNA level of genes involved in lipid accumulation and lipogenesis, including *Pparγ, Cd36, Fabp4, Mgat1, Scd-1* and *Fas*, and an elevated gene expression for adaptive thermogenesis and fatty acid β oxidation, such as *Ucp1, Ucp3, Pgc-1α, Pgc-1β, Pparα, Pparδ, Cpt1-α* and *Cpt1-β* in obese animals. These results suggest that the overexpression of the *Il-15/sIl-15Rα* gene is an effective approach in treating diet-induced obesity and its associated metabolic complications.

3.2. INTRODUCTION

The high prevalence of obesity in children and adults represents a major public health problem worldwide[146, 164]. Regular exercise and physical activities are common strategies to manage obesity and its associated chronic conditions, including hypertension, coronary heart disease, type 2 diabetes mellitus, and age-related muscle wasting [165]. The molecular basis for an exercise-based strategy is that following physical activity several "myokines," most notably interleukin (IL)-6, IL-10, IL-15 and fibroblast growth factor (FGF)-21, are released from skeletal muscle resulting in a positive endocrine effect on body composition [99, 166, 167]. IL-6 and FGF-21 are shown to enhance adaptive thermogenesis in adipose tissue by consuming energy as heat

through uncoupling adenosine triphosphate production, and thus exert a beneficial effect on body fat utilization [159, 168]. IL-10, an anti-inflammatory cytokine, works to modulate obesity-induced low-grade inflammation and to regulate metabolic homeostasis [169]. IL-15, originally characterized as a stimulator for T and nature killer (NK) cell development [4, 170], functions as a circulating regulator of body composition. In a recent study, Nielsen *et al.* showed a negative association between circulating IL-15 levels and body-mass index, total fat, trunk fat, and limb fat mass in humans [138]. In pre-clinical studies, mice with targeted deletion of IL-15 showed higher level of body fat than did wild-type mice [90]. Whereas, IL-15 transgenic mice, engineered for elevated plasma concentrations of IL-15, exhibited lower body fat and resistance to diet-induced obesity [150]. Using adipogenic cell cultures, several studies have shown activity of IL-15 in inhibiting lipogenesis and increasing lipolysis [89-91, 93].

Different from other myokines, such as IL-6 that are secreted directly from skeletal muscle into blood circulation, IL-15 and soluble IL-15 receptor alpha (IL-15Rα) interact intracellularly with high affinity forming IL-15/sIL-15Rα complexes that are subsequently secreted into blood circulation [171]. IL-15 stays in blood circulation as a complex with increased stability and circulation half-life [172, 173]. The signal transduction of IL-15 is achieved through interactions of receptor complexes consisting of IL-15Rα, IL-2Rβ, and IL-2Rγ [174]. The IL-2Rβ and IL-2Rγ subunits are expressed on various cell types and responsible for signal transduction, while IL-15Rα has a high binding affinity to the receptor complexes [174]. At a molecular level, IL-15/sIL-15Rα complexes are the biologically active form of IL-15.

Our previous study successfully demonstrated the activity of IL-15 in blocking high fat diet (HFD)-induced obesity, insulin resistance and fatty liver development using the well-established hydrodynamic gene transfer technique [175]. Here, using the same technique, we

assessed the effect of IL-15/sIL-15Rα on reducing the body weight of obese mice and obesity-associated metabolic disorders. We demonstrated that *Il-15/sIl-15Rα* gene transfer is effective in inducing weight loss of obese mice and improves glucose homeostasis and insulin sensitivity.

3.3. MATERIALS AND METHODS

3.3.1. Plasmids

AG209 DP muIL-15sRα+IL-15 plasmids carrying mouse *IL-15/sIL15-Rα* genes were provided from Dr. Barbara K Felber (NCI) [171]. The plasmid was constructed with pCMV-kan backbone, which contains simian and human dual CMV promoters, the bovine growth hormone (BGH) polyadenylation site, and the kanamycin resistance gene [176-178]. The expression of mouse IL-15 gene was driven by simian CMV promoter and the IL-15 sequence was codon-optimized by removing RNA processing and instability sequences and substituted with the leader sequence from the mouse granulocyte-macrophage colony-stimulating factor (GM-CSF). The soluble form of mouse IL-15Rα (sIL-15Rα, amino acids 1–205) was expressed from the human CMV promoter and sIL-15Rα sequence was codon-optimized by introducing multiple silent point mutations, which resulted in enhanced stability of mRNA. All coding sequences were verified by sequencing. The mouse IL-15 and sIL-15Rα proteins are corresponding to GenBankTM accession number and NP-032383 and NP-032384. The DNA plasmids were isolated using endotoxin free preparation procedures through cesium chloride-ethidium bromide gradient ultracentrifugation and kept in saline at −80°C until use. Purity of the plasmid preparations was determined by optical density (260 and 280 nm) and 1% agarose gel electrophoresis.

3.3.2. Animals and animal treatments

The animal studies were under the surveillance of Institutional Animal Care and Use Committee (IACUC, University of Georgia, Athens, GA) and were performed according to the experimental protocol (# A2014 07-008-Y1-A0). Male C57BL/6 mice (8-9 weeks old, 24~26 g) were used for all experiments (Charles River Laboratories, Wilmington, MA). The study animals were kept in a pathogen-free environment under a standard light-dark cycle condition. Obese mice (52 $\pm$ 2 g) were developed by feeding animals with a high fat diet (HFD) (60% kcal from fats, Bio-Serv Frenchtown, NJ; #F3282) for 20 weeks. Age-matched lean mice were kept on a regular chow diet (60% kcal from carbohydrates, LabDiet, St Louis, MO). The food consumption was measured by the difference between the amount provided and the amount left in three days. EchoMRI-100 system (EchoMRI, Houston, TX, USA) was used to measure the mouse body composition.

The hydrodynamic gene delivery was performed according to an established procedure with some modifications [159, 168]. Briefly, 2.0-2.5 ml saline solution (equivalent to 8% lean mass of a mouse) containing either 2 μg of AG209 DP muIL-15sRα+IL-15 plasmid or empty vector was injected through tail vein within 5-8 s. Mice were continuously fed a predetermined diet. Blood, body weight, body composition, and food intake were measured at the desired time points. Blood was collected using a Microvette-CB300-LH from Fisher Scientific (Pittsburgh, PA) at the desired time points and mouse IL-15/sIL-15 complex levels in serum were determined using ELISA kit (eBioscience, San Diego, CA). Mouse serum and various tissue samples were collected after euthanizing the mice for biochemical and histological examinations.

3.3.3. Histochemical, Oil Red O and Nile Red Examination

For histochemical examination using hematoxylin and eosin (H&E) staining, tissue samples from the liver, WAT and BAT were collected from the euthanized mice, fixed in 10% neutrally buffered formalin and embedded into paraffin. H&E staining was performed using tissue sections at a thickness of 5 μm with a commercial kit purchased from BBC Biochemical (Atlanta, GA). For Oil-red O and Nile red staining, frozen liver sections were made at 8 μm using a Cryostat and fixed in 10% neutrally buffered formalin for 30 min. These sections were stained with either 0.2% Oil Red O working solution (Electron Microscopy Sciences, Hatfield, PA) for 15 min, or Nile red working solution (Sigma, St. Louis, MO) for 5 min. Microscopic examination was performed using the NIS-Elements imaging platform from Nikon Instruments Inc. (Melville, NY).

3.3.4. Hepatic lipid analysis

A quantitative determination of hepatic lipids was performed using the Folch procedure [156]. Two to three hundreds micrograms of liver samples were homogenized in a 2:1 volume mixture of chloroform and methanol, and centrifuged at 4℃, 12,000 r.p.m. for 20 min. The lower phase was collected, and air dried. The lipids were then dissolved by the triton-isopropanol solution (3%). The hepatic triglyceride and cholesterol levels were further measured by a commercial kit (Thermo-Scientific, Middletown, VA)

3.3.5. Evaluation of glucose homeostasis and insulin sensitivity

The glucose response and insulin sensitivity were determined by insulin tolerance test (ITT) and intraperitoneal glucose tolerance test (IPGTT). The IPGTT is performed one week

before the end of the experiments, and mice were intraperitoneally (*i.p.*) injected with 2 g/kg glucose after hours fasting. Similarly, the ITT is carried out by injecting 0.75 U/kg insulin (Humulin from Eli Lilly, Indianapolis, IN) intraperitoneally to animals bearing 4 hours fasting. Blood glucose levels for both tests were determined using glucose test strips and glucose meters (Nipro Diagnostics Inc, Fort Lauderdale, FL) at the time of 0, 30, 60, and 120 min. Blood insulin level was determined using a commercial Insulin ELISA kit (Mercodia Developing Diagnostics, Winston Salem, NC). The HOMA-IR values were expressed based on the fasting glucose and insulin levels: HOMA-IR = (fasting insulin (ng/ml) × fasting plasma glucose (mg/dl)/405).

3.3.6. Gene expression analysis by real-time PCR

The mRNA level of target genes expression in mouse liver, muscle, WAT, and BAT was determined by the ABI StepOne Plus Real-Time PCR system. Briefly, TRIzol reagents (Invitrogen, Carlsbad, CA) and RNeasy kit (QIAGEN, Valencia, CA) were used to extract total RNA from the tissue samples. Then one μg of isolated RNA was reverse transcribed to cDNA by using a commercial kit (OriGene, Rockville, MD). Quantification of target gene expression was achieved by the real-time PCR (qPCR) and using SYBR Green as the detection reagent. ΔΔCt method and melting curve analysis were performed for all quantitative PCR products. The results were presented by normalizing the mRNA level of target genes with the internal control GAPDH mRNA. All primers used in this study were ordered from Sigma (St. Louis, MO) and sequences are summarized in Table 3.1.

3.3.7. Statistical Analysis

Student's t-test was used for all statistical analyzes. The data were considered as statistically significant when P value <0.05. No animals were excluded from data analysis. Researchers were not blinded for performing experiments and data analysis. Data were presented as mean ± s.d.

3.4. RESULTS

3.4.1. Il-15/sIl-15Rα gene transfer induces weight loss in obese mice

The time dependent *IL-15/sIL-15Rα* expression after hydrodynamic delivery of 2 μg of AG209 DP muIL-15sRα+IL-15 plasmids was examined in obese mice (Figure 3.1a). A total of six hydrodynamic tail vein injections of AG209 DP muIL-15sRα+IL-15 or pcDNA3.1 plasmids were performed on days 0, 10, 20, 48, 58 and 68. Circulating IL-15/sIL-15Rα protein reached the peak level, ~100 ng/ml, one day after each injection and declined to the baseline in 10 days. Blood chemistry analysis showed no significant increase in serum concentrations of liver specific enzymes (AST, ALT) at the end of experiments, indicating that the procedures are safe (Figure 3.1b). These results prove that *Il-15/sIl-15Rα* gene expression can be successfully achieved and peak level regained through repeated hydrodynamic gene delivery.

The therapeutic effect of *Il-15/sIl-15Rα* gene expression on obese mice was shown in Figure 3.1c-f. Mice showed a significant reduction in body weight starting as early as day 6 after receiving the first *Il-15/sIl-15Rα* gene transfer, and reached a steady state with an average body weight of 44 g in 18 days (Figure 3.1c). Due to the absence of *Il-15/sIl-15Rα* gene expression, animals previously injected with IL-15/sIL-15Rα plasmids started to regain body weight 27 days after the initial treatment. Additional gene transfers were performed when the animals regained

body weight previously lost (53 ± 1.8g). Obese mice injected with *IL-15/sIL-15Rα* plasmids started weight loss and reached an average body weight of 48 ± 1.9 g, about 6 g lower compared to the control mice (54.1 ± 1.8g) at the end of experiment. The size of the two groups of mice is visually differentiable (Figure 3.1d). Body composition analysis using the EchoMRI-100 system (EchoMRI, Houston, TX, USA) revealed that the *Il-15/sIl-15Rα* gene transfer is fully correlated with time-dependent fat mass reduction without changing lean mass (Figures 3.1e and 3.1f). Reduction of body weight did not change the average food intake of the animals (Figure 3.1g). However, a transient increase of food intake is seen in the animals when they regain the body weight and the IL-15/sIL-15Rα is low.

To examine whether *Il-15/sIl-15Rα* gene transfer affects body weight only in obese mice, we performed the same set of experiments using age-matched lean mice fed with a chow diet. Three hydrodynamic tail vein injections of AG209 DP muIL-15sRα+IL-15 or pcDNA3.1 empty plasmids were performed every 10 days. Each injection generates similar IL-15/sIL-15Rα expression profile without inducing an increase of serum concentration of AST and ALT in age-matched lean mice (Figures 3.7a and 3.7b). However, the *Il-15/sIl-15Rα* gene transfer did not induce weight loss in age-matched mice fed a regular chow compared to the control mice injected with empty plasmids (Supplementary Figure 3.7c-f). In addition, the *Il-15/sIl-15Rα* gene transfer did not change food intake in age-matched lean mice (Supplementary Figure 3.7g). Together, these results demonstrate that the activity of Il-15/sIl-15Rα in reducing body weight is specific to obese mice.

3.4.2. Il-15/sIl-15Rα gene transfer reduced hypertrophy in adipocytes

In order to explore the impact of *Il-15/sIl-15Rα* gene transfer on body fat reduction, we collected different types of adipose tissues from the control and IL-15/sIL-15Rα treated mice. Compared to the control mice injected with empty plasmid, *Il-15/sIl-15Rα* gene transfer resulted in significant reduction of average size and weight of fat pads including inguinal (IWAT), epididymal (EWAT), perirenal (PWAT) white adipose tissues, and brown adipose tissue (BAT), by ~ 1.6, ~ 0.6, ~ 1.8 and ~ 0.1 g, respectively (Figures 3.2a and 3.2b). Accordingly, H&E staining results showed that *Il-15/sIl-15Rα* gene transfer significantly reduced the size of adipocytes in IWAT, EWAT, and PWAT, and increased the density of cellular matrix in BAT (Figure 3.2c). Quantification analysis using the imaging system confirmed that the average diameter of adipocytes in control mice is 149.5 ± 13.3 μm, compared with 78.7 ± 5.1 μm in mice transferred with *Il-15/sIl-15Rα* gene (Figure 3.2d).

To investigate how *Il-15/sIl-15Rα* gene transfer affects the energy utilization in obese mice, we measured the mRNA levels of genes in IWAT and BAT involved in adaptive thermogenesis. Obese mice transferred with the *Il-15/sIl-15Rα* gene showed a marked increase in the mRNA level of uncoupling protein 1 (*Ucp-1)* (BAT: ~1.6 fold; IWAT: ~8.1 fold) and *Ucp-3* (BAT: ~1.4 fold; IWAT: ~1.9 fold), compared to mice injected with control plasmids (Figure 3.3a). In addition, *Il-15/sIl-15Rα* gene transfer increased the expression of peroxisome proliferator-activated receptor gamma coactivator-1*α* (*Pgc-1α*) and *Pgc-1β* in IWAT by ~2.4 and ~1.5 folds, respectively (Figure 3.3b). Taken together, these data suggest that *Il-15/sIl-15Rα* gene transfer reduces the hypertrophy and enhances the energy expenditure in adipose tissues.

3.4.3. Il-15/sIl-15Rα gene transfer alleviates obesity associated fatty liver

Since fatty liver is commonly associated with obesity, we evaluated the impact of *Il-15/sIl-15Rα* gene transfer on lipid levels in the liver. Histological images showed extensive vacuoles in liver sections in obese mice, indicating a higher level of fat accumulation (Figure 3.4a). In comparison, the transfer of the *Il-15/sIl-15Rα* gene in obese mice noticeably reduced the total amount of vacuoles. Oil-red O and Nile red staining also showed significant reduction of lipid droplets in the liver sections, suggesting alleviation of hepatic steatosis in mice with *Il-15/sIl-15Rα* gene transfer. Consistently, *Il-15/sIl-15Rα* gene transfer greatly reduced the liver weight, and hepatic triglyceride and total cholesterol levels in obese mice (Figures 3.4b-d). In addition, age-matched lean mice with *Il-15/sIl-15Rα* gene transfer showed a reduction in hepatic triglyceride level, indicating the improvement of lipid metabolism in the liver (Figure 3.8a-c). Collectively, these data demonstrate that *Il-15/sIl-15Rα* gene transfer alleviates HFD-induced hepatic steatosis.

3.4.4. Il-15/sIl-15Rα gene transfer alters transcription of genes involved in lipid metabolism

Real time PCR analysis was performed to investigate how *Il-15/sIl-15Rα* gene transfer modulated the transcription of genes involved in lipid accumulation, lipogenesis, and fatty acid β oxidation in the liver and muscle. In the liver (Figures 3.5a and 3.5b), *Il-15/sIl-15Rα* gene transfer markedly suppressed the expression of key genes involved in lipid accumulation and lipogenesis in obese mice, including peroxisome proliferator-activated receptor gamma (*Pparγ-1*, 38%), *Pparγ-2* (59%), cluster of differentiation 36 (*Cd36*, 51%), fatty acid binding protein (*Fabp4*, 40%), monoacylglycerol O-acyltransferase 1 (*Mgat1*, 71%), stearoyl-CoA desaturase-1 (*Scd1*, 88%), and fatty acid synthase (*Fas*, 43%). Different from that of obese mice, *Il-15/sIl-*

15Rα gene transfer in age matched mice only repressed the mRNA levels of *Scd1* (41%) and *Fas* (37%) without significantly change in other genes (Figures 3.9a and 3.9b). In contrast, *Il-15/sIl-15Rα* gene transfer slightly, but significantly, increased the mRNA level of *Pparα* (~1.3 fold) and carnitine palmitoyl-transferase 1 (*Cpt1α*, ~1.3 fold), both of which are key genes involved in fatty acid β oxidation (Figures 3.5a and 3.5b). In addition, *Il-15/sIl-15Rα* gene transfer slightly increased mRNA levels of genes critical for fatty acid β oxidation, such as *Pparδ* (~1.2 fold), *Pgc-1α* (~1.3 fold), and *Cpt1β* (~1.4 fold) and suppressed the expression of genes responsible for lipogenesis, including *Scd1* (57%) and *Fas* (39%) in muscle (Figures 3.5c and 3.5d).

3.4.5. Il-15/sIl-15Rα gene transfer improves glucose homeostasis and insulin sensitivity

Glucose intolerance and insulin resistance are characteristics of type-2 diabetes and commonly associated with obesity. As such, we performed an intraperitoneal glucose tolerance test (IPGTT) and insulin tolerance test (ITT) to assess the impact of *Il-15/sIl-15Rα* gene transfer on glucose homeostasis and insulin sensitivity in obese mice. IPGTT showed that transfer of the *Il-15/sIl-15Rα* gene lead to a lower peak level and a markedly improved glucose profile (Figure 3.6a). Consistently, the calculated area under the curve (AUC) of IPGTT showed a much higher clearance rate after *i.p* injection of glucose (Figure 3.6b). Compared to the control, ITT revealed that mice with *Il-15/sIl-15Rα* gene transfer were more sensitive in response to insulin injection (Figure 3.6c). In addition, obese mice transferred with *Il-15/sIl-15Rα* gene showed larger decreases of their fasting blood glucose (control: ~224 mg/dL, IL-15/sIL-15Rα: ~130 mg/dl) and fasting blood insulin (control: ~7.9 ng/ml, IL-15/sIL-15Rα: ~3.6 ng/ml) (Figures 3.6d and 3.6e). Similarly, a reduction in calculated HOMA-IR suggests that *Il-15/sIl-15Rα* gene transfer improved the insulin sensitivity compared to the control (Figure 3.6f). In age-matched lean mice,

Il-15/sIl-15Rα gene transfer also showed a slight improvement of glucose metabolism (Figure 3.8d-g). A real time PCR analysis reveals a ~40% reduction of the mRNA level of glucose 6-phosphotase (*G6p*) in the liver, indicating *Il-15/sIl-15Rα* gene transfer reduced the gluconeogenesis (Figure 3.6g). Taken together, these results demonstrate that *Il-15/sIl-15Rα* gene transfer improves glucose homeostasis and insulin sensitivity.

3.5. DISCUSSION

In this study, we evaluated the therapeutic effects of *Il-15/sIl-15Rα* gene transfer on HFD-induced obesity and its associated metabolic symptoms. Our results demonstrate that *Il-15/sIl-15Rα* gene transfer *via* hydrodynamic tail vein injection in obese mice induces weight loss and fat mass reduction (Figures 3.1 and 3.2), alleviates obesity associated fatty liver (Figure 3.4), and improves glucose homeostasis and insulin sensitivity (Figure 3.6). Mechanistically, these beneficial effects are associated with an increased expression of genes for adaptive thermogenesis in adipose tissue (Figure 3.3). Moreover, *Il-15/sIl-15Rα* gene transfer suppressed the expression of genes involved in lipid accumulation and lipogenesis, and increased the expression of genes important for fatty acid β oxidation in liver and muscle (Figure 3.5).

Induction of weight loss in obese mice is dependent on the IL-15/sIL-15Rα level in circulation (Figures 3.1a and 3.1c). This conclusion is in agreement with a previous study that delivered the human *Il-15* gene into obese B6 mice [90, 107]. In addition, evidence suggests that IL-15 has a direct impact on adipose tissue without altering the food intake in animals [88, 90, 175]. Our data showed that the hydrodynamic delivery of the *Il-15/sIl-15Rα* gene reduced fat mass in obese animals (Figure 3.1c-f) without changing food intake (Figure 3.1g and 3.7g). However, there is a transient induction of food intake accompanied with ascending bodyweight gain in animals when

we temporally suspended the IL-15/sIL-15Rα treatment (Figures 3.1a and 3.1g). This observation may be partially due to the changes of circulating peripheral hormones which are involved in appetite regulation following weight loss [179].

Our results in Figure 3.1c showed that *Il-15/sIl-15Rα* gene transfer induced a maximum of ~15% body weight loss in obese mice 18 days after the initial treatment. This result is in agreement with previous studies where approximately 12% body weight loss in obese mice was achieved by IL-15 overexpression [90, 107, 180]. These observations are also in agreement with clinical studies where high intensity and frequency exercise induced and maintained the magnitude of weight loss by 10-14% in obese patients [181-183]. The maintenance of body weight may partially be explained by adjustment in homeostatic feedback system, where energy utilization shifts to a preference for carbohydrate use and spares dietary fat for deposition [179, 184].

Several lines of evidence indicate that IL-15 has direct effects on regulating adiposity. Using murine 3T3-L1 adipocytes cell line, IL-15 treatment was able to decrease lipid deposition in differentiated and mature adipocytes *in vitro* [89-91]. Treatment with IL-15 in adult mice and rats led to reduced size in white adipose tissue and shrinkage of adipocytes, suggesting an anti-adipogenic role of the IL-15 [92, 180]. In line with previous reports, *Il-15/sIl-15Rα* gene transfer dramatically reduced the size (Figure 3.2a) and weight (Figure 3.2b) of fat pads. Meanwhile, histological analysis revealed a smaller diameter of adipocytes in the adipose tissue (Figures 3.2c and 3.2d), indicating that *Il-15/sIl-15Rα* gene transfer promotes adipose tissue shrinkage, which contributes to the whole body weight loss (Figures 3.1c and 3.1d). Furthermore, Almendro *et al.* demonstrated that IL-15 treatment up-regulated the expression of *Ucp1* and *Ucp3* in rat BAT, suggesting the potential role of IL-15 in mediating uncoupling of adenosine triphosphate production as a mechanism to dissipate energy [185]. In addition, previous studies have shown that

IL-15 targeted adipocytes, through inhibition of lipogenic enzyme expression and activity, resulted in a decrease in the lipogenic rate and carcass fat [93, 175, 186]. In line with these studies, our data showed that obese mice with *Il-15/sIl-15Rα* gene transfer exhibited an increase in the transcription of thermogenic genes including *Ucp1*, *Ucp3*, *Pgc1α* and *Pgc1β* in BAT and IWAT (Figures 3.3a and 3.3b). As well, *Il-15/sIl-15Rα* gene transfer in obese mice suppressed the transcription of *Scd-1* and *Fas*, the key genes for lipogenesis in the liver and muscle (Figures 3.5b and 3.5d). These results suggest that *Il-15/sIl-15Rα* gene transfer reduces adipocyte deposition, at least in part, through increasing adaptive thermogenesis in adipose tissue, and repressing lipogenesis in the liver.

Members of the nuclear receptor superfamily PPARs, play various physiological roles in regulating lipid accumulation and fatty acid catabolism [187-189]. PPARγ plays a central role in mediating adipogenesis and insulin sensitivity [187-189]. Evidence suggests that the development of hepatic steatosis is correlated with *Pparγ* up-regulation n in the liver, and that the inhibition of the hepatic PPARγ pathway is responsible for the alleviation of liver steatosis [190-192]. Our results show that the transfer of the *Il-15/sIl-15Rα* gene markedly suppressed the mRNA level of *Pparγ* and its target genes in obese mice, but not in age-matched lean mice, suggesting that activation of the hepatic PPARγ pathway is important for liver steatosis development (Figures 3.4, 3.5a and 3.9a). In addition, Almendro *et al.* demonstrated that part of IL-15 activity on lipid oxidation is mediated by means of up-regulation of PPARα and PPARδ in the liver and muscle [105]. A subsequent study by the same group also showed an increase in *Pparα* and *Pparδ* mRNA levels in BAT after IL-15 administration, which resulted in up-regulation of genes that code for enzymes for β oxidation [185]. Consistent with these findings, our results show that *Il-15/sIl-15Rα* gene transfer increased the expression of *Pparα* and *Pparδ* genes in the liver and muscle, leading

to a corresponding increase of the mRNA level of their target genes involved in β oxidation, including *Cpt1-α, Cpt1-β* and *Pgc1-α* (Figure 3.5).

Studies have shown the beneficial role of IL-15 in mediating glucose intolerance and insulin resistance. By stimulating glucose uptake in skeletal muscle with the administration of IL-15, improved glucose homeostasis and insulin sensitivity are achieved [106, 107]. Our previous study provided direct evidence demonstrating that *Il-15* gene transfer protects mice from HFD-induced hyperinsulinemia and hyperglycemia [175]. Consistent with this previous study, the results of current study clearly show that *Il-15/sIl-15Rα* gene transfer markedly reduces obesity-induced high blood glucose level and insulin resistance, as reflected by an improved IPGTT and ITT profile, and reduced HOMA-IR (Figure 3.6). A small, but significant improvement of insulin sensitivity and glucose homeostasis is also seen in age-matched lean mice (Figure 3.8d-g). Taken together, our study suggests that *Il-15/sIl-15Rα* gene transfer improves obesity-associated glucose homeostasis and insulin sensitivity.

In summary, we demonstrate in this study that the hydrodynamic delivery of the *Il-15/sIl-15Rα* gene in obese mice enhances lipid and glucose metabolism, consequently leading to bodyweight reduction, alleviation of fatty liver, and improvement of glucose homeostasis. These findings suggest that *Il-15/sIl-15Rα* gene transfer could be an effective approach in treating HFD-induced obesity and its associated metabolic complications. Further studies need to focus on evaluation of the long-term effect of *Il-15/sIl-15Rα* gene transfer due to the profound immunomodulatory properties of IL-15 in regulating the activity of natural killer cells and $CD4^+$ and $CD8^+$ T cells. The fact that repeated gene transfer needs to be performed to sustain therapeutic level of IL-15 in blood would suggest additional effort in achieving regulated *Il-15* gene expression. Repeated gene transfer is less desirable as far as gene therapy is concerned.

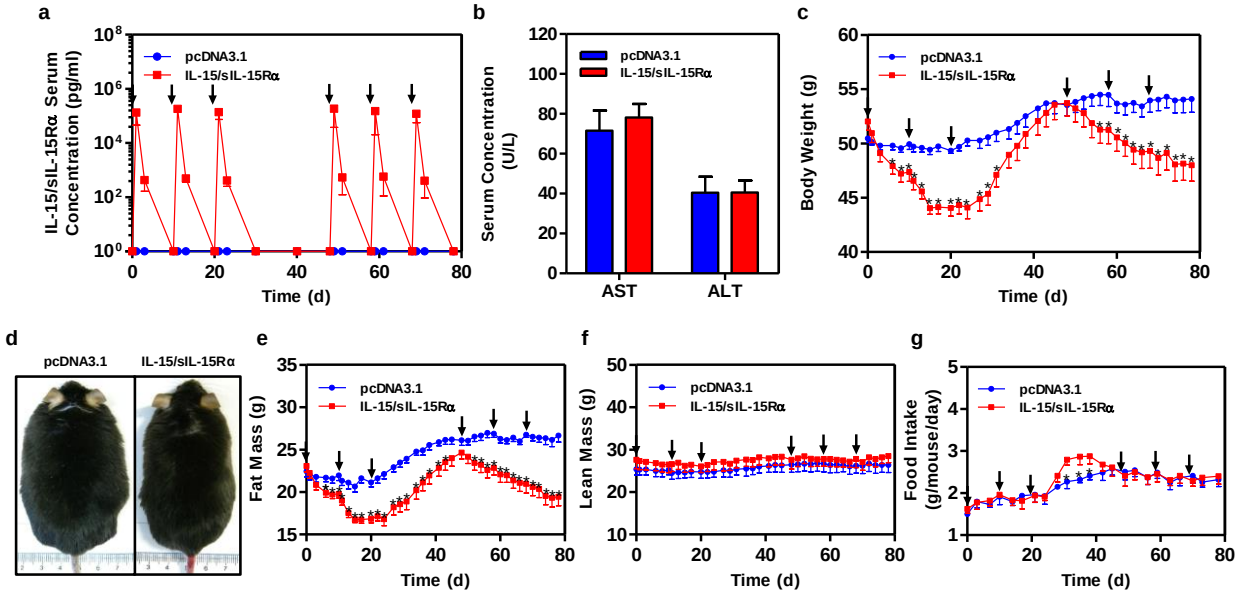

Figure 3.1. Effects of gene transfer on body weight, fat mass and food intake of obese mice. Obese mice were hydrodynamically injected with 2 μg of plasmid carrying *IL-15/sIL-15Rα* genes or pcDNA3.1 empty vector. (**a**) Serum concentration of IL-15/sIL-15Rα as a function of time; (**b**) Plasma concentrations of aspartate aminotransferase (AST) and alanine aminotransferase (ALT) at the end of experiments; (**c**) Time dependent body weight of obese mice; (**d**) Representative images of obese mice injected with pcDNA3.1 empty vector (left) or plasmid carrying *IL-15/sIL-15Rα* genes (right); (**e**) Time dependent fat mass; (**f**) Time dependent lean mass; and (**g**) Time dependent food intake. (●) Animals injected with pcDNA3.1 empty vector, (■) Animals injected plasmid carrying *IL-15/sIL-15Rα* genes. Results represent mean ± SD (n=5). * $P<0.05$ compared with control obese mice injected with empty vector. Arrows indicate the time of gene transfer.

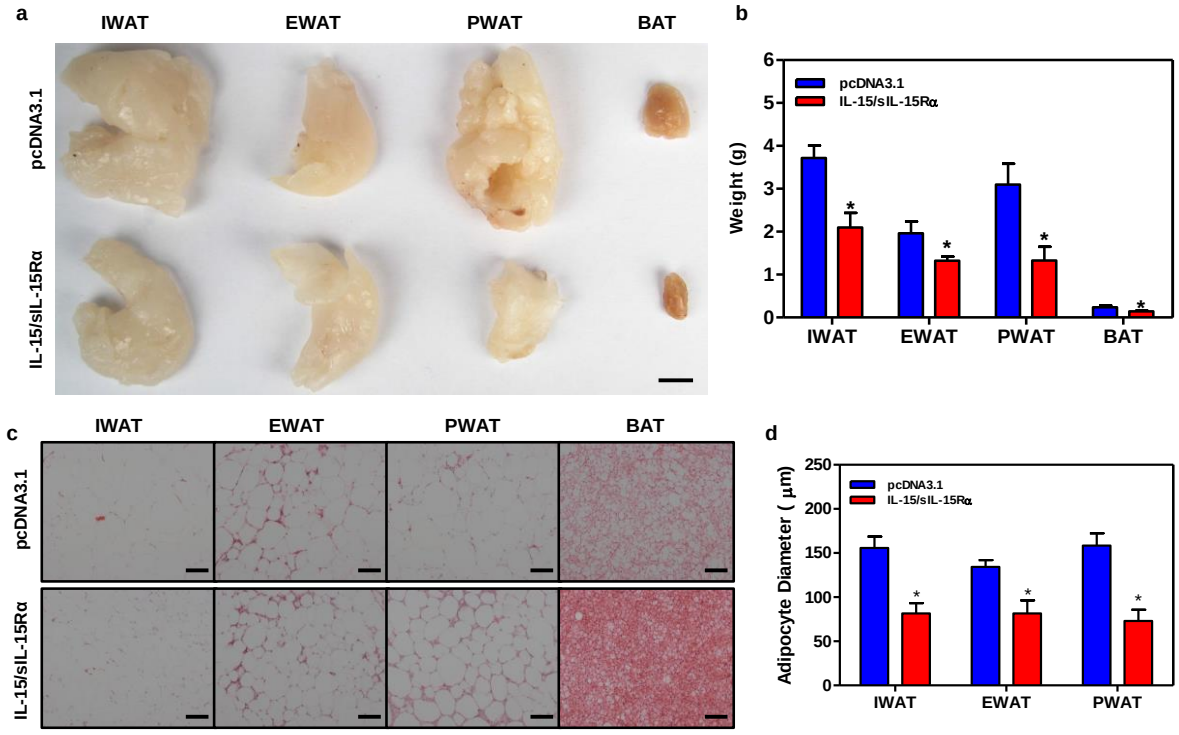

Figure 3.2. ***Il-15/sIl-15Rα*** **gene transfer reduced hypertrophy of adipocytes in obese mice.** Obese mice were sacrificed at the end of experiment and different fat pads were collected and examined. (**a**) Representative image of inguinal white adipose tissue (IWAT), epididymal white adipose tissue (EWAT), perirenal white adipose tissue (PWAT) and brown adipose tissue (BAT), bar represents 1 cm (**b**) Weight of different fat pads; (**c**) Images of H&E staining of IWAT, EWAT, PWAT and BAT. Bars represent 100 μm**;** (**d**) Average diameter of adipocytes in WAT (calculated from 400 randomly selected cells from 5 tissue slides). Data represent mean ± SD (n=5). * P<0.05 compared with control mice injected with empty plasmids.

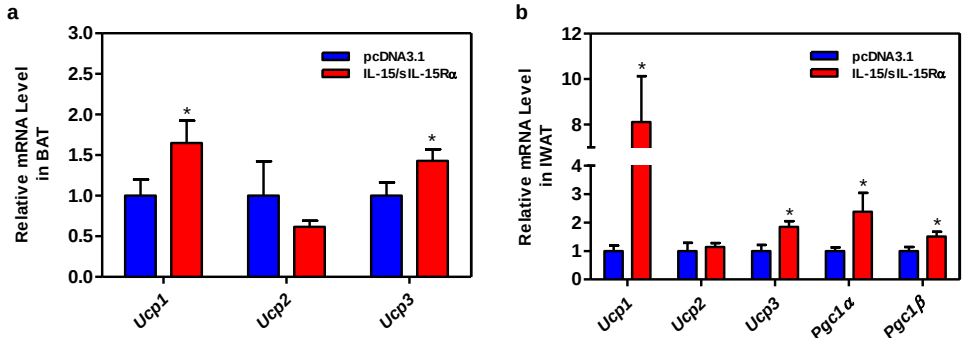

Figure 3.3. Impact of *Il-15/sIl-15Rα* gene transfer on mRNA levels of genes involved in thermogenesis in adipose tissues. Relative mRNA levels of genes involved in thermogenesis were determined in (**a**) BAT and (**b**) IWAT through q-PCR. Each data point represents mean ± SD (n=5). * $P<0.05$ compared with control mice.

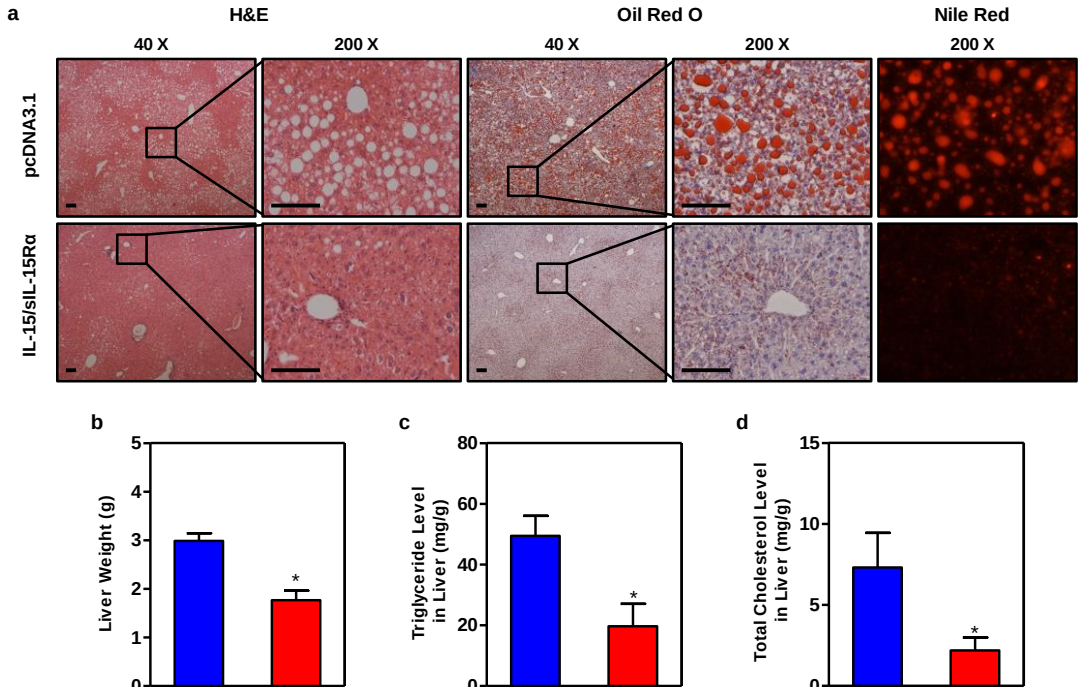

Figure 3.4. ***Il-15/sIl-15Rα*** **gene transfer alleviates fatty liver.** (**a**) Representative images of H&E, oil-red O and Nile red staining of the liver sections; Bars represent 100 μm; (**b**) Liver weight; (**c**) Hepatic triglyceride (TG) level; and (**d**) total cholesterol (TC) level in the liver. Results represent mean ± SD (n=5). * $P<0.05$ compared with control mice injected with empty plasmids.

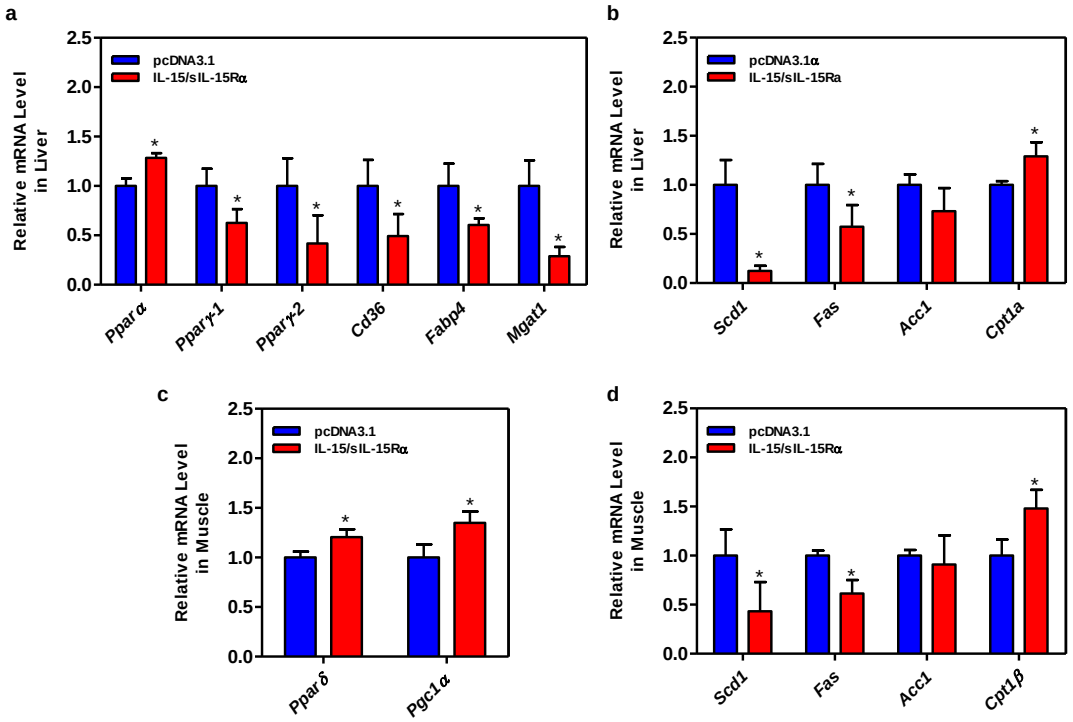

Figure 3.5. ***Il-15/sIl-15Rα*** **gene transfer alters the mRNA level of genes involved in lipid metabolism.** (**a-b**) Relative mRNA levels of genes involved in metabolic homeostasis in liver; (**c-d**) Relative mRNA levels of genes involved in lipogenesis and fatty acid β oxidation in muscle. Data represent mean ± SD (n=5). * P<0.05 compared with control mice.

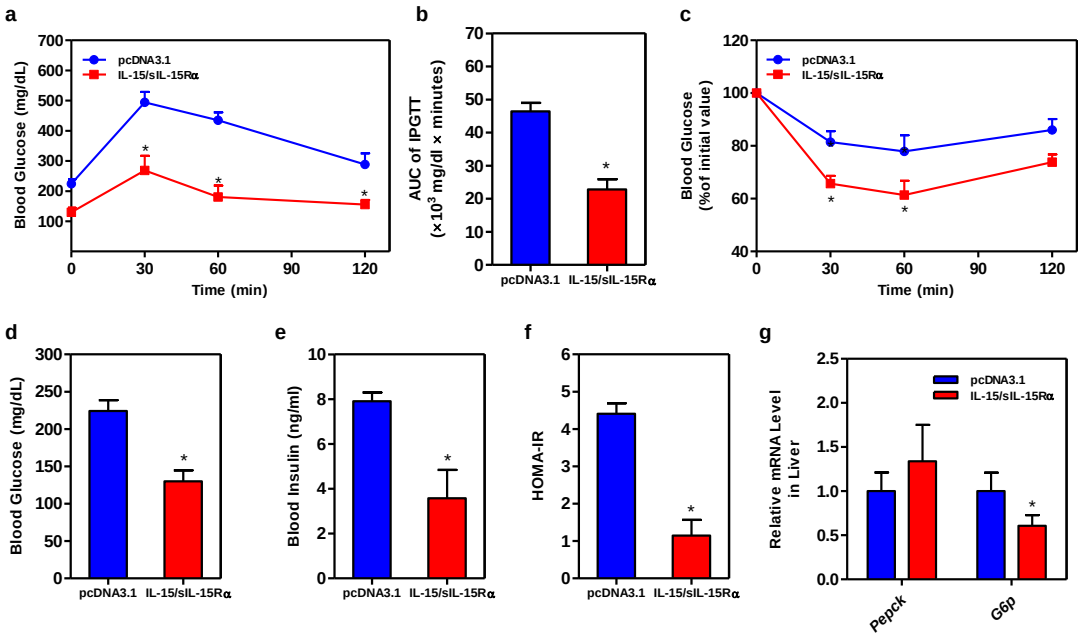

Figure 3.6. *Il-15/sIl-15Rα* gene transfer improves glucose homeostasis and insulin sensitivity. (**a**) Time dependent change of blood glucose concentration in IPGTT; (**b**) AUC of IPGTT; (**c**) Time dependent change of blood glucose concentration in ITT; (**d**) Fasting blood glucose level; (**e**) Fasting blood insulin level; (**f**) Results of HOMA-IR analysis for insulin resistance; and (**g**) Relative mRNA levels of genes involved in glucose metabolism in liver. IPGTT: intraperitoneal glucose tolerance test, AUC: area under curve, ITT: insulin tolerance test, HOMA-IR: Homeostasis model assessment of insulin resistance. (●) Mice injected with pcDNA3.1 empty plasmids; and (■) Mice injected with IL-15/sIL-15Rα plasmids. Results represent mean ± SD (n=5). * $P<0.05$ compared with control mice.

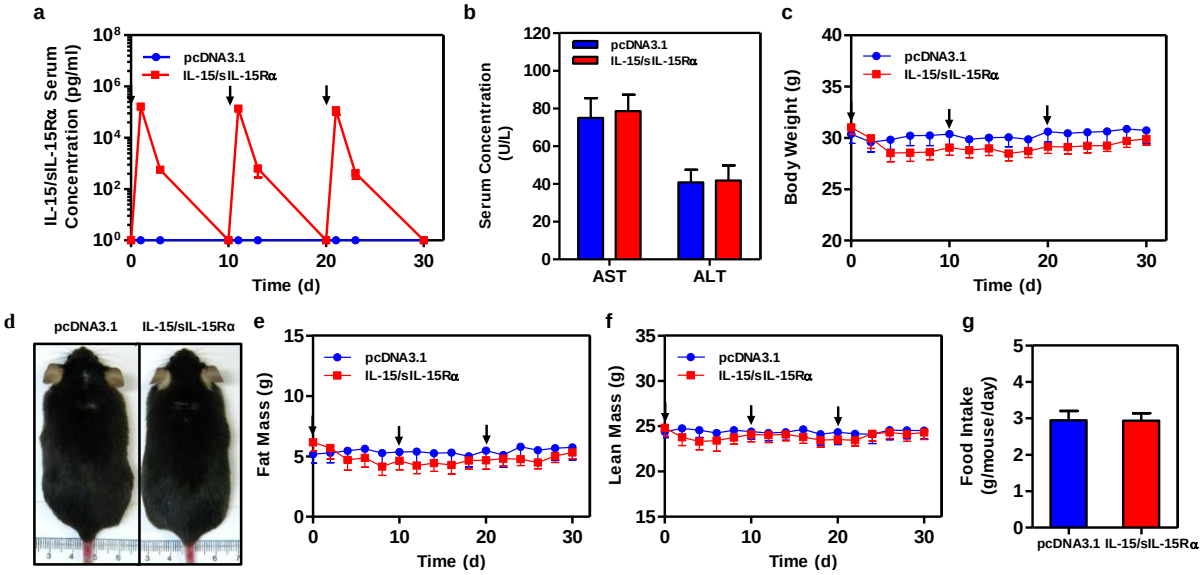

Figure 3.7. *Il-15/sIl-15Rα* gene transfer didn't induce weight loss in age-matched mice on a regular chow diet. Age-matched lean mice were hydrodynamically injected with 2 μg of IL-15/sIL-15Rα or pcDNA 3.1 empty plasmids. (**a**) Circulating IL-15/sIL-15Rα level as a function of time; (**b**) Plasma AST and ALT levels at the end of experiment; (**c**) Time dependent change of body weight; (**d**) Representative images of lean mice injected with empty plasmids (left) or IL-15/sIL-15Rα plasmids (right); (**e**) Time dependent change of fat mass; (**f**) Time dependent change of lean mass; and (**g**) Food intake. (●) Animals injected with empty plasmids; and (■) Animals injected with IL-15/sIL-15Rα plasmids. Data represent mean ± SD (n=5). * $P<0.05$ compared with control mice injected with empty plasmids.

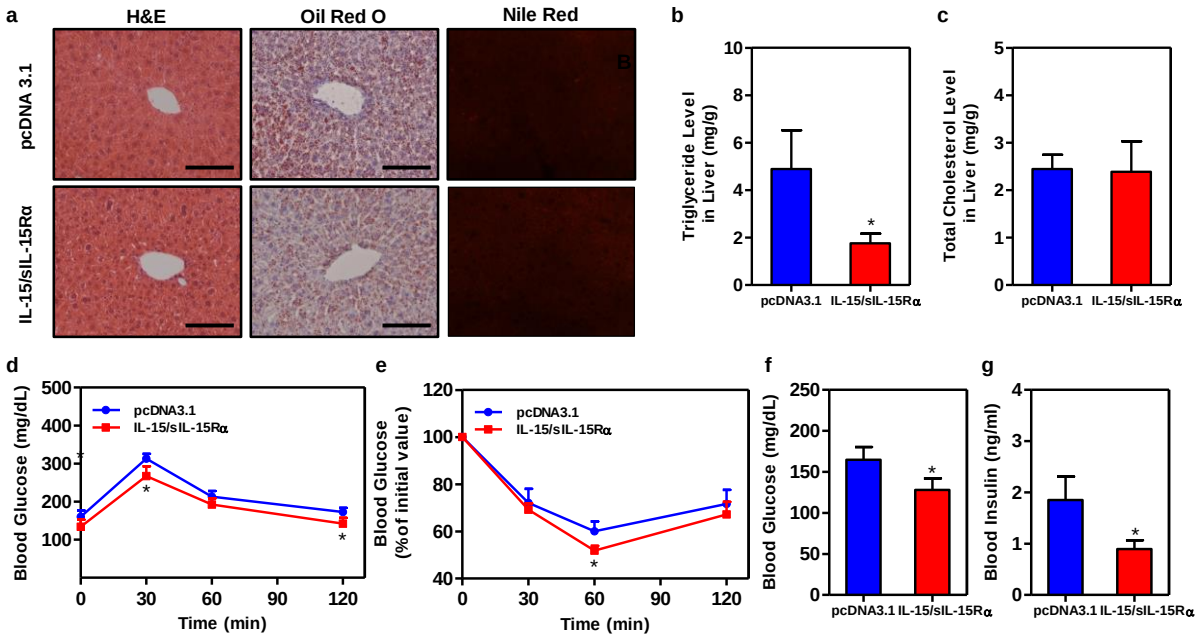

Figure 3.8. ***Il-15/sIl-15Rα*** **gene transfer slightly improves lipid and glucose metabolism in age-matched mice.** (**a**) Images of liver sections stained with H&E, oil-red O or Nile red, Bars represent 100 μm; (**b-c**) Relative TG and TC level in the liver; (**d**) Time dependent change of blood glucose concentration in IPGTT; (**e**) Time dependent change of blood glucose concentration in ITT; (**f**) Fasting blood glucose level; and (**g**) Fasting blood insulin level. (●) Mice injected with empty plasmids; and (■) Mice injected with IL-15/sIL-15Rα plasmids. Results represent mean ± SD (n=5). * P<0.05 compared with control mice.

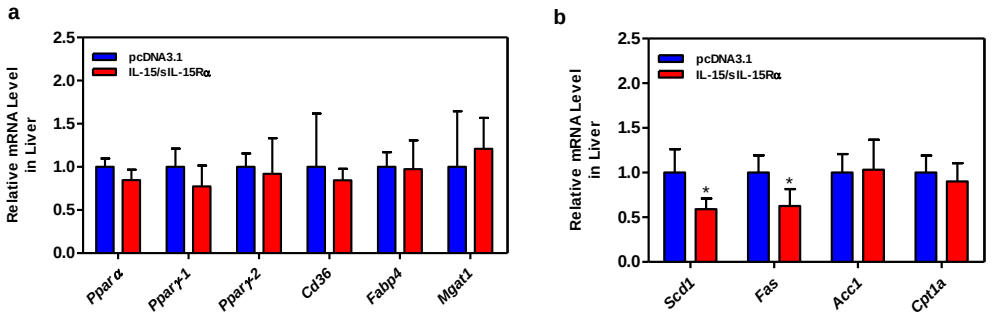

Figure 3.9. *Il-15/sIl-15Rα* gene transfer alters the mRNA level of genes involved in thermogenesis and lipid metabolism in age-matched normal mice. (**a**) Relative mRNA levels of nuclear receptor and their target genes in liver; and (**b**) Relative mRNA levels of genes involved in lipogenesis and fatty acid β oxidation in liver. Each data point represents mean ± SD (n=5). * $P<0.05$ compared with control mice injected with empty plasmids.

Table 3.1. Primer sequences for real time PCR analysis of gene expression

Gene	Forward primer sequence	Reverse primer sequence
Acc-1	ATGGGCGGAATGGTCTCTTTC	TGGGGACCTTGTCTTCATCAT
Cd36	CCTTAAAGGAATCCCCGTGT	TGCATTTGCCAATGTCTAGC
Cpt1α	CTCCGCCTGAGCCATGAAG	CACCAGTGATGATGCCATTCT
Cpt1β	GCACACCAGGCAGTAGCTTT	CAGGAGTTGATTCCAGACAGGT
Fas	GGAGGTGGTG ATAGCCGGTAT	TGGGTAATCCATAGAGCCCAG
Fabp4	AAGGTGAAGAGCATCATAACCC	TCACGCCTTTCATAACACATTCC
Gapdh	AGGTCGGTGTGAACGGATTTG	TGTAGACCATGTAGTTGAGGTCA
G6p	CGACTCGCTATCTCCAAGTGA	GTTGAACCAGTCTCCGACCA
Mgat1	TGGTGCCAGTTTGGTTCCAG	TGCTCTGAGGTCGGGTTCA
Pdk4	AGGGAGGTCGAGCTGTTCTC	GGAGTGTTCACTAAGCGGTCA
Pepck	CTGCATAACGGTCTGGACTTC	CAGCAACTGCCCGTACTCC
Pgc-1α	GAAGTGGTGTAGCGACCAATC	AATGAGGGCAATCCGTCTTCA
Pgc-1β	TTGTAGAGTGCCAGGTGCTG	GATGAGGGAAGGGACTCCTC
Pparα	TGTCGAATATGTGGGGACAA	AATCTTGCAGCTCCGATCAC
Pparγ-1	GGAAGACCACTCGCATTCCTT	GTAATCAGCAACCATTGGGTCA
Pparγ-2	TCGCTGATGCACTGCCTATG	GAGAGGTCCACAGAGCTGATT
Pparδ	TCCATCGTCAACAAAGACGGG	ACTTGGGCTCAATGATGTCAC
Scd1	TTCTTGCGATACACTCTGGTGC	CGGGATTGAATGTTCTTGTCGT
Ucp1	AGGCTTCCAGTACCATTAGGT	CTGAGTGAGGCAAAGCTGATTT
Ucp2	GCGTTCTGGGTACCATCCTA	GCTCTGAGCCCTTGGTGTAG
Ucp3	ATGAGTTTTGCCTCCATTCG	GGCGTATCATGGCTTGAAAT

CHAPTER 4

IL-15/sIL-15Rα GENE TRANSFER SUPPRESSES LEWIS LUNG CANCER GROWTH IN THE LUNGS, LIVER AND KIDNEYS

Hao Sun and Dexi Liu. (2016).

Cancer Gene Therapy; **23**: 54-60.

4.1. ABSTRACT

Nearly 40% of people with lung cancer have tumor growth in other organs at the time of diagnosis. Current treatment strategies for patients with late-stage lung cancer are primarily palliative and only showed modest efficacy. The current study takes advantage of the hydrodynamic gene delivery technique to evaluate the antitumor activity of interleukin (IL)-15/sIL-15Rα on lung tumors growing in the lungs, liver and kidneys. We demonstrate that hydrodynamic tail vein injection of 2 μg of AG209 DP muIL-15sRα+IL-15 plasmid resulted in serum IL-15/sIL-15Rα reaching a peak level of ~ 10 μg ml^{-1} 1 day after the injection and gradually declined to ~ 5 ng ml^{-1} within 3 days. Quantitative PCR analysis revealed that overexpression of IL-15/sIL-15Rα induced the activation of natural killer and T cells, evidenced by increased mRNA levels of marker genes including *granzyme B, perforin, Ifn-γ, T-bet* and *Cd8* in the lungs, liver and kidneys. Importantly, transfer of the Il-15/sIl-15Rα gene alone, or in combination with gemcitabine chemotherapy, significantly inhibited the tumor growth in these three organs and prolonged median survival time of treated mice by 1.7- and 3.3-fold, respectively. The therapeutic benefits are principally blockade and elimination of tumor growth in the liver and kidneys. Taken together, these results suggest that IL-15/sIL-15Rα-based gene therapy could be an effective approach to treat late-stage lung cancer with metastases in other organs.

4.2. INTRODUCTION

Lung cancer is a leading cause of death for cancer patients, both in men and in women worldwide [193]. Approximately 30–40% of lung cancer patients developed tumor metastases in other organs at the time of diagnosis [194]. Clinically, treatment for lung cancer with metastases is

primarily palliative involving systemic chemotherapy and/or radiation therapy [195]. Limited progress has been made demonstrating modest efficacy of current treatments, with the overall 5-year survival rate for stage-4 lung cancer at around 4% [193]. Thus, there is an urgent need to develop therapies that are more effective for late-stage lung cancer patients. Emerging evidence supports a strategy of cytokine-based immunotherapy to enhance the immune response that targets cancer cells in patients with tumor metastasis [196]. Modest successes have been achieved with interleukin (IL)-2 or interferon alpha (IFN-α) based immunotherapy in treating patients with metastatic melanoma and renal cell carcinoma [197, 198]. Thus, IL-15, a cytokine sharing the common receptor components with IL-2 (IL-2R/15Rβ-γc), also becomes a potential candidate for cytokine-based cancer immunotherapy [199].

IL-15 is a potent innate and adaptive immune stimulator for generation, proliferation and induction of cytotoxic T lymphocytes, natural killer (NK) cells and NKT cells [200]. Compared with IL-2, IL-15 shows no obvious adverse effects in animals, including activation-induced cell death in T cells or expansion of T regulatory cells [199]. Upon activation, IL-15 and IL-15Rα interact intracellularly with high affinity ($Kd \approx 10^{-11}$ M), resulting in formation of membrane-bound IL-15/IL-15Rα complexes, which are found in activated monocytes and dendritic cells [34, 171]. The membrane-bound IL-15/IL-15Rα complexes induce the signal transduction primarily through the JAK1/JAK3 and STAT3/STAT5 pathways on neighboring effector T, B and NK cells through cell-to-cell contact ('trans-presentation') [34]. Recent studies demonstrate that when IL-15/IL-15Rα complexes are cleaved from the cell surface, the soluble form of IL-15/IL-15Rα complexes (IL-15/sIL-15Rα) is released [201]. This soluble form of IL-15/sIL-15Rα complexes increases the bioavailability and extends the circulation half-life of IL-15 in blood, resulting in enhanced activity in proliferation and activation of cytotoxic T, NK and NKT cells *in vivo* [114, 201].

Both membrane-bound and soluble forms of IL-15/IL-15Rα complexes have been tested for their antitumor activity in preclinical mouse models [39, 113, 114, 202-205]. Using the genetically modified dendritic cells to express membrane-bound IL-15/IL-15Rα complexes, Steel et al. [203] showed enhanced immune responses against a neu (Erbb2)-positive mammary cancer in mice, and restored the impaired CD4+ T-helper functions. In addition, direct administration of preformed IL-15/sIL-15Rα protein or transfer of the Il-15/sIl-15Rα gene showed profound proliferation and activation of NK and cytotoxic CD8+ cells, leading to an inhibition of tumor growth in vivo [113, 202, 204-207]. The therapeutic benefits of IL-15/sIL-15Rα for the treatment of lung cancer have yet to be assessed.

In this study, we employed a well-established hydrodynamic gene transfer technique and assessed the antitumor activity of IL-15/sIL-15Rα for the eradication of lung tumor growth in multiple organs. We report that Il-15/sIl-15Rα gene transfer is effective in inhibiting lung tumor growth in the lungs, liver and kidneys. Our results suggest a possible application of Il-15/sIl-15Rα gene transfer for treatment of late-stage lung cancer with metastasis.

4.3. MATERIALS AND METHODS

4.3.1. Plasmids

The plasmid expressing the mouse IL-15/sIL-15Rα (AG209 DP muIL-15sRα+IL-15) complex was generously provided by Dr. Barbara K. Felber (NCI) [171]. This plasmid consists of two expression compartments (Figure 1a), which drives the gene expression of mouse IL-15 and the soluble form of mouse IL-15Rα (sIL-15Rα, amino acids 1–205) separately. The GenBank accession numbers of mouse IL-15 and sIL-15Rα proteins are NP-032383 and NP-032384, respectively. The sequence of mouse IL-15 was optimized *via* the substitution of the signal

peptide with mouse GM-CSF and the elimination of instability elements that enhanced the mRNA stability. Similarly, the sequence of mouse sIL-15Rα was codon-optimized by introducing multiple silent point mutations to remove RNA instability sequences. The gene expression of mouse IL-15 and sIL-15Rα is driven by siman or human CMV promoter, and the optimized sequence was chemically synthesized and validated *via* sequencing [171]. The plasmids were amplified by *E. coli*-based culture growth and purified by the cesium chloride-ethidium bromide gradient ultracentrifugation procedures. The prepared plasmids were stored in saline at − 80 °C until use and plasmids purity was determined by 1% agarose gel electrophoresis and measured *via* 260-280 nm optical density.

4.3.2. Cells

LL/2 cells (Lewis Lung Carcinoma) were purchased from ATCC (Manassas, VA). The luciferase-tagged LL/2 cells (LL/2-Luc) were created using Lenti viral vectors containing luciferase reporter gene. About 2×10^6 LL/2-Luc cells were seeded into a 100 × 20 mm cell culture dish and cultured in DMEM (ATCC) with 10% FBS (Atlanta Biologics, Atlanta, GA) and 1% penicillin/streptomycin (Life Technologies, Grand Island, NY). At 80% confluence, the medium was removed and each plate was treated with 3 ml of 0.25% Trypsin/2.21 mM EDTA solution (Corning, Corning, NY) at room temperature for 8 min. Cell suspension was mixed with 5 ml of serum containing medium. The mixture was passed through a membrane filter with an average pore size of 40 μm (BD Falcon, Franklin Lakes, NJ) and centrifuged for 3 min at room temperature at 1300 r.p.m. Cell pellet was re-suspended in a serum-free medium; and cell concentration was adjusted to the desirable level and confirmed by the method of hemocytometric cell counting.

4.3.3. Animals and animal treatments

The IACUC approved all animal-related experiments in this study under the protocol of A2014 07-008-Y1-A0 (University of Georgia, Athens, Georgia). All experimental mice were housed in a light-dark 12-12 hour cycle without the contact of pathogens. Only female C57BL/6 mice (7-8 weeks, 18-20g) were used and purchased from Charles River Laboratories (Wilmington, MA).

The tumor cell suspension and plasmid solution were injected using a hydrodynamics-based procedure [154, 208]. Briefly, for cell delivery, 10^6 LL/2-Luc cells suspended in 1.6–1.8 ml serum-free medium (equivalent to 9% body weight of a mouse) were injected through the tail vein within 5–8 s. Tumor-bearing mice were randomly divided into groups for different treatments. For gene delivery, the same volume of saline solution containing either 2 μg of AG209 DP muIL-15sRα+IL-15 or pCMV empty plasmids was injected *via* the tail vein following the previously established procedure [154]. Gemcitabine (LC Laboratory, Woburn, MA) was diluted in saline and injected intraperitoneally at a dose of 120 mg kg− 1. Mice were killed for tissue collection, and biochemical and histological examinations. The mouse IL-15/sIL-15 complex levels in the serum were determined using commercial ELISA kit (eBioscience, San Diego, CA). The investigators were not blinded for performing the experiments and for analyzing the data.

4.3.4. Histochemical examination

H&E staining was used to verify the existence of micro-tumor development in the lung, liver, and kidneys. The tissue samples were collected from the killed mice and fixed in the buffered formalin (10%) for at least 48 hours. Then the tissue samples underwent the gradient

dehydration process by using the increased ratio of ethanol/water (v/v) and embedded in paraffin for 16 h. The H&E staining used the five μm tissue sections and performed by a commercial kit (BBC Biochemical, Atlanta, GA). The micro-tumors were examined by using the NIS-Elements imaging platform microscopic (Nikon Instruments Inc. Melville, NY).

4.3.5. Bioluminescence imaging

IVIS Imaging Systems (Perkin-Elmer, Akron, OH) were used to detect the bioluminescence intensity stimulated by the firefly luciferin. The Firefly D-luciferin was purchased from Perkin-Elmer (Akron, OH) and stored in PBS at -20 ℃ in a concentration of 15 mg ml^{-1}. The animals were anesthetized with isoflurane (Abbott Laboratories, Irving, TX), *i.p.* injected with firefly luciferin at a dose of 150 mg kg^{-1}, and then imaged with IVIS Imaging Systems after 15 min. The grayscale images were captured in a 24-cm view field and set as the background level. All bioluminescence images were then acquired using the fixed parameters (Exposure time: 60s; binning factor: 4; f/stop: 1.2; and filter: open). The total luminescent intensity for each mouse was calculated automatically by using the Living Image Software (Perkin-Elmer) and expressed as p s^{-1} cm^{-2} sr^{-1} (photons per second per cm^2 per steradian).

4.3.6. Analysis of luciferase activity

After the animals were killed, tissue samples from the assigned organs were harvested and kept at − 80 °C until use. The tissue samples (~150 mg) were homogenized in 1 ml of lysis buffer using a tissue homogenizer (Dremel, Racine, WI). Tissue homogenates were centrifuged at 12,000 r.p.m. using Microfuge (Beckman Coulter, Brea, CA) for 10 min at 4 ℃, and the

supernatants were collected. Ten microliters of supernatant was taken for the luciferase assay according to the previously described procedure [154].

4.3.7. Gene expression analysis by real-time PCR

The samples from mouse lungs, liver and kidneys were homogenized using TRIzol reagents from Invitrogen (Carlsbad, CA) total RNA isolation. A commercial kit from OriGene (Rockville, MD) was used for reverse-transcription PCR (RT-PCR) to transcribe one microgram of extracted RNA to the same amount of cDNA. Quantitative PCR (qPCR) was then performed on the ABI StepOne Plus Real-Time PCR system, which was purchased from Applied Biosystems (Grand Island, NY), to quantify the mRNA level of target gene expression. SYBR Green is used as a detection reagent, and the data was normalized to the internal control (GAPDH mRNA) by ΔΔCt method. A melting curve was also included to verify all quantitative PCR products had a single DNA duplex. All primers sequence are summarized in Table 1 and synthesized by Sigma (St Louis, MO)

4.3.8. Statistical Analysis

One-way analysis of variance and student's t-test (Graph Pad Prism Software, La Jolla, CA) were used to determine the statistical significance. The data were expressed as mean ± s.d. and considered as a statistical difference when the P-value is less than 0.05 ($P<0.05$)

4.4. RESULTS

4.4.1. Hydrodynamic gene transfer results in a rapid increase in serum concentration of IL-15/sIL-15Rα without inducing liver damage

Hydrodynamic delivery of 2 μg of AG209 DP muIL-15sRα+IL-15 plasmids (Figure 4.1a) was performed on C57BL/6 mice according to the established procedure [154]. Serum concentration of IL-15/sIL-15Rα reached peak level at ~ 10 μg ml^{-1} 1 day after the injection and gradually declined to ~ 5 ng ml^{-1} within 3 days (Figure 4.1b). Three days after the injection, blood chemistry tests showed no significant increase in the serum level of liver-specific enzymes of AST or ALT, indicating no liver damage with the gene transfer (Figure 4.1c). Histochemical examination of the liver (Figure 1d) revealed no difference in the liver structure between mice with or without gene transfer. These results prove that a high level of Il-15/sIl-15Rα gene expression can be successfully achieved by hydrodynamic gene delivery.

4.4.2. Il-15/sIl-15Rα gene transfer activates NK and T cells in the lungs, liver and kidneys.

IL-15 has a major role in supporting and maintaining the activity of NK and T cells [14]. To analyze the effects of IL-15/sIL-15Rα expression on NK and T cells, we measured the mRNA levels of marker genes for activated NK and T cells in the lungs, liver and kidneys. Three days after hydrodynamic injection of IL-15/sIL-15Rα plasmids, a significant increase in the mRNA level of *granzyme B* (lungs,~ 150-fold; liver, ~ 310-fold; kidneys, ~ 93-fold) and *perforin* (lungs, ~ 72-fold; liver, ~ 128-fold; kidneys, ~ 16-fold) was seen (Figure 4.2a and b). In addition, transcription of *Ifn-γ*, a type II interferon produced primarily by NK cells and cytotoxic T lymphocytes, and its dominant T-box transcription factor TBX21 (*T-bet*), was also significantly increased in the same organs (Figure 4.2c and d). Further, Il-15/sIl-15Rα gene transfer resulted in

an increase in $CD8^+$ cytotoxic T cells, but not in $CD4^+$ T-helper cells, in the lungs, liver and kidneys (Figure 4.2e and f). Together, these results suggest that Il-15/sIl-15Rα gene transfer is potent in inducing the NK and T cell activation in these three organs.

4.4.3. Il-15/sIl-15Rα gene transfer significantly inhibits tumor growth in the lungs, liver and kidneys

To evaluate the activity of IL-15/sIL-15Rα against Lewis lung tumor growth in different organs, we utilized the method of hydrodynamics- based cell delivery to seed and grow tumor cells in the lungs, liver and kidneys [208]. Bio-imaging revealed efficient delivery and progression of tumor cells in the lungs, liver and kidneys (Figure 4.6a). Eight days after the initial tumor cell injection, all mice developed macroscopic tumor nodules (Figure 4.6b). Tumor growth in these organs was confirmed by the presence of tumor nodules identified from the surface of the lungs (mean, 17; range, 13–25), liver (mean, 35; range, 31–40) and kidneys (mean, 3; range, 1–6) (Figure 4.6c). Assessment of luciferase activity in different organs 8 days after tumor cell injection concludes that tumor growth remained confined to the lungs, liver and kidneys (Figure 4.6d).

The therapeutic effect of IL-15/sIL-15Rα on tumor growth in the lungs, liver and kidneys is shown in Figure 4.3. Two micrograms of AG209 DP muIL-15sRα+IL-15 plasmids was transferred into tumor bearing mice 3 days after tumor cell delivery. Ten days later, animals transferred with the Il-15/sIl-15Rα gene showed significantly lower tumor load on the surface of the lungs, liver and kidneys (Figure 4.3a). H&E staining of the tissue sections from these organs shows a smaller microscopic tumor (Figure 4.3b). The total number of tumor nodules in IL-15/sIL-15Rα-treated mice is ~ 62% less than that of control in the lungs, ~ 89% less in the liver

and ~ 92% less in the kidneys (Figure 4.3c). These results suggest that *Il-15/sIl-15Rα* gene transfer is effective in suppressing tumor growth in the lungs, liver and kidneys.

4.4.4. Combination of Il-15/sIl-15Rα gene therapy and gemcitabine chemotherapy enhances antitumor effects.

We next examined the combined effects of *Il-15/sIl-15Rα* gene therapy and gemcitabine-mediated chemotherapy. For comparison purpose, individual treatment with gemcitabine or IL-15/sIL-15Rα plasmid was also included. Chemotherapy was conducted by intraperitoneal injection of gemcitabine (120 mg kg^{-1}) on days 3, 8 and 12 after hydrodynamic tumor cell inoculation. Gene therapy was carried out with hydrodynamic delivery of 2 μg per mouse of IL-15/sIL-15Rα plasmid on days 3 and 12. The treatment employed the combination of the two individual treatment procedures. Bioluminescent imaging 6 h after tumor cell injection showed successful seeding of tumor cells (Figure 4.4a). Compared with control mice with a rapid progression of cancer development, mice with gemcitabine treatment showed suppression of tumor growth as assessed on day 8 after tumor cell injection. Similarly, animals with Il-15/sIl-15Rα gene transfer showed excellent antitumor activity in the liver and kidneys, but a moderate activity in the lungs. No luminescent signals were detected in animals receiving the combined treatment of gemcitabine and Il-15/sIl-15Rα gene transfer.

Interestingly, luminescence reappeared in the lungs of animals with combined treatments starting on day 12 after cell injection, indicating growth of the tumor cells in the lungs (Figure 4.4b). The survival curve of all treated animals is shown in Figure 4.4c. Compared with control animals showing a median survival time of 10 days after hydrodynamic tail vein injection of tumor cells, animals with *Il-15/sIl-15Rα* gene therapy lived an average of 17 days. Similar

increase in median survival time was also seen in the gemcitabine-treated animals (17 days, 1.75-fold longer than that of control animals). Combined treatment resulted in the best outcome, a median survival time of 33 days, 3.3-fold longer than that of control animals.

4.4.5. IL-15/sIL15Rα-based therapies show predominant antitumor activity in the liver and kidneys.

Further examination was carried out to confirm the antitumor efficacy of IL-15/sIL-15Rα-based gene therapy. Animals in each treatment group were killed before their death, and organs were collected for tumor identification. Results in Figure 4.5a reveal that treatment with *Il-15/sIL-15Rα* gene transfer alone or in combination with gemcitabine was more effective in blocking tumor growth in the liver and kidneys, but failed to suppress tumor growth in the lungs. This conclusion is also supported by luciferase assay (Figure 4.5b). Taken together, these results suggest that IL-15/sIL-15Rα-based therapies are more effective in suppressing tumor growth in the liver and kidneys.

4.5. DISCUSSION

In the present work, we evaluated the effects of IL-15/sIL-15Rα gene therapy on Lewis lung tumors growing in the lungs, liver and kidneys. Our results demonstrated that transfer of the *Il-15/sIl-15Rα* gene using hydrodynamic delivery resulted in peak level of circulating IL-15/sIL-15Rα and activation of NK and T cells in these organs (Figures 4.1 and 4.2). *Il-15/sIl-15Rα* gene transfer resulted in the suppression of tumor growth and enhanced antitumor activity of gemcitabine when gene therapy and chemotherapy were combined (Figures 4.3 and 4.4).

Mechanistically, we demonstrate that Il-15/sIl-15Rα gene transfer is effective in blocking tumors in the liver and kidneys, but not as effective in the lungs (Figure 4.5).

Hydrodynamic delivery of codon-optimized IL-15/sIL-15Rα plasmid is effective and safe to achieve a high level of IL-15/sIL-15Rα expression (Figure 4.1). Previous reports demonstrated that a pharmacologic dose at 10 ng ml^{-1} of IL-15 in the serum is the minimum requirement for rapid mobilization and activation of NK cells in peripheral organs such as the lungs [171]. The AG209 DP muIL-15sRα+IL-15 plasmid was chosen for this study because of its optimized features of a strong CMV promoter, a better leader sequence of granulocyte-macrophage colony-stimulating factor and optimized coding sequences (Figure 4.1a). Serum concentration peaked at ~ 10 μg ml^{-1} and was achieved with 2 μg of plasmid injection (Figure 4.1b) with no liver toxicity detectable 3 days after the injection (Figure 4.1c and d).

Transfer of the *Il-15/sIl-15Rα* gene induces the activation of NK and T cells in the lungs, liver and kidneys, resulting in effective suppression of tumor growth in these three organs (Figures 4.2 and 4.3). Indeed, a previous study has shown that hydrodynamic delivery of the *Il-15/sIl-15Rα* gene induces a significant increase in NK, T and $CD8^+$ memory T cell distribution in the lungs, liver and spleen[171]. In tumor-bearing animals, Cheng *et al.* [202] demonstrated that delivery of IL-15/sIL-15Rα containing DNA plasmid induces the expansion and infiltration of tumor-specific $CD8^+$ T cells in tumor-bearing liver, where the cytotoxic function is enhanced. Chang *et al.* [204] also showed compelling evidence that administration of adeno-associated virus vector containing the *Il-15/sIl-15Rα* gene remarkably enhanced NK cell cytolytic activity in a liver metastatic model. In line with these studies, our results showed that *Il-15/sIl-15Rα* gene transfer significantly enhanced the NK and T cell activity in the environment of the lungs, liver and kidneys, as evidenced by increased mRNA levels of marker genes, including *granzyme B,*

perforin, Ifn-γ, T-bet and *Cd8* (Figure 4.2a–e), leading to a significant inhibition of tumor growth (Figure 4.3). Furthermore, transfer of the *Il-15/sIl-15Rα* gene did not alter the transcription of *Cd4* (Figure 4.2f). This result is in agreement with a previous study where treatment with IL-15/sIL-15Rα did not significantly increase the overall number of total $CD4^+$ population or regulatory $CD4^+$ T cells [171, 202], indicating that *Il-15/sIl-15Rα* gene transfer activated an antitumor immune pathway without inducing immune suppressive pathways in the lungs, liver and kidneys.

Results in Figure 4 show that combining *Il-15/sIl-15Rα* gene therapy with gemcitabine chemotherapy yields a better therapeutic outcome for tumors growing in multiple organs including the lungs, liver and kidneys. This finding is in line with a previous report that indicates that IL-15 administration increased the antitumor activity of chemotherapeutic agents, cyclophosphamide, in mice bearing rhabdomyosarcoma [123, 178]. Moreover, as an Food and Drug Administration (FDA)-approved first-line chemotherapeutic agent for patients with early and advanced stage non-small cell lung cancer, gemcitabine administration also demonstrated enhanced antitumor activity when combined with IFN-β [209, 210]. This may be partially due to the selective elimination of the myeloid-derived suppressor cells after gemcitabine administration, where the tumor-derived immunosuppressive environment was diminished and antitumor response, induced by immunotherapy, was improved [211].

Assessments of tumor burden in the lungs, liver and kidneys of animals, immediately before being killed, due to tumor burden, reveal that *Il-15/sIl-15Rα* gene transfer reduced tumor load in the liver and kidneys, but not in the lungs (Figure 4.5a). The same level of luciferase activity was seen in the lungs of all the animals regardless of the type of treatment provided (Figure 4.5b). The differential treatment effects on the lungs and liver/kidneys suggest the existence of different, and organ specific, responses to the serum IL-15/sIL-15Rα. It has been

previously shown that cytokine-based immune therapy is superior in inducing the local infiltration and activation of $CD8^+$ T and NK cells into the tumors in the liver and kidneys, leading to the destruction of established tumors in these two organs [202, 212, 213]. In contrast, lung tumors tend to generate an immunosuppressive environment where tumor cells are able to recruit immunosuppressive factors to impair the cytotoxic T or NK cell function, thus resulting in continued tumor growth [214]. Consistent with these studies, we observed an improved antitumor activity in the lungs at earlier time points with a combination therapy of gemcitabine and *Il-15/sIl-15Rα* gene transfer (Figure 4.4a). It appears that the tumors in the lungs become resistance to the treatment later, leading to aggressive subsequent tumor growth (Figure 4.4b). In fact, gemcitabine resistant tumor growth in the lungs has been previously reported [215]. Although modest success has been demonstrated in overcoming the tumor immune escape in the lungs using the PD-1 immune checkpoint inhibitor antibody [216], a different strategy is needed to cope with drug-resistant tumors in the lungs.

In conclusion, we demonstrate in this study that hydrodynamic delivery of AG209 DP muIL-15sRα+IL-15 plasmid results in a high level of serum IL-15/sIL-15Rα and activation of NK and T cells in the lungs, liver and kidneys. Delivery of the Il-15/sIl-15Rα gene alone, or in combination with gemcitabine, showed remarkable therapeutic benefits in the treatment of tumors growing in the liver and kidneys. Our findings warrant further investigation for possible use of Il-15/sIl-15Rα gene transfer for treatment of late stage lung cancer where the tumor has already metastasized to the liver and kidneys.

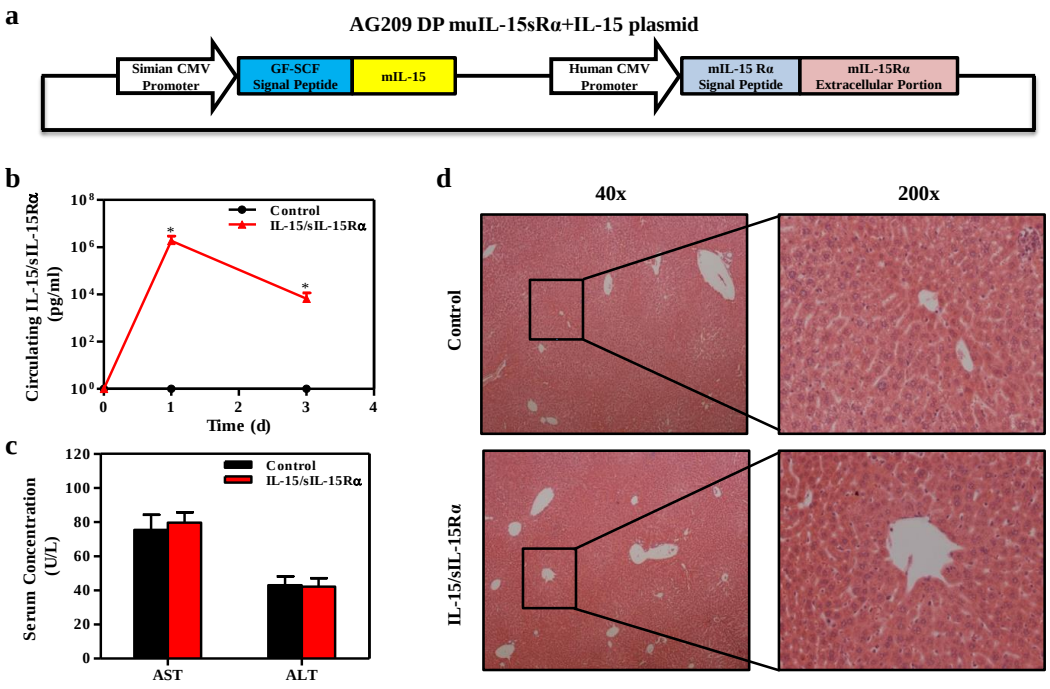

Figure 4.1. Impact of hydrodynamic *Il-15/sIl-15Rα* gene transfer. Mice were hydrodynamically injected with 2 μg AG209 DP muIL-15sRα+IL-15 or pcDNA3.1 plasmid. **(a)** Schematic representation of AG209 DP muIL-15sRα+IL-15 plasmid construct; **(b)** Serum concentration of IL-15/IL-15Rα protein post gene transfer; **(c)** Plasma aspartate aminotransferase (AST) and alanine aminotransferase (ALT) levels; and **(d)** Representative images of H&E staining of mouse liver. Samples in (b) and (c) were collected 3 days after hydrodynamic injection. Results represent mean ± SD (n=5). * P<0.05 comparing to control animals injected with pcDNA3.1 empty plasmid.

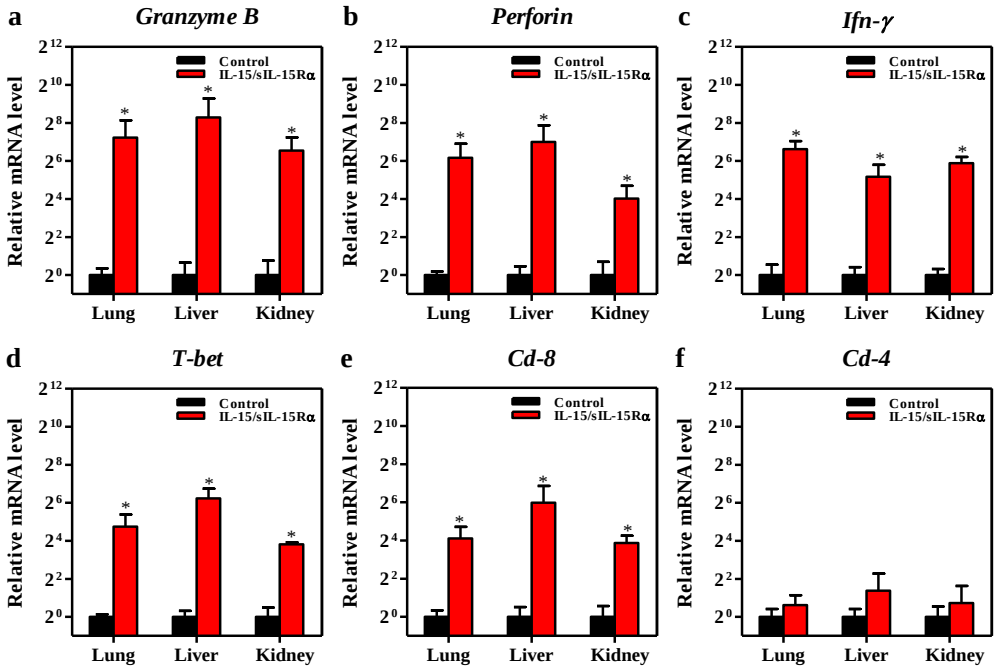

Figure 4.2. *Il-15/sIl-15Rα* gene transfer increases mRNA level of activation marker genes of NK and T cells. Animals were hydrodynamically injected with 2 μg AG209 DP muIL-15sRα+IL-15 or pcDNA3.1 control plasmid. Lungs, liver and kidneys were harvested 3 days later. Relative mRNA levels of marker genes for NK and T cell activation including **(a)** *Granzyme B*; **(b)** *Perforin*; **(c)** Ifn-γ; **(d)** *T-bet*; **(e)** *Cd-8*; and **(f)** *Cd4* were determined using RT-PCR. Data represents mean ± s.d (n=5). * $P<0.05$ comparing to control mice.

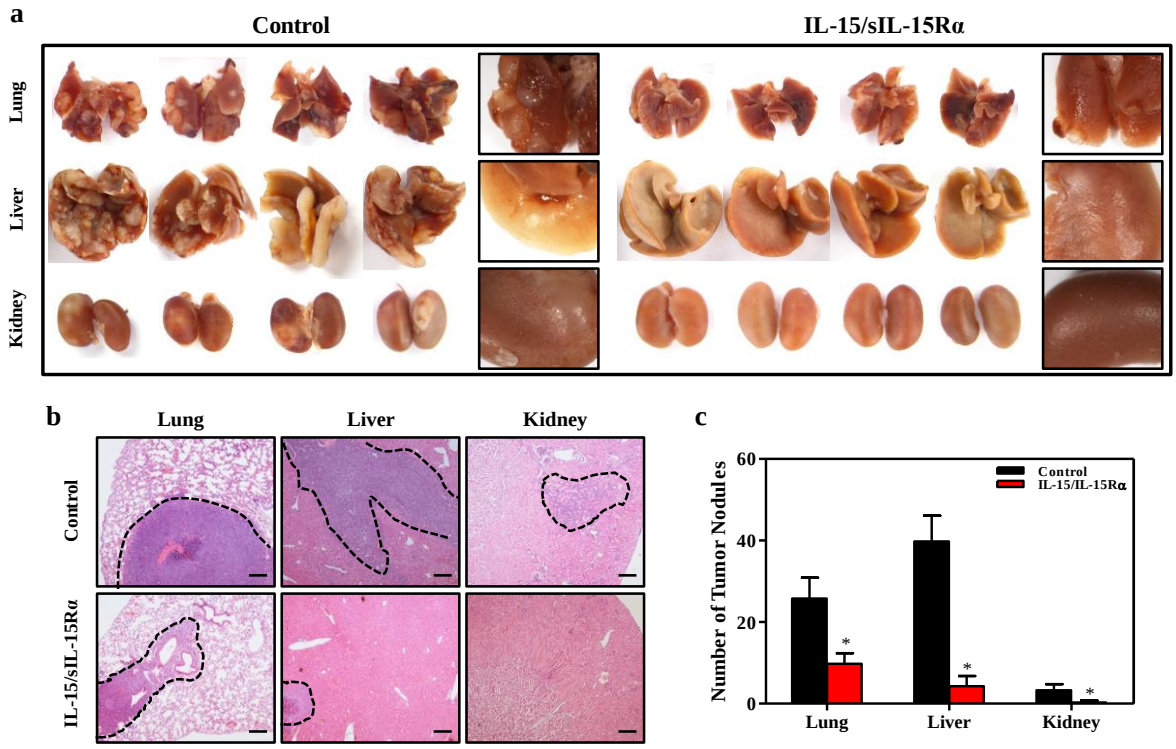

Figure 4.3. ***Il-15/sIl-15Rα*** **gene transfer inhibited tumor growth in the lungs, liver and kidneys.** Animals were hydrodynamically injected with LL/2-Luc cells (10^6 cells/mouse). Three days after tumor injection, animals received hydrodynamic injection of 2 μg/mouse of AG209 DP muIL-15sRα+IL-15 plasmid or pcDNA3.1 control plasmid. All animals were sacrificed 10 days after tumor injection. **(a)** Tumor loads in the lungs, liver and kidneys. Right panel represents enlarged organ pictures of treated and control animals. **(b)** Representative H&E staining of tissue sections from the lungs, liver and kidneys. Bar represents 200 μm. **(c)** Number of nodules in the lungs, liver and kidneys. Results represent mean ± s.d (n=4). * P<0.05 comparing to control animals. Numbers of tumor nodules were counted under the dissecting microscope. Areas circled with dotted lines are microscopic tumor identified by H&E staining.

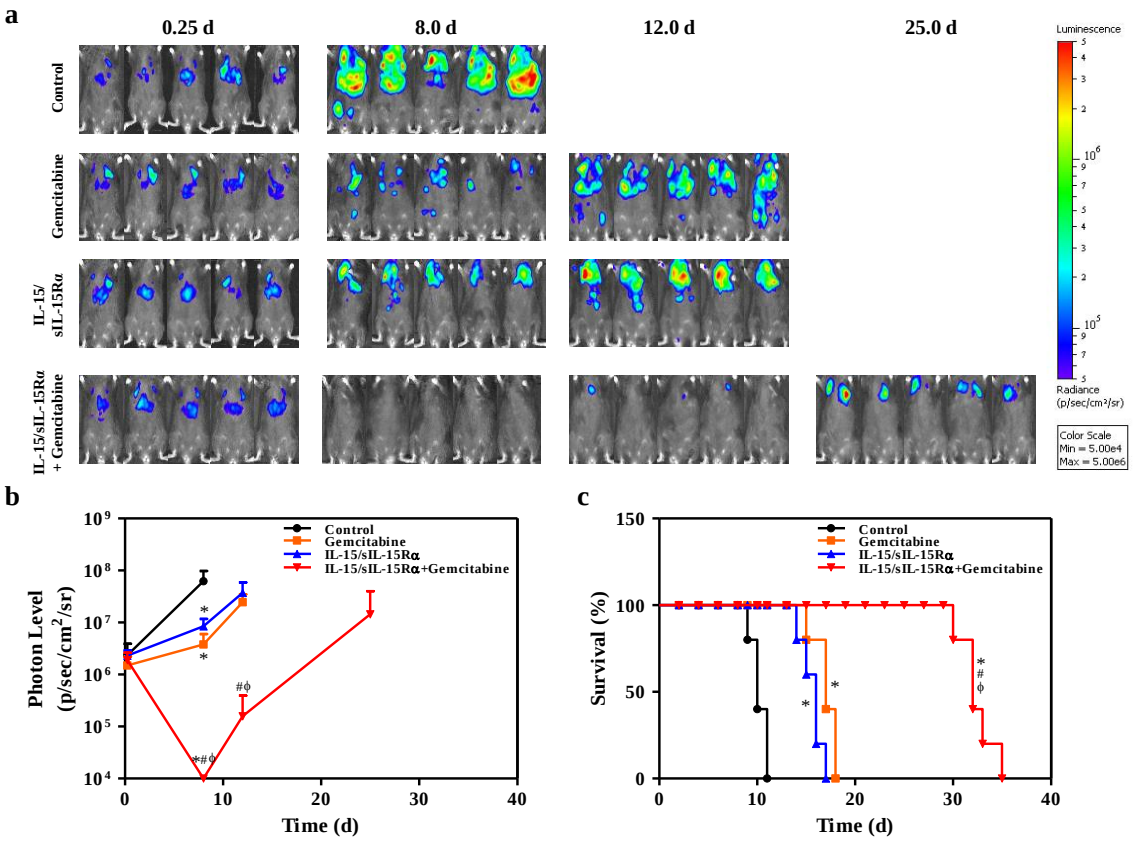

Figure 4.4. Antitumor activities of *Il-15/sIl-15Rα* gene therapy, chemotherapy, or in combination. Animals inoculated with LL2-Luc cells were treated with saline, gemcitabine (120 mg/kg/mouse), AG209 DP muIL-15sRα+IL-15 plasmid (2 μg/mouse), or in combination at designated time. **(a)** Bioluminescence images taken at 0.25, 8.0, 12.0 and 25.0 days post tumor cell inoculation; **(b)** Time dependent bioluminescence intensity in different treatment groups; and **(c)** Survival curves of animals with different treatments (n=5, P <0.05 for pooled data, log-rank test). Data represent mean ± s.d (n=5). **P*<0.05 comparing to control animal; # *P*<0.05 comparing to animals treated with gemcitabine; ϕ *P*<0.05 comparing to animals with *Il-15/sIl-15Rα* gene transfer.

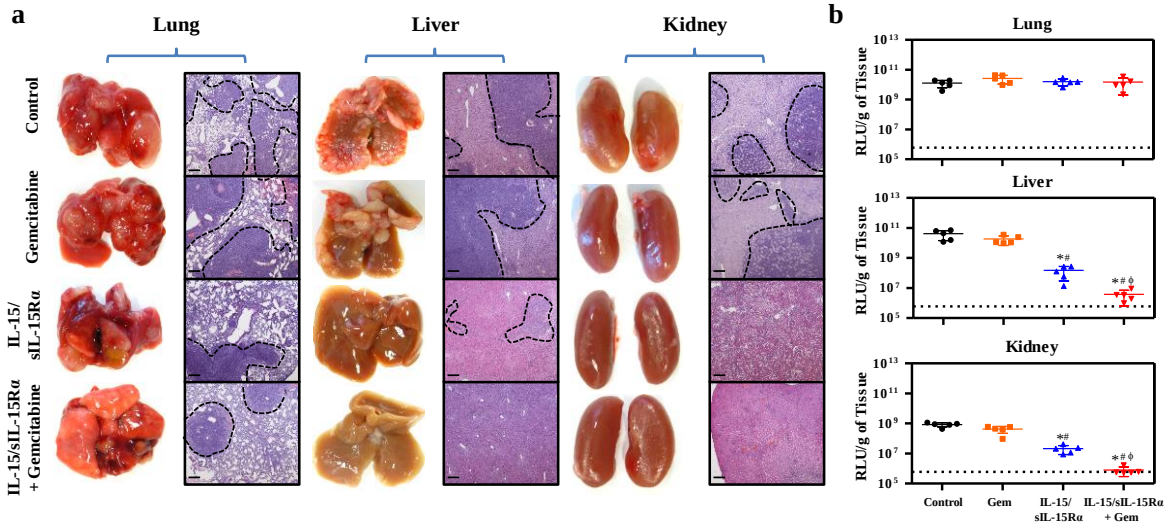

Figure 4.5. *Il-15/sIl-15Rα* gene therapy showed predominant antitumor activity in the liver and kidneys. Selected animals in each treatment group were sacrificed prior to their death and organs collected. **(a)** Photos and images of H&E staining of tumor bearing lungs, liver, and kidneys. Bar represents 200 μm. **(b)** Relative luciferase activity per gram of tissue. Data represents mean ± s.d (n=5). * $P<0.05$ comparing to control animal; # $P<0.05$ comparing to animals treated with gemcitabine; and ϕ $P<0.05$ comparing to animals with *Il-15/sIl-15Rα* gene transfer. Areas surrounded by dotted lines are microscopic tumors identified by H&E staining.

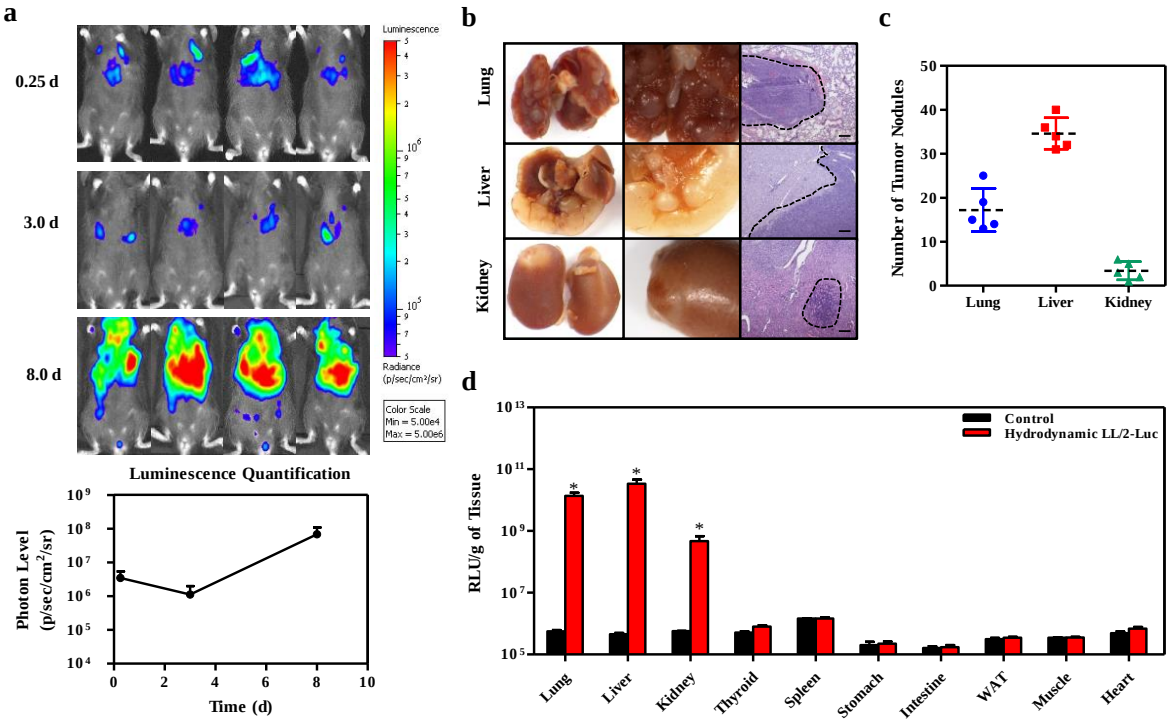

Figure 4.6. Establishment of tumor growth in the lungs, liver and kidneys. Animals were hydrodynamically injected with luciferase tagged LL/2 cells (106 cells/mouse). Normal mice were used as control. **(a)** Bioluminescence images and quantification of photon level in tumor bearing mice after 0.25, 3 or 8 days of tumor cell injection. **(b)** Representative photo and images of H&E staining of the lungs, liver and kidneys. Bar represents 200 μm. **(c)** Number of nodules in the lung, liver and kidneys. **(d)** Relative luciferase activity in the selected organs. Samples in (b) to (d) were collected 8 days after hydrodynamic cell delivery. Each data represent mean ± s.d (n=5). * $P<0.05$ comparing to control animals. Numbers of tumor nodules were counted under the dissecting microscope. Areas circled with dotted lines are microscopic tumor identified by H&E staining.

Table 4.1. Primer sequences for real time PCR analysis of gene expression

Gene	***Forward primer sequence***	***Reverse primer sequence***
Cd4	AGGTGATGGGACCTACCTCTC	GGGGCCACCACTTGAACTAC
Cd8	CCGTTGACCCGCTTTCTGT	CGGCGTCCATTTTCTTTGGAA
Gapdh	AGGTCGGTGTGAACGGATTTG	TGTAGACCATGTAGTTGAGGTCA
Granzyme b	CCACTCTCGACCCTACATGG	GGCCCCCAAAGTGACATTTATT
Ifn-γ	ATGAACGCTACACACTGCATC	CCATCCTTTTGCCAGTTCCTC
Perforin	AGCACAAGTTCGTGCCAGG	GCGTCTCTCATTAGGGAGTTTTT
T-bet	AGCAAGGACGGCGAATGTT	GGGTGGACATATAAGCGGTTC

CHAPTER 5

PERSPECTIVES OF IL-15 THERAPEUTICS

IL-15 was first classified as a T lymphocytes growth factor in 1994 by two laboratories [4, 40]. Burton *et al*. first identified IL-15 as a 14 kDa lymphokine secreted by the leukemia virus-1 infected human cell line (HuT-102), which could stimulate the proliferation and activation of T lymphocytes and large granular lymphocytes [40]. Grabstein *et al.*, on the other hand, isolated a 14–15 kDa cytokine (named IL-15) from the epithelial cell line supernatant, which shows similar biological functions with IL-2 [4]. Since then, extensive studies have been conducted to investigate the biological function and therapeutic implications of IL-15, primarily focusing on cancer immunotherapy and, more recently, the treatment of metabolic disorders.

5.1. IL-15 AND ITS APPLICATIONS IN CANCER THERAPY

Numerous preclinical studies have been conducted demonstrating the therapeutic activity of IL-15 against cancer [127, 129, 135, 140]. The earlier work showed that overexpression of IL-15 in mice significantly suppresses tumor growth and prolongs the survival of animals to 8 months compared to 6 weeks for control mice intravenously injected with MC38 colon carcinoma cells [217]. A mechanistic study by Klebanoff *et al*. demonstrated that mice transferred with the IL-15 gene have stronger tumor-reactive $CD8^+$ T cells [218]. Studies by Yu *et al.* [219, 220] and Zhang *et al*. [127] also reported strong tumor suppression activity of IL-15 in mice carrying PC26, MC38 colon cancer, or TRAMP-C2 prostate cancers.

Early successes in animal studies led to significant efforts in exploring the therapeutic potential of IL-15 and its toxicity in non-human primates [47, 141-143, 221, 222]. Using virus-infected rhesus macaques as a model, Munger *et al.* reported a 3-fold induction of peripheral $CD8^+$ and NK cells in animals with twice-weekly subcutaneous injections of 10 or 100 μg/kg rIL-15 for four weeks [141]. Similar results were obtained using an intravenous bolus infusion [142, 143] and continuous infusion [221]. Only transient neutropenia has been observed in these studies, without clinical chemistry test changes and induction of organ failure and VLS [142]. In addition, no animals developed autoimmune disorders or antibodies to the administered IL-15.

To date, *E. coli*-produced rhIL-15 has been used in five clinical trials for cancer immunotherapy (Table 1.1). The objectives of these trials are focused on assessing its toxicity profile, including the dose-related adverse events and maximum tolerance dose, and evaluating the anti-tumor activity after rIL-15 administration. In a published clinical study [144], rhIL-15 was designed to be infused intravenously (*i.v*) at a daily dose of 3 μg/kg/day for 12 days to patients bearing various metastatic cancers. Due to the development of unexpected side effects, such as grade-3 hypotension and thrombocytopenia, in two patients with a dose of 3 μg/kg/day, the study further adjusted its dosing strategies and included two lower doses at 1.0 and 0.3 μg/kg/day [144]. The maximum tolerated dose of rhIL-15 was finalized as 0.3 μg/kg/day, since all nine patients receiving 12 doses showed no signs of toxicity [144]. However, patients did show modest capillary leak [144]. The pharmacokinetic results demonstrated that the maximum concentration (C_{max}) after bolus *i.v* infusion of rhIL-15 was 43,800, 15,900 and 12,060 pg/ml at the dose of 3.0, 1.0 and 0.3μg/kg/day, respectively [144]. In addition, the half-lives ($t_{1/2}$) for these three doses were very similar, at 2.4, 2.7 and 2.7 h [144]. Importantly, administration of rhIL-15 showed a modest anti-tumor activity [144]. Five patients showed a reduction of their tumor lesions by 10% to 30%, and

two patients demonstrated clearance of tumors in the lung [144]. However, a C_{max}-related toxicity was observed with intravenous bolus injection of IL-15. When exceeding C_{max} of 43,800 pg/ml, bolus infusion of rIL-15 showed a transient induction of pro-inflammatory cytokines release, which led to multiple adverse events [144]. Compared to intravenous bolus injection, subcutaneous or continuous intravenous infusion (CIV) appears much better in avoiding high C_{max} levels [142, 221]. At the dose of 20 μg/kg/day, the C_{max} for rhIL-15 bolus infusion was 720 ng/ml, whereas the Cmax for subcutaneous infusion and CIV of rhIL-15 were 50 ng/ml and 4 ng/ml, respectively [142, 221]. Moreover, comparing only 4-fold induction of memory $CD8^+$ T cells obtained by bolus infusion, CIV administration of rhIL-15 was able to stimulate the proliferation of memory $CD8^+$ T cells by 80- to 100-fold, whereas subcutaneous IL-15 led to a modest proliferation of memory $CD8^+$ T cells by 10-fold [142, 221].

Some efficacy has been seen in human trials for the treatment of metastatic malignancy, but the overall outcome was less satisfactory [144]. The major challenge seems to be the lack of a method that maintains a therapeutic level of IL-15 in the blood with optimal activity to stimulate the proliferation and differentiation of $CD8^+$ T and NK cells. Additionally, more studies have shown that monomeric IL-15 may not be the best choice for cancer treatment. IL-15 and sIL-15Rα complexes seem to work better by showing a longer blood half-life and improved biological activity. Therefore, future research direction should be geared toward exploring the possibility of using a pre-associated IL-15/IL-15Rα complex as the therapeutic agent for IL-15-based therapy.

5.2. IL-15 AND METABOLIC HOMEOSTASIS

As early as 1995, Quinn *et al.* proposed that IL-15 plays an critical role in stimulating the differentiation of muscle fibers and myocytes for contractile proteins accumulation [100]. Since then, studies have been conducted to investigate this activity of IL-15 in muscle and muscle-related functions.

About 40% of body weight is made up of skeletal muscle, and it is considered the largest organ in non-obese humans. Muscle cells are known for their capacity to produce high levels of several secreted factors [223]. Pedersen *et al.* demonstrated in 2003 that muscle cells produce cytokines and other peptides that exert endocrine effects, which were later named "myokines" [224]. Riechman *et al.* demonstrated that the blood concentration of IL-15 increased in young men and women during a 10-week period of physical training that focused on resistance endurance [225]. Similarly, elevated expression of IL-15 in plasma and skeletal muscle was observed in a treadmill exercise with rats on a high-fat diet [152].

Clinical investigations revealed that the level of circulating IL-15 was negatively associated with BMI and the mass of total fat, trunk, and limb fat in human subjects [138]. IL-15 knock-out mice showed a higher amount of body fat than the wild type.[90] Conversely, mice transferred with the *Il-15* gene showed lower levels of fat accumulation and were resistant to high-fat diet-induced obesity.[150] These results suggest that IL-15 acts as a key reciprocal regulator, which influences the body weight and fat deposition by adjusting the protein synthesis and metabolic rate in the skeletal muscle and adipose tissue [99].

The therapeutic potential of IL-15 as an anti-obese agent has been evaluated in several animal studies. Carbo *et al.* demonstrated that administration of recombinant IL-15 protein resulted in ~33% fat mass reduction, ~20% decrease in circulating triacylglycerols, ~47%

reduction of hepatic lipogenic rate, and ~36% decrease in plasma VLDL in rats [92]. Furthermore, a study by Nielsen *et al.* revealed ~26% decrease in trunk fat mass in IL-15-transfected mice fed a high-fat diet [138]. In agreement with these animal studies, results from the work summarized in this dissertation show that *Il-15* gene transfer by hydrodynamic delivery blocks high-fat diet-induced body weight gain (Chapter 2). The benefits generated also include ~67% reduction in total fat mass, alleviation of adiposity and fatty liver, and improvement of insulin resistance. Results in Chapter 3 further show that transfer of the *Il-15/sIl-15Rα* gene into obese mice induced ~15% body weight loss. Meanwhile, the fact that *Il-15/sIl-15Rα* gene transfer did not induce weight loss in regular mice fed a chow diet indicates that the activity of IL-15/sIL-15Rα in reducing body weight is specific to obese mice. It is also evident that transfer of the *Il-15/sIl-15Rα* gene enhanced lipid and glucose metabolism, and consequently led to the alleviation of fatty liver, and improvement of glucose homeostasis.

Similar to IL-15-based immunotherapy for the treatment of cancer, IL-15-based treatment of obesity and obesity-associated metabolic diseases may gain significant advances when monomeric IL-15 is replaced with IL-15/sIL-15Rα complexes, due to their superior circulation half-life in blood and higher biological activities. The challenge, however, is the regulation of the IL-15 level in a therapeutic window without inducing the toxic effects.

5.3. FUTURE PERSPECTIVE

The future direction of IL-15-based pharmaceutics may lie in the improvement of its biologic activity by coupling IL-15 with sIL-15Rα. The combination of sIL-15Rα with IL-15 presents a number of advantages over monomeric IL-15. Mechanistically, IL-15/sIL-15Rα represents physiological form since IL-15 is produced as a heterodimer in association with sIL-

15Rα [31, 34]. In addition, IL-15/sIL-15Rα can be efficiently generated in mammalian cells and properly glycosylated [226]. Due to the larger overall protein size and glycosylation, the IL-15/IL-15Rα complex has a much longer $T_{1/2}$ in the plasma compared to the monomeric IL-15 [226]. Significant evidence is available in support of such a notion. For example, cell culture studies have shown that inclusion of sIL-15Rα is able to increase the IL-15 mediated proliferation of NK and $CD8^+$ T cells, which could not be achieved with IL-15 alone at similar concentration [114, 226, 227]. In a human immune system (HIS) mouse model, administration of preformed rhIL-15 covalently linked by the human IL-15Rα 'sushi' domain (IL-15/IL-15Rα-sushi) resulted in development of NK cells in HIS mice and $CD8^+$ T cell proliferation which did not occur when IL-15 was used alone [205, 228]. Moreover, administration of pre-formed IL-15/sIL-15Rα induced the preferential expansion of memory $CD8^+$ T cells in B6 mice [206].

Efforts have been made to demonstrate the therapeutic advantages of IL-15/sIL-15Rα in cancer therapy. Steel *et al.* reported that overexpression of membrane-bound IL-15/sIL-15Rα complexes in DCs is able to induce the immune activities to suppress the *neu* (*Erbb2*)-positive mammary tumor growth in animals [203]. Bessard *et al.* demonstrated high anti-tumor activity using the IL-15 and sIL-15Rα fusion protein in mice bearing metastatic colorectal and melanoma cancer [205]. In mice bearing B16 melanoma or TRAMP-C2 renal tumors, the IL-15/sIL-15Rα complex has shown greater efficacy in prolonging survival time of tumor-bearing mice [206]. Consistently, the results presented in this dissertation confirm that transfer of *Il-15/sIl-15Rα* gene is effective in activating NK and T cells in the lungs, liver and kidneys, leading to an effective suppression of Lewis lung tumor growth in these organs and prolonged animal survival time (Chapter 4).

In contrast, less information is available in applying IL-15/sIL-15Rα to mediate metabolic homeostasis. This is likely due to the lack of a full understanding of the role that IL-15Rα plays in controlling body composition and metabolic activity [229]. However, studies in obese rats have reported lower expression of IL-15Rα mRNA and protein in adipose tissues [152], and treadmill running was able to restore IL-15Rα expression in adipose tissue, resulting in a reduction of body weight and elevation of plasma IL-15 concentration in diet-induced obese rats [152]. Studies by O' Connell *et al.* showed that IL-15 directly induces the level of pro-oxidative gene expression in skeletal muscle through a mechanism that requires the interactions between IL-15 and IL-15Rα *in vitro*, suggesting the functional roles of IL-15Rα in supporting IL-15 mediated metabolic activity [230]. In this dissertation study, we are the first to use the IL-15/sIL-15Rα combination to treat obesity and obesity-associated metabolic disorders (Chapter 3). Our results showed that transfer of the *Il-15/sIl-15Rα* gene in obese mice induces lipid and glucose metabolism, consequently leading to the body weight reduction, alleviation of fatty liver, and improvement of glucose homeostasis.

It is worth noting that clinical trials have been or are being conducted to assess the therapeutic effect of IL-15 pre-association with sIL-15Rα or with sIL-15Rα IgG1-Fc (Table 1.1). Altor BioScience Corporation has launched several dose-escalation clinical trials in patients with different cancers using ALT-803, a combination of pre-associated mutant IL-15 and IL-15Rα sushi domain linked to a single Fc fragment of IgG1 (ClinicalTrials: NCT01946789, NCT02099539, NCT02138734, NCT02384954 and NCT01885897). Admune Therapeutics LLC, which is in conjunction with the NCI, is running a clinical trial by subcutaneously injecting the heterodimer IL-15/sIL-15Rα into patients with metastatic malignancy (ClinicalTrials:

NCT02452268). It is highly anticipated that these ongoing studies will provide valuable information regarding IL-15/sIL-15Rα therapy.

Although direct injection of rIL-15 or pre-associated rIL-15/sIL-15Rα shows efficacy in the treatment of cancer and obesity, expression of IL-15 or IL-15/sIL-15Rα through gene transfer appears more desirable as it eliminates the procedures of protein production, formulation development, and repeated administration. In therapy, the gene therapy-based approach is a great advantage because the patients will be able to produce their proteins whenever needed. With a proper control of the level and persistence of gene expression, one would be able to maintain the therapeutic concentration of IL-15/sIL-15Rα without the risk of C_{max}-associated toxicities.

A critical aspect of gene therapy is gene delivery using either viral, nonviral, or physical methods. Yu *et al.* have explored the use of a recombinant adeno-associated virus (rAAV) vector carrying the *hIl-15* gene to maintain the expression of the *Il-15* gene in mice with experimental breast cancer [231]. The results showed that administration of rAAV-constructed hIL-15 delayed the development of tumors and prolonged the survival rate. Similarly, Yiang *et al.* performed rAAV-mediated *hIl-15* gene transfer into mice prior to tumor cell inoculation and reported suppression of development of human cervical cancer [232]. Moreover, also employing rAAV vector (AAV-8), Chang *et al.* employed IL-15/sIL-15Rα to treat metastatic hepatocellular carcinoma in mice [204]. The results demonstrated that overexpression of the *Il-15/sIl-15Rα* gene potentiated anti-tumor activity by increasing the expansion of hepatic NK cells [204].

Other viral vectors to express the *Il-15* gene in experimental animals have also been utilized. Using vesicular stomatitis virus (VSV), Stephenson *et al.* demonstrated that intravenous injection of a VSV vector with the *hIl-15* gene (VSV-hIL-15) induced anti-tumor activity in animals bearing established colorectal carcinoma and pulmonary metastases [233]. Moreover, Barra

et al. demonstrated that adenoviral vector-mediated *Il-15* gene transfer induced weight loss in obese mice fed on a high-fat diet without altering food intake [90]. *Il-15* gene transfer reduced lipid deposition in adipocytes, and improved glucose homeostasis and insulin sensitivity in the response to oral glucose administration [90, 107].

Non-viral gene transfer approaches have also been tested for IL-15 therapeutics. Using novel cationic nano gel, and heparin-polyethyleneimine (HPEI) complexed with plasmid carrying the *hIl-15* gene, Zhou *et al.* showed that overexpression of *Il-15* gene transfer significantly inhibited the growth of B16-F10 and CT26 tumor cells in mouse lung, while IL-15 induced the infiltration of cytotoxic NK and T cells into tumor sites and was accompanied by increased TNF-α and IFN-γ production, and ultimately resulted in the apoptosis of tumor cells [234]. In an orthotopic bladder cancer model inoculated with MBT-2 cells, Matsumoto *et al.* employed liposomal carrier for *Il-15* gene delivery and reported higher $CD8^+$ T cell infiltration into tumor sites and growth inhibition of subcutaneously injected MBT-2 cells [235]. Similarly, using the approach of intra-tumor injection of plasmids carrying the *hIl-15* gene coupled with electroporation, Ugen *et al.* showed an enhanced anti-tumor response in mice bearing B16-F10 melanoma cells [236].

Compared to the above-mentioned methods for gene transfer, the hydrodynamics-based procedure provides an effective means for convenient gene delivery [157]. Using this method, combined gene transfer of plasmids carrying the *Il-15* and *Il-21* genes exerted a synergistic stimulation of NK cells and showed a potent anti-tumor effect against established metastatic lymphoma in liver [122]. Similarly, hydrodynamic delivery of IL-15/sIL-15Rα-Fc plasmids showed therapeutic effects on both well-established metastatic and autochthonous liver tumor in mice [202]. The work summarized in this dissertation also employed the hydrodynamics-based procedure to

achieve over-expression of IL-15 in the form of either IL-15 or IL-15/sIL-15Rα complexes. The results confirm that the method of hydrodynamic gene transfer is effective in delivering the *Il-15* or *Il-15/sIl-15Rα* gene to mouse liver, and generating high serum level of IL-15 or IL-15/sIL-15Rα in the blood. Elevation in the protein level of IL-15 blocks high-fat diet-induced obesity, insulin resistance, and development of fatty liver (Chapter 2). Similarly, *Il-15/sIl-15Rα* gene transfer in obese mice results in the reduction of body weight and improvement in glucose homeostasis and insulin sensitivity (Chapter 3). In addition, hydrodynamic transfer of *Il-15/sIl-15Rα* genes into mice carrying the Lewis lung tumor in the lungs, liver, and kidneys prolongs the survival time of tumor-bearing animals (Chapter 4).

Collectively, the results from previous studies provide strong evidence in support of applying IL-15-based gene therapy to the treatment of cancer and metabolic diseases, such as obesity. Further studies need to focus on improving not only the methods of gene delivery, but also the gene expression system for sustained gene expression with potential for regulation.

An alternative approach coupling IL-15 therapy with other strategies is worth considering. During tumor development, tumor cells tend to generate a tumor-derived immunosuppressive microenvironment, which inhibits the infiltration of effector T and NK cells into the tumor bed and suppresses their cytotoxic activity, and ultimately results in the "helpless state" of immune effector cells that thereby promotes the tumor progression [213]. It is also recognized that the poor efficacy of IL-15-mediated immunotherapy might be due to the process known as tumor tolerization [213]. The tumor cells can alter the level of effector immune mediators in response to IL-15-based therapy, including the change of co-stimulatory and -inhibitory molecule levels and the ratio of APCs and cytotoxic T and T_{reg} cells [213]. Alteration of these immune mediators could result in the development of the immunosuppressive environment in

tumor sites and the deactivation of the anti-tumor activity, including the suppression of APCs functions, inhibiting the T and NK cells cytotoxicity, and inducing the T_{reg} activity [237]. Additionally, tumor cells are capable of up-regulating inhibitory T cell surface ligands, such as program death-ligand 1 (PD-L1), to enhance the T-cell anergy and to suppress the T-cell activity [237]. Myeloid-derived suppressor cells (MDSCs) are also involved in tumor development by inducing multiple immunosuppressive compensates, including the releasing of IL-10, TGF-β, arginase and nitric oxide and induction of reactive oxidative species, to deactivate effector T and NK cells [211].

In order to conquer the issue of tumor-derived immune-suppression environment, a strategy of combining IL-15 with additional approaches has been considered to remove the inhibitory checkpoints that mediate negative T-cell signaling pathways. The combination of IL-15 treatment with PD-L1 or CTLA-4 antibodies significantly reduced the expression of PD-1 on $CD8^+$ T cells' surface, and significantly prolonged the survival rate of tumor-bearing animals when compared to single treatment alone [129, 220]. In agreement with this conclusion, the study summarized in Chapter 4 of this dissertation showed combining *Il-15/sIl-15Rα* gene therapy with gemcitabine chemotherapy manifested a marked prolongation of animal survival, and yielded a better therapeutic outcome for tumors growing in multi-organs including the lungs, liver, and kidneys. The improved therapy is likely achieved through selective elimination of the myeloid-derived suppressor cells by administered gemcitabine [211]. Further studies appear necessary to test the possibility of combined therapy with IL-15 or IL-15/sIL-15Rα with additional cytokines, antibodies or chemicals with defined activities. Efforts are needed to develop strategies to couple the effect of IL-15-based therapy with a different approach that would enhance lipid metabolism,

or control of diet intake to accomplish the goal of maintaining energy homeostasis and preventing obesity.

In conclusion, evidence collected from the cell culture, laboratory animal, and human studies of IL-15 and the IL-15/sIL-15Rα systems opens the possibility for the rational design of improved IL-15 pharmaceutics. The dissertation study has extended the current IL-15 therapeutics and provided strong evidence in support of applying IL-15-based gene therapy to treatments of cancer and metabolic diseases. Although further studies are needed to optimize the forms of IL-15 and to modulate IL-15-related toxicity, the prospects are good that the goal of developing clinically applicable IL-15-based therapeutics will be achieved in the near future.

REFERENCES

1. Anderson DM, Johnson L, Glaccum MB, Copeland NG, Gilbert DJ, Jenkins NA *et al.* Chromosomal Assignment and Genomic Structure of Il15. *Genomics* 1995; **25**(3)**:** 701-706.

2. Canals A, Grimm DR, Gasbarre LC, Lunney JK, Zarlenga DS. Molecular cloning of cDNA encoding porcine interleukin-15. *Gene* 1997; **195**(2)**:** 337-339.

3. Krause H, Jandrig B, Wernicke C, BulfonePaus S, Pohl T, Diamantstein T. Genomic structure and chromosomal localization of the human interleukin 15 gene (IL-15). *Cytokine* 1996; **8**(9)**:** 667-674.

4. Grabstein KH, Eisenman J, Shanebeck K, Rauch C, Srinivasan S, Fung V *et al.* Cloning of a T-Cell Growth-Factor That Interacts with the Beta-Chain of the Interleukin-2 Receptor. *Science* 1994; **264**(5161)**:** 965-968.

5. Pettit DK, Bonnert TP, Eisenman J, Srinivasan S, Paxton R, Beers C *et al.* Structure-function studies of interleukin 15 using site-specific mutagenesis, polyethylene glycol conjugation, and homology modeling. *J. Biol. Chem.* 1997; **272**(4)**:** 2312-2318.

6. Kurys G, Tagaya Y, Bamford R, Hanover JA, Waldmann TA. The long signal peptide isoform and its alternative processing direct the intracellular trafficking of interleukin-15. *J. Biol. Chem.* 2000; **275**(39)**:** 30653-9.

7. Fehniger TA, Caligiuri MA. Interleukin 15: biology and relevance to human disease. *Blood* 2001; **97**(1)**:** 14-32.

8. Budagian V, Bulanova E, Paus R, Bulfone-Paus S. IL-15/IL-15 receptor biology: A guided tour through an expanding universe. *Cytokine Growth Factor. Rev.* 2006; **17**(4)**:** 259-280.

9. Meazza R, Verdiani S, Biassoni R, Coppolecchia M, Gaggero A, Orengo AM *et al.* Identification of a novel interleukin-15 (IL-15) transcript isoform generated by alternative splicing in human small cell lung cancer cell lines. *Oncogene* 1996; **12**(10)**:** 2187-92.

10. Gaggero A, Azzarone B, Andrei C, Mishal Z, Meazza R, Zappia E *et al.* Differential intracellular trafficking, secretion and endosomal localization of two IL-15 isoforms. *Eur. J. Immunol.* 1999; **29**(4)**:** 1265-1274.

11. Kurys G, Tagaya Y, Bamford R, Hanover JA, Waldmann TA. The long signal peptide isoform and its alternative processing direct the intracellular trafficking of interleukin-15. *J. Biol. Chem.* 2000; **275**(39)**:** 30653-30659.

12. Onu A, Pohl T, Krause H, Bulfone-Paus S. Regulation of IL-15 secretion via the leader peptide of two IL-15 isoforms. *J. Immunol.* 1997; **158**(1)**:** 255-62.

13. Prinz M, Hanisch UK, Kettenmann H, Kirchhoff F. Alternative splicing of mouse IL-15 is due to the use of an internal splice site in exon 5. *Mol. Brain Res.* 1998; **63**(1)**:** 155-162.

14. Steel JC, Waldmann TA, Morris JC. Interleukin-15 biology and its therapeutic implications in cancer. *Trends Pharmacol. Sci.* 2012; **33**(1)**:** 35-41.

15. Musso T, Calosso L, Zucca M, Millesimo M, Ravarino D, Giovarelli M *et al.* Human monocytes constitutively express membrane-bound, biologically active, and interferon-gamma-upregulated interleukin-15. *Blood* 1999; **93**(10)**:** 3531-3539.

16. Mattei F, Schiavoni G, Belardelli F, Tough DF. IL-15 is expressed by dendritic cells in response to type IIFN, double-stranded RNA, or lipopolysaccharide and promotes dendritic cell activation. *J. Immunol.* 2001; **167**(3)**:** 1179-1187.

17. Azimi N, Brown K, Bamford RN, Tagaya Y, Siebenlist U, Waldmann TA. Human T cell lymphotropic virus type I Tax protein trans-activates interleukin 15 gene transcription through an NF-kappaB site. *Proc. Natl. Acad. Sci. U. S. A.* 1998; **95**(5)**:** 2452-7.

18. Ogasawara K, Hida S, Azimi N, Tagaya Y, Sato T, Yokochi-Fukuda T *et al.* Requirement for IRF-1 in the microenvironment supporting development of natural killer cells. *Nature* 1998; **391**(6668)**:** 700-3.

19. Bamford RN, DeFilippis AP, Azimi N, Kurys G, Waldmann TA. The 5' untranslated region, signal peptide, and the coding sequence of the carboxyl terminus of IL-15 participate in its multifaceted translational control. *J. Immunol.* 1998; **160**(9)**:** 4418-26.

20. Giri JG, Kumaki S, Ahdieh M, Friend DJ, Loomis A, Shanebeck K *et al.* Identification and Cloning of a Novel Il-15 Binding-Protein That Is Structurally Related to the Alpha-Chain of the Il-2 Receptor. *EMBO J.* 1995; **14**(15)**:** 3654-3663.

21. Hatakeyama M, Tsudo M, Minamoto S, Kono T, Doi T, Miyata T *et al.* Interleukin-2 receptor beta chain gene: generation of three receptor forms by cloned human alpha and beta chain cDNA's. *Science* 1989; **244**(4904)**:** 551-6.

22. Takeshita T, Asao H, Ohtani K, Ishii N, Kumaki S, Tanaka N *et al.* Cloning of the gamma chain of the human IL-2 receptor. *Science* 1992; **257**(5068)**:** 379-82.

23. Anderson DM, Kumaki S, Ahdieh M, Bertles J, Tometsko M, Loomis A *et al.* Functional

characterization of the human interleukin-15 receptor alpha chain and close linkage of IL15RA and IL2RA genes. *J. Biol. Chem.* 1995; **270**(50)**:** 29862-9.

24. Chae DW, Nosaka Y, Strom TB, Maslinski W. Distribution of IL-15 receptor alpha-chains on human peripheral blood mononuclear cells and effect of immunosuppressive drugs on receptor expression. *J. Immunol.* 1996; **157**(7)**:** 2813-9.

25. Dubois S, Magrangeas F, Lehours P, Raher S, Bernard J, Boisteau O *et al.* Natural splicing of exon 2 of human interleukin-15 receptor alpha-chain mRNA results in a shortened form with a distinct pattern of expression. *J. Biol. Chem.* 1999; **274**(38)**:** 26978-84.

26. Mortier E, Bernard J, Plet A, Jacques Y. Natural, proteolytic release of a soluble form of human IL-15 receptor alpha-chain that behaves as a specific, high affinity IL-15 antagonist. *J. Immunol.* 2004; **173**(3)**:** 1681-1688.

27. Giri JG, Ahdieh M, Eisenman J, Shanebeck K, Grabstein K, Kumaki S *et al.* Utilization of the beta and gamma chains of the IL-2 receptor by the novel cytokine IL-15. *EMBO J.* 1994; **13**(12)**:** 2822-30.

28. Miyazaki T, Kawahara A, Fujii H, Nakagawa Y, Minami Y, Liu ZJ *et al.* Functional activation of Jak1 and Jak3 by selective association with IL-2 receptor subunits. *Science* 1994; **266**(5187)**:** 1045-7.

29. Miyazaki T, Liu ZJ, Kawahara A, Minami Y, Yamada K, Tsujimoto Y *et al.* Three distinct IL-2 signaling pathways mediated by bcl-2, c-myc, and lck cooperate in hematopoietic cell proliferation. *Cell* 1995; **81**(2)**:** 223-31.

30. Giron-Michel J, Giuliani M, Fogli M, Brouty-Boye D, Ferrini S, Baychelier F *et al.* Membrane-bound and soluble IL-15/IL-15Ralpha complexes display differential signaling and functions on human hematopoietic progenitors. *Blood* 2005; **106**(7)**:** 2302-10.

31. Mortier E, Woo T, Advincula R, Gozalo S, Ma A. IL-15R alpha chaperones IL-15 to stable dendritic cell membrane complexes that activate NK cells via trans presentation. *J. Exp. Med.* 2008; **205**(5)**:** 1213-1225.

32. Lorenzen I, Dingley AJ, Jacques Y, Grotzinger J. The structure of the interleukin-15 alpha receptor and its implications for ligand binding. *J. Biol. Chem.* 2006; **281**(10)**:** 6642-6647.

33. Wu Z, Xue HH, Bernard J, Zeng R, Issakov D, Bollenbacher-Reilley J *et al.* The IL-15 receptor {alpha} chain cytoplasmic domain is critical for normal IL-15Ralpha function but is not required for trans-presentation. *Blood* 2008; **112**(12)**:** 4411-9.

34. Dubois S, Mariner J, Waldmann TA, Tagaya Y. IL-15Ralpha recycles and presents IL-15

In trans to neighboring cells. *Immunity* 2002; **17**(5)**:** 537-47.

35. Bergamaschi C, Jalah R, Kulkarni V, Rosati M, Zhang GM, Alicea C *et al.* Secretion and Biological Activity of Short Signal Peptide IL-15 Is Chaperoned by IL-15 Receptor Alpha In Vivo. *J. Immunol.* 2009; **183**(5)**:** 3064-3072.

36. Chirifu M, Hayashi C, Nakamura T, Toma S, Shuto T, Kai H *et al.* Crystal structure of the IL-15-IL-15Ralpha complex, a cytokine-receptor unit presented in trans. *Nat. Immunol.* 2007; **8**(9)**:** 1001-7.

37. Olsen SK, Ota N, Kishishita S, Kukimoto-Niino M, Murayama K, Uchiyama H *et al.* Crystal Structure of the interleukin-15.interleukin-15 receptor alpha complex: insights into trans and cis presentation. *J. Biol. Chem.* 2007; **282**(51)**:** 37191-204.

38. Ring AM, Lin JX, Feng D, Mitra S, Rickert M, Bowman GR *et al.* Mechanistic and structural insight into the functional dichotomy between IL-2 and IL-15. *Nat. Immunol.* 2012; **13**(12)**:** 1187-+.

39. Stoklasek TA, Schluns KS, Lefrancois L. Combined IL-15/IL-15R alpha immunotherapy maximizes IL-15 activity in vivo. *J. Immunol.* 2006; **177**(9)**:** 6072-6080.

40. Burton JD, Bamford RN, Peters C, Grant AJ, Kurys G, Goldman CK *et al.* A lymphokine, provisionally designated interleukin T and produced by a human adult T-cell leukemia line, stimulates T-cell proliferation and the induction of lymphokine-activated killer cells. *Proc. Natl. Acad. Sci. U. S. A.* 1994; **91**(11)**:** 4935-9.

41. Kanegane H, Tosato G. Activation of naive and memory T cells by interleukin-15. *Blood* 1996; **88**(1)**:** 230-5.

42. Zhang X, Sun S, Hwang I, Tough DF, Sprent J. Potent and selective stimulation of memory-phenotype CD8+ T cells in vivo by IL-15. *Immunity* 1998; **8**(5)**:** 591-9.

43. Yajima T, Nishimura H, Ishimitsu R, Watase T, Busch DH, Pamer EG *et al.* Overexpression of IL-15 in vivo increases antigen-driven memory CD8+ T cells following a microbe exposure. *J. Immunol.* 2002; **168**(3)**:** 1198-203.

44. Kennedy MK, Glaccum M, Brown SN, Butz EA, Viney JL, Embers M *et al.* Reversible defects in natural killer and memory CD8 T cell lineages in interleukin 15-deficient mice. *J. Exp. Med.* 2000; **191**(5)**:** 771-80.

45. Lodolce JP, Boone DL, Chai S, Swain RE, Dassopoulos T, Trettin S *et al.* IL-15 receptor maintains lymphoid homeostasis by supporting lymphocyte homing and proliferation. *Immunity* 1998; **9**(5)**:** 669-76.

46. Oh S, Perera LP, Terabe M, Ni L, Waldmann TA, Berzofsky JA. IL-15 as a mediator of CD4(+) help for CD8(+) T cell longevity and avoidance of TRAIL-mediated apoptosis.

Proc. Natl. Acad. Sci. U. S. A. 2008; **105**(13)**:** 5201-5206.

47. Berger C, Berger M, Hackman RC, Gough M, Elliott C, Jensen MC *et al.* Safety and immunologic effects of IL-15 administration in nonhuman primates. *Blood* 2009; **114**(12)**:** 2417-2426.

48. Marks-Konczalik J, Dubois S, Losi JM, Sabzevari H, Yamada N, Feigenbaum L *et al.* IL-2-induced activation-induced cell death is inhibited in IL-15 transgenic mice. *Proc. Natl. Acad. Sci. U. S. A.* 2000; **97**(21)**:** 11445-11450.

49. Huntington ND, Puthalakath H, Gunn P, Naik E, Michalak EM, Smyth MJ *et al.* Interleukin 15-mediated survival of natural killer cells is determined by interactions among Bim, Noxa and Mcl-1. *Nat. Immunol.* 2007; **8**(8)**:** 856-863.

50. Petrovas C, Mueller YM, Dimitriou ID, Bojczuk PM, Mounzer KC, Witek J *et al.* HIV-specific CD8+ T cells exhibit markedly reduced levels of Bcl-2 and Bcl-xL. *J. Immunol.* 2004; **172**(7)**:** 4444-53.

51. Wilkinson PC, Liew FY. Chemoattraction of human blood T lymphocytes by interleukin-15. *J. Exp. Med.* 1995; **181**(3)**:** 1255-9.

52. Perera LP, Goldman CK, Waldmann TA. IL-15 induces the expression of chemokines and their receptors in T lymphocytes. *J. Immunol.* 1999; **162**(5)**:** 2606-2612.

53. Estess P, Nandi A, Mohamadzadeh M, Siegelman MH. Interleukin 15 induces endothelial hyaluronan expression in vitro and promotes activated T cell extravasation through a CD44-dependent pathway in vivo. *J. Exp. Med.* 1999; **190**(1)**:** 9-19.

54. Liu CC, Perussia B, Young JD. The emerging role of IL-15 in NK-cell development. *Immunol. Today* 2000; **21**(3)**:** 113-6.

55. Leclercq G, Debacker V, de Smedt M, Plum J. Differential effects of interleukin-15 and interleukin-2 on differentiation of bipotential T/natural killer progenitor cells. *J. Exp. Med.* 1996; **184**(2)**:** 325-36.

56. Lyman SD, Jacobsen SE. c-kit ligand and Flt3 ligand: stem/progenitor cell factors with overlapping yet distinct activities. *Blood* 1998; **91**(4)**:** 1101-34.

57. Mrozek E, Anderson P, Caligiuri MA. Role of interleukin-15 in the development of human CD56+ natural killer cells from CD34+ hematopoietic progenitor cells. *Blood* 1996; **87**(7)**:** 2632-40.

58. Carson WE, Fehniger TA, Haldar S, Eckhert K, Lindemann MJ, Lai CF *et al.* A potential role for interleukin-15 in the regulation of human natural killer cell survival. *J. Clin. Invest.* 1997; **99**(5)**:** 937-43.

59. Suzuki H, Duncan GS, Takimoto H, Mak TW. Abnormal development of intestinal intraepithelial lymphocytes and peripheral natural killer cells in mice lacking the IL-2 receptor beta chain. *J. Exp. Med.* 1997; **185**(3)**:** 499-505.

60. Castillo EF, Stonier SW, Frasca L, Schluns KS. Dendritic Cells Support the In Vivo Development and Maintenance of NK Cells via IL-15 Trans-Presentation. *J. Immunol.* 2009; **183**(8)**:** 4948-4956.

61. Park SY, Saijo K, Takahashi T, Osawa M, Arase H, Hirayama N *et al.* Developmental defects of lymphoid cells in Jak3 kinase-deficient mice. *Immunity* 1995; **3**(6)**:** 771-82.

62. Imada K, Bloom ET, Nakajima H, Horvath-Arcidiacono JA, Udy GB, Davey HW *et al.* Stat5b is essential for natural killer cell-mediated proliferation and cytolytic activity. *J. Exp. Med.* 1998; **188**(11)**:** 2067-2074.

63. Carson WE, Giri JG, Lindemann MJ, Linett ML, Ahdieh M, Paxton R *et al.* Interleukin (Il)-15 Is a Novel Cytokine That Activates Human Natural-Killer-Cells Via Components of the Il-2 Receptor. *J. Exp. Med.* 1994; **180**(4)**:** 1395-1403.

64. Ross ME, Caligiuri MA. Cytokine-induced apoptosis of human natural killer cells identifies a novel mechanism to regulate the innate immune response. *Blood* 1997; **89**(3)**:** 910-8.

65. Fehniger TA, Shah MH, Turner MJ, VanDeusen JB, Whitman SP, Cooper MA *et al.* Differential cytokine and chemokine gene expression by human NK cells following activation with IL-18 or IL-15 in combination with IL-12: implications for the innate immune response. *J. Immunol.* 1999; **162**(8)**:** 4511-20.

66. Zhang C, Zhang JH, Niu JF, Zhang J, Tian ZG. Interleukin-15 improves cytotoxicity of natural killer cells via up-regulating NKG2D and cytotoxic effector molecule expression as well as STAT1 and ERK1/2 phosphorylation. *Cytokine* 2008; **42**(1)**:** 128-136.

67. Prlic M, Blazar BR, Farrar MA, Jameson SC. In vivo survival and homeostatic proliferation of natural killer cells. *J. Exp. Med.* 2003; **197**(8)**:** 967-976.

68. Elpek KG, Rubinstein MP, Bellemare-Pelletier A, Goldrath AW, Turley SJ. Mature natural killer cells with phenotypic and functional alterations accumulate upon sustained stimulation with IL-15/IL-15R alpha complexes. *Proc. Natl. Acad. Sci. U. S. A.* 2010; **107**(50)**:** 21647-21652.

69. Bernasconi NL, Traggiai E, Lanzavecchia A. Maintenance of serological memory by polyclonal activation of human memory B cells. *Science* 2002; **298**(5601)**:** 2199-2202.

70. Armitage RJ, Macduff BM, Eisenman J, Paxton R, Grabstein KH. Il-15 Has Stimulatory Activity for the Induction of B-Cell Proliferation and Differentiation. *J. Immunol.* 1995; **154**(2)**:** 483-490.

71. Park CS, Yoon SO, Armitage RJ, Choi YS. Follicular dendritic cells produce IL-15 that enhances germinal center B cell proliferation in membrane-bound form. *J. Immunol.* 2004; **173**(11)**:** 6676-6683.

72. Badolato R, Ponzi AN, Millesimo M, Notarangelo LD, Musso T. Interleukin-15 (IL-15) induces IL-8 and monocyte chemotactic protein 1 production in human monocytes. *Blood* 1997; **90**(7)**:** 2804-9.

73. Musso T, Calosso L, Zucca M, Millesimo M, Ravarino D, Giovarelli M *et al.* Human monocytes constitutively express membrane-bound, biologically active, and interferon-gamma-upregulated interleukin-15. *Blood* 1999; **93**(10)**:** 3531-9.

74. Neely GG, Epelman S, Ma LL, Colarusso P, Howlett CJ, Amankwah EK *et al.* Monocyte Surface-Bound IL-15 Can Function as an Activating Receptor and Participate in Reverse Signaling. *The Journal of Immunology* 2004; **172**(7)**:** 4225-4234.

75. Krutzik SR, Tan B, Li HY, Ochoa MT, Liu PT, Sharfstein SE *et al.* TLR activation triggers the rapid differentiation of monocytes into macrophages and dendritic cells. *Nat. Med.* 2005; **11**(6)**:** 653-660.

76. D'Agostino P, Milano S, Arcoleo F, Di Bella G, La Rosa M, Ferlazzo V *et al.* Interleukin-15, as interferon-gamma, induces the killing of Leishmania infantum in phorbol-myristate-acetate-activated macrophages increasing interleukin-12. *Scand. J. Immunol.* 2004; **60**(6)**:** 609-614.

77. Ohteki T, Suzue K, Maki C, Ota T, Koyasu S. Critical role of IL-15-IL-15R for antigen-presenting cell functions in the innate immune response. *Nat. Immunol.* 2001; **2**(12)**:** 1138-1143.

78. Dubois SP, Waldmann TA, Muller JR. Survival adjustment of mature dendritic cells by IL-15. *Proc. Natl. Acad. Sci. U. S. A.* 2005; **102**(24)**:** 8662-8667.

79. Pulendran B, Dillon S, Joseph C, Curiel T, Banchereau J, Mohamadzadeh M. Dendritic cells generated in the presence of GM-CSF plus IL-15 prime potent CD8(+) Tc1 responses in vivo. *Eur. J. Immunol.* 2004; **34**(1)**:** 66-73.

80. Mohamadzadeh M, Berard F, Essert G, Chalouni C, Pulendran B, Davoust J *et al.* Interleukin 15 skews monocyte differentiation into dendritic cells with features of Langerhans cells. *J. Exp. Med.* 2001; **194**(7)**:** 1013-1019.

81. Ruckert R, Brandt K, Bulanova E, Mirghomizadeh F, Paus R, Bulfone-Paus S. Dendritic cell-derived IL-15 controls the induction of CD8 T cell immune responses. *Eur. J. Immunol.* 2003; **33**(12)**:** 3493-3503.

82. Ferlazzo G, Pack M, Thomas D, Paludan C, Schmid D, Strowig T *et al.* Distinct roles of

IL-12 and IL-15 in human natural killer cell activation by dendritic cells from secondary lymphoid organs. *Proc. Natl. Acad. Sci. U. S. A.* 2004; **101**(47)**:** 16606-16611.

83. Mortier E, Woo T, Advincula R, Gozalo S, Ma A. IL-15Ralpha chaperones IL-15 to stable dendritic cell membrane complexes that activate NK cells via trans presentation. *J. Exp. Med.* 2008; **205**(5)**:** 1213-25.

84. Cassatella MA, McDonald PP. Interleukin-15 and its impact on neutrophil function. *Curr. Opin. Hematol.* 2000; **7**(3)**:** 174-177.

85. Hoontrakoon R, Chu HW, Gardai SJ, Wenzel SE, McDonald P, Fadok VA *et al.* Interleukin-15 inhibits spontaneous apoptosis in human eosinophils via autocrine production of granulocyte macrophage-colony stimulating factor and nuclear factor-kappaB activation. *Am. J. Respir. Cell Mol. Biol.* 2002; **26**(4)**:** 404-12.

86. Musso T, Caloss L, Zucca M, Millesimo M, Puliti M, Bulfone-Paus S *et al.* Interleukin-15 activates proinflammatory and antimicrobial functions in polymorphonuclear cells. *Infect. Immun.* 1998; **66**(6)**:** 2640-2647.

87. Bouchard A, Ratthe C, Girard D. Interleukin-15 delays human neutrophil apoptosis by intracellular events and not via extracellular factors: role of Mcl-1 and decreased activity of caspase-3 and caspase-8. *J. Leukoc. Biol.* 2004; **75**(5)**:** 893-900.

88. Alvarez B, Carbo N, Lopez-Soriano J, Drivdahl RH, Busquets S, Lopez-Soriano FJ *et al.* Effects of interleukin-15 (IL-15) on adipose tissue mass in rodent obesity models: evidence for direct IL-15 action on adipose tissue. *Biochim. Biophys. Acta* 2002; **1570**(1)**:** 33-7.

89. Barra NG, Palanivel R, Denou E, Chew MV, Gillgrass A, Walker TD *et al.* Interleukin-15 modulates adipose tissue by altering mitochondrial mass and activity. *PLoS One* 2014; **9**(12)**:** e114799.

90. Barra NG, Reid S, MacKenzie R, Werstuck G, Trigatti BL, Richards C *et al.* Interleukin-15 contributes to the regulation of murine adipose tissue and human adipocytes. *Obesity (Silver Spring)* 2010; **18**(8)**:** 1601-7.

91. Quinn LS, Strait-Bodey L, Anderson BG, Argiles JM, Havel PJ. Interleukin-15 stimulates adiponectin secretion by 3T3-L1 adipocytes: evidence for a skeletal muscle-to-fat signaling pathway. *Cell Biol. Int.* 2005; **29**(6)**:** 449-57.

92. Carbo N, Lopez-Soriano J, Costelli P, Alvarez B, Busquets S, Baccino FM *et al.* Interleukin-15 mediates reciprocal regulation of adipose and muscle mass: a potential role in body weight control. *Biochim. Biophys. Acta* 2001; **1526**(1)**:** 17-24.

93. Ajuwon KM, Spurlock ME. Direct regulation of lipolysis by interleukin-15 in primary pig adipocytes. *Am. J. Physiol. Regul. Integr. Comp. Physiol.* 2004; **287**(3)**:** R608-11.

94. Sugiura T, Harigai M, Kawaguchi Y, Takagi K, Fukasawa C, Ohsako-Higami S *et al.* Increased IL-15 production of muscle cells in polymyositis and dermatomyositis. *Int. Immunol.* 2002; **14**(8)**:** 917-24.

95. Stegall T, Krolick KA. Myocytes respond to both interleukin-4 and interferon-gamma: Cytokine responsiveness with the potential to influence the severity and course of experimental myasthenia gravis. *Clin. Immunol.* 2000; **94**(2)**:** 133-139.

96. Quinn LS, Anderson BG, Drivdahl RH, Alvarez B, Argiles JM. Overexpression of interleukin-15 induces skeletal muscle hypertrophy in vitro: Implications for treatment of muscle wasting disorders. *Exp. Cell Res.* 2002; **280**(1)**:** 55-63.

97. Nieman DC, Davis JM, Henson DA, Walberg-Rankin J, Shute M, Dumke CL *et al.* Carbohydrate ingestion influences skeletal muscle cytokine mRNA and plasma cytokine levels after a 3-h run. *J. Appl. Physiol.* 2003; **94**(5)**:** 1917-1925.

98. Riechman SE, Balasekaran G, Roth SM, Ferrell RE. Association of interleukin-15 protein and interleukin-15 receptor genetic variation with resistance exercise training responses. *J. Appl. Physiol.* 2004; **97**(6)**:** 2214-2219.

99. Quinn LS, Anderson BG. Interleukin-15, IL-15 Receptor-Alpha, and Obesity: Concordance of Laboratory Animal and Human Genetic Studies. *J Obes* 2011; **2011:** 456347.

100. Quinn LS, Haugk KL, Grabstein KH. Interleukin-15: a novel anabolic cytokine for skeletal muscle. *Endocrinology* 1995; **136**(8)**:** 3669-72.

101. Florini JR, Ewton DZ, Coolican SA. Growth hormone and the insulin-like growth factor system in myogenesis. *Endocr. Rev.* 1996; **17**(5)**:** 481-517.

102. Busquets S, Figueras MT, Meijsing S, Carbo N, Quinn LS, Almendro V *et al.* Interleukin-15 decreases proteolysis in skeletal muscle: a direct effect. *Int. J. Mol. Med.* 2005; **16**(3)**:** 471-6.

103. Carbo N, Lopez-Soriano J, Costelli P, Busquets S, Alvarez B, Baccino FM *et al.* Interleukin-15 antagonizes muscle protein waste in tumour-bearing rats. *Br. J. Cancer* 2000; **83**(4)**:** 526-531.

104. Fuster G, Busquets S, Figueras M, Ametller E, Fontes de Oliveira CC, Olivan M *et al.* PPARdelta mediates IL15 metabolic actions in myotubes: effects of hyperthermia. *Int. J. Mol. Med.* 2009; **24**(1)**:** 63-8.

105. Almendro V, Busquets S, Ametller E, Carbo N, Figueras M, Fuster G *et al.* Effects of interleukin-15 on lipid oxidation: disposal of an oral [(14)C]-triolein load. *Biochim. Biophys. Acta* 2006; **1761**(1)**:** 37-42.

106. Busquets S, Figueras M, Almendro V, Lopez-Soriano FJ, Argiles JM. Interleukin-15 increases glucose uptake in skeletal muscle. An antidiabetogenic effect of the cytokine. *Biochim. Biophys. Acta* 2006; **1760**(11)**:** 1613-7.

107. Barra NG, Chew MV, Holloway AC, Ashkar AA. Interleukin-15 treatment improves glucose homeostasis and insulin sensitivity in obese mice. *Diabetes Obes. Metab.* 2012; **14**(2)**:** 190-3.

108. Angiolillo AL, Kanegane H, Sgadari C, Reaman GH, Tosato G. Interleukin-15 promotes angiogenesis in vivo. *Biochem. Biophys. Res. Commun.* 1997; **233**(1)**:** 231-237.

109. Oppenheimer-Marks N, Brezinschek RI, Mohamadzadeh M, Vita R, Lipsky PE. Interleukin 15 is produced by endothelial cells and increases the transendothelial migration of T cells in vitro and in the SCID mouse-human rheumatoid arthritis model in vivo. *J. Clin. Investig.* 1998; **101**(6)**:** 1261-1272.

110. Barry M, Bleackley RC. Cytotoxic T lymphocytes: All roads lead to death. *Nat. Rev. Immunol.* 2002; **2**(6)**:** 401-409.

111. Waldmann TA. Interleukin-15 in the treatment of cancer. *Expert Rev. Clin. Immunol.* 2014; **10**(12)**:** 1689-701.

112. Zhu XY, Marcus WD, Xu WX, Lee HI, Han KP, Egan JO *et al.* Novel Human Interleukin-15 Agonists. *J. Immunol.* 2009; **183**(6)**:** 3598-3607.

113. Epardaud M, Elpek KG, Rubinstein MP, Yonekura AR, Bellemare-Pelletier A, Bronson R *et al.* Interleukin-15/interleukin-15R alpha complexes promote destruction of established tumors by reviving tumor-resident CD8+ T cells. *Cancer Res.* 2008; **68**(8)**:** 2972-83.

114. Dubois S, Patel HJ, Zhang M, Waldmann TA, Muller JR. Preassociation of IL-15 with IL-15R alpha-IgG1-Fc enhances its activity on proliferation of NK and CD8+/CD44high T cells and its antitumor action. *J. Immunol.* 2008; **180**(4)**:** 2099-106.

115. Jakobisiak M, Golab J, Lasek W. Interleukin 15 as a promising candidate for tumor immunotherapy. *Cytokine Growth Factor. Rev.* 2011; **22**(2)**:** 99-108.

116. Habibi M, Kmieciak M, Graham L, Morales JK, Bear HD, Manjili MH. Radiofrequency thermal ablation of breast tumors combined with intralesional administration of IL-7 and IL-15 augments anti-tumor immune responses and inhibits tumor development and metastasis. *Breast Cancer Res. Treat.* 2009; **114**(3)**:** 423-431.

117. Kimura K, Nishimura H, Matsuzaki T, Yokokura T, Nimura Y, Yoshikai Y. Synergistic effect of interleukin-15 and interleukin-12 on antitumor activity in a murine malignant pleurisy model. *Cancer Immunol. Immunother.* 2000; **49**(2)**:** 71-77.

118. Lasek W, Golab J, Maslinski W, Switaj T, Balkowiec EZ, Stoklosa T *et al.* Subtherapeutic doses of interleukin-15 augment the antitumor effect of interleukin-12 in a B16F10 melanoma model in mice. *Eur. Cytokine Netw.* 1999; **10**(3)**:** 345-56.

119. Pouw N, Treffers-Westerlaken E, Kraan J, Wittink F, ten Hagen T, Verweij J *et al.* Combination of IL-21 and IL-15 enhances tumour-specific cytotoxicity and cytokine production of TCR-transduced primary T cells. *Cancer Immunol. Immunother.* 2010; **59**(6)**:** 921-931.

120. Huarte E, Fisher J, Turk MJ, Mellinger D, Foster C, Wolf B *et al.* Ex vivo expansion of tumor specific lymphocytes with IL-15 and IL-21 for adoptive immunotherapy in melanoma. *Cancer Lett.* 2009; **285**(1)**:** 80-88.

121. Zeng R, Spolski R, Finkelstein SE, Oh SK, Kovanen PE, Hinrichs CS *et al.* Synergy of IL-21 and IL-15 in regulating CD8(+) T cell expansion and function. *J. Exp. Med.* 2005; **201**(1)**:** 139-148.

122. Kishida T, Asada H, Itokawa Y, Cui FD, Shin-Ya M, Gojo S *et al.* Interleukin (IL)-21 and IL-15 genetic transfer synergistically augments therapeutic antitumor immunity and promotes regression of metastatic lymphoma. *Mol. Ther.* 2003; **8**(4)**:** 552-558.

123. Chapoval AI, Fuller JA, Kremlev SG, Kamdar SJ, Evans R. Combination chemotherapy and IL-15 administration induce permanent tumor regression in a mouse lung tumor model: NK and T cell-mediated effects antagonized by B cells. *J. Immunol.* 1998; **161**(12)**:** 6977-84.

124. Evans R, Fuller JA, Christianson G, Krupke DM, Troutt AB. IL-15 mediates anti-tumor effects after cyclophosphamide injection of tumor-bearing mice and enhances adoptive immunotherapy: the potential role of NK cell subpopulations. *Cell. Immunol.* 1997; **179**(1)**:** 66-73.

125. Cao S, Troutt AB, Rustum YM. Interleukin 15 protects against toxicity and potentiates antitumor activity of 5-fluorouracil alone and in combination with leucovorin in rats bearing colorectal cancer. *Cancer Res.* 1998; **58**(8)**:** 1695-9.

126. Weiss JM, Back TC, Scarzello AJ, Subleski JJ, Hall VL, Stauffer JK *et al.* Successful immunotherapy with IL-2/anti-CD40 induces the chemokine-mediated mitigation of an immunosuppressive tumor microenvironment. *Proc. Natl. Acad. Sci. U. S. A.* 2009; **106**(46)**:** 19455-19460.

127. Zhang M, Yao Z, Dubois S, Ju W, Muller JR, Waldmann TA. Interleukin-15 combined with an anti-CD40 antibody provides enhanced therapeutic efficacy for murine models of colon cancer. *Proc. Natl. Acad. Sci. U. S. A.* 2009; **106**(18)**:** 7513-8.

128. Wysocka M, Benoit BM, Newton S, Azzoni L, Montaner LJ, Rook AH. Enhancement of

the host immune responses in cutaneous T-cell lymphoma by CpG oligodeoxynucleotides and IL-15. *Blood* 2004; **104**(13)**:** 4142-4149.

129. Yu P, Steel JC, Zhang ML, Morris JC, Waldmann TA. Simultaneous Blockade of Multiple Immune System Inhibitory Checkpoints Enhances Antitumor Activity Mediated by Interleukin-15 in a Murine Metastatic Colon Carcinoma Model. *Clin. Cancer Res.* 2010; **16**(24)**:** 6019-6028.

130. Perera PY, Lichy JH, Waldmann TA, Perera LP. The role of interleukin-15 in inflammation and immune responses to infection: implications for its therapeutic use. *Microbes Infect.* 2012; **14**(3)**:** 247-261.

131. Tovey MG, Lallemand C. Adjuvant Activity of Cytokines. *Vaccine Adjuvants* 2010; **626:** 287-309.

132. Hu XD, Chen ST, Li JY, Yu DH, Yi Z, Cai H. An IL-15 adjuvant enhances the efficacy of a combined DNA vaccine against Brucella by increasing the CD8(+) cytotoxic T cell response. *Vaccine* 2010; **28**(12)**:** 2408-2415.

133. Eickhoff CS, Vasconcelos JR, Sullivan NL, Blazevic A, Bruna-Romero O, Rodrigues MM *et al.* Co-administration of a plasmid DNA encoding IL-15 improves long-term protection of a genetic vaccine against Trypanosoma cruzi. *PLoS Negl. Trop. Dis.* 2011; **5**(3)**:** e983.

134. Merkel TJ, Perera PY, Kelly VK, Verma A, Llewellyn ZN, Waldmann TA *et al.* Development of a highly efficacious vaccinia-based dual vaccine against smallpox and anthrax, two important bioterror entities. *Proc. Natl. Acad. Sci. U. S. A.* 2010; **107**(42)**:** 18091-6.

135. Oh S, Berzofsky JA, Burke DS, Waldmann TA, Perera LP. Coadministration of HIV vaccine vectors with vaccinia viruses expressing IL-15 but not IL-2 induces long-lasting cellular immunity. *Proc. Natl. Acad. Sci. U. S. A.* 2003; **100**(6)**:** 3392-7.

136. Villinger F, Miller R, Mori K, Mayne AE, Bostik P, Sundstrom JB *et al.* IL-15 is superior to IL-2 in the generation of long-lived antigen specific memory CD4 and CD8 T cells in rhesus macaques. *Vaccine* 2004; **22**(25-26)**:** 3510-3521.

137. Halwani R, Boyer JD, Yassine-Diab B, Haddad EK, Robinson TM, Kumar S *et al.* Therapeutic vaccination with simian immunodeficiency virus (SIV)-DNA+IL-12 or IL-15 induces distinct CD8 memory subsets in SIV-infected macaques. *J. Immunol.* 2008; **180**(12)**:** 7969-7979.

138. Nielsen AR, Hojman P, Erikstrup C, Fischer CP, Plomgaard P, Mounier R *et al.* Association between interleukin-15 and obesity: interleukin-15 as a potential regulator of fat mass. *J. Clin. Endocrinol. Metab.* 2008; **93**(11)**:** 4486-93.

139. Baluna R, Vitetta ES. Vascular leak syndrome: a side effect of immunotherapy. *Immunopharmacology* 1997; **37**(2-3)**:** 117-32.

140. Munger W, DeJoy SQ, Jeyaseelan R, Sr., Torley LW, Grabstein KH, Eisenmann J *et al.* Studies evaluating the antitumor activity and toxicity of interleukin-15, a new T cell growth factor: comparison with interleukin-2. *Cell. Immunol.* 1995; **165**(2)**:** 289-93.

141. Mueller YM, Petrovas C, Bojczuk PM, Dimitriou LD, Beer B, Silvera P *et al.* Interleukin-15 increases effector memory CD8(+) T cells and NK cells in simian immunodeficiency virus-infected macaques. *J. Virol.* 2005; **79**(8)**:** 4877-4885.

142. Waldmann TA, Lugli E, Roederer M, Perera LP, Smedley JV, Macallister RP *et al.* Safety (toxicity), pharmacokinetics, immunogenicity, and impact on elements of the normal immune system of recombinant human IL-15 in rhesus macaques. *Blood* 2011; **117**(18)**:** 4787-95.

143. Lugli E, Goldman CK, Perera LP, Smedley J, Pung R, Yovandich JL *et al.* Transient and persistent effects of IL-15 on lymphocyte homeostasis in nonhuman primates. *Blood* 2010; **116**(17)**:** 3238-48.

144. Conlon KC, Lugli E, Welles HC, Rosenberg SA, Fojo AT, Morris JC *et al.* Redistribution, hyperproliferation, activation of natural killer cells and CD8 T cells, and cytokine production during first-in-human clinical trial of recombinant human interleukin-15 in patients with cancer. *J. Clin. Oncol.* 2015; **33**(1)**:** 74-82.

145. Yanovski SZ, Yanovski JA. Obesity Prevalence in the United States - Up, Down, or Sideways? *N. Engl. J. Med.* 2011; **364**(11)**:** 987-989.

146. Hill JO, Wyatt HR, Reed GW, Peters JC. Obesity and the environment: Where do we go from here? *Science* 2003; **299**(5608)**:** 853-855.

147. Martins C, Morgan L, Truby H. A review of the effects of exercise on appetite regulation: an obesity perspective. *Int. J. Obes.* 2008; **32**(9)**:** 1337-47.

148. Steensberg A, Fischer CP, Keller C, Moller K, Pedersen BK. IL-6 enhances plasma IL-1ra, IL-10, and cortisol in humans. *Am. J. Physiol. Endocrinol. Metab.* 2003; **285**(2)**:** E433-7.

149. Li A, Dubey S, Varney ML, Dave BJ, Singh RK. IL-8 directly enhanced endothelial cell survival, proliferation, and matrix metalloproteinases production and regulated angiogenesis. *J. Immunol.* 2003; **170**(6)**:** 3369-76.

150. Quinn LS, Anderson BG, Strait-Bodey L, Stroud AM, Argiles JM. Oversecretion of interleukin-15 from skeletal muscle reduces adiposity. *Am. J. Physiol. Endocrinol. Metab.* 2009; **296**(1)**:** E191-202.

151. Pedersen BK, Febbraio MA. Muscles, exercise and obesity: skeletal muscle as a secretory organ. *Nat. Rev. Endocrinol.* 2012; **8**(8)**:** 457-65.

152. Yang H, Chang J, Chen W, Zhao L, Qu B, Tang C *et al.* Treadmill exercise promotes interleukin 15 expression in skeletal muscle and interleukin 15 receptor alpha expression in adipose tissue of high-fat diet rats. *Endocrine* 2013; **43**(3)**:** 579-85.

153. Quinn LS, Anderson BG, Conner JD, Wolden-Hanson T. IL-15 overexpression promotes endurance, oxidative energy metabolism, and muscle PPARdelta, SIRT1, PGC-1alpha, and PGC-1beta expression in male mice. *Endocrinology* 2013; **154**(1)**:** 232-45.

154. Liu F, Song Y, Liu D. Hydrodynamics-based transfection in animals by systemic administration of plasmid DNA. *Gene Ther.* 1999; **6**(7)**:** 1258-66.

155. Livak KJ, Schmittgen TD. Analysis of relative gene expression data using real-time quantitative PCR and the 2(T)(-Delta Delta C) method. *Methods* 2001; **25**(4)**:** 402-408.

156. Folch J, Lees M, Sloane Stanley GH. A simple method for the isolation and purification of total lipides from animal tissues. *J. Biol. Chem.* 1957; **226**(1)**:** 497-509.

157. Suda T, Liu D. Hydrodynamic gene delivery: its principles and applications. *Mol. Ther.* 2007; **15**(12)**:** 2063-9.

158. Nielsen AR, Pedersen BK. The biological roles of exercise-induced cytokines: IL-6, IL-8, and IL-15. *Appl. Physiol. Nutr. Metab.* 2007; **32**(5)**:** 833-9.

159. Gao M, Ma Y, Cui R, Liu D. Hydrodynamic delivery of FGF21 gene alleviates obesity and fatty liver in mice fed a high-fat diet. *J. Control. Release* 2014; **185:** 1-11.

160. Fuster G, Almendro V, Fontes-Oliveira CC, Toledo M, Costelli P, Busquets S *et al.* Interleukin-15 affects differentiation and apoptosis in adipocytes: implications in obesity. *Lipids* 2011; **46**(11)**:** 1033-42.

161. Almendro V, Fuster G, Ametller E, Costelli P, Pilla F, Busquets S *et al.* Interleukin-15 increases calcineurin expression in 3T3-L1 cells: possible involvement on in vivo adipocyte differentiation. *Int. J. Mol. Med.* 2009; **24**(4)**:** 453-8.

162. Barra NG, Chew MV, Reid S, Ashkar AA. Interleukin-15 treatment induces weight loss independent of lymphocytes. *PLoS One* 2012; **7**(6)**:** e39553.

163. Lopez-Soriano J, Carbo N, Almendro V, Figueras M, Ribas V, Busquets S *et al.* Rat liver lipogenesis is modulated by interleukin-15. *Int. J. Mol. Med.* 2004; **13**(6)**:** 817-819.

164. Ogden CL, Carroll MD, Kit BK, Flegal KM. Prevalence of Childhood and Adult Obesity in the United States, 2011-2012. *Jama-J Am Med Assoc* 2014; **311**(8)**:** 806-814.

165. Egan B, Zierath JR. Exercise metabolism and the molecular regulation of skeletal muscle adaptation. *Cell Metab.* 2013; **17**(2)**:** 162-84.

166. Nieman DC, Davis JM, Henson DA, Walberg-Rankin J, Shute M, Dumke CL *et al.* Carbohydrate ingestion influences skeletal muscle cytokine mRNA and plasma cytokine levels after a 3-h run. *J Appl Physiol (1985)* 2003; **94**(5)**:** 1917-25.

167. Pedersen BK, Febbraio MA. Muscles, exercise and obesity: skeletal muscle as a secretory organ. *Nature Reviews Endocrinology* 2012; **8**(8)**:** 457-465.

168. Ma Y, Gao M, Sun H, Liu D. Interleukin-6 gene transfer reverses body weight gain and fatty liver in obese mice. *Biochim. Biophys. Acta* 2015; **1852**(5)**:** 1001-11.

169. Gao M, Zhang C, Ma Y, Bu L, Yan L, Liu D. Hydrodynamic delivery of mIL10 gene protects mice from high-fat diet-induced obesity and glucose intolerance. *Mol. Ther.* 2013; **21**(10)**:** 1852-61.

170. Tagaya Y, Bamford RN, DeFilippis AP, Waldmann TA. IL-15: a pleiotropic cytokine with diverse receptor/signaling pathways whose expression is controlled at multiple levels. *Immunity* 1996; **4**(4)**:** 329-36.

171. Bergamaschi C, Rosati M, Jalah R, Valentin A, Kulkarni V, Alicea C *et al.* Intracellular interaction of interleukin-15 with its receptor alpha during production leads to mutual stabilization and increased bioactivity. *J. Biol. Chem.* 2008; **283**(7)**:** 4189-99.

172. Pedersen BK, Steensberg A, Schjerling P. Muscle-derived interleukin-6: possible biological effects. *J. Physiol.* 2001; **536**(Pt 2)**:** 329-37.

173. Waldmann TA, Tagaya Y. The multifaceted regulation of interleukin-15 expression and the role of this cytokine in NK cell differentiation and host response to intracellular pathogens. *Annu. Rev. Immunol.* 1999; **17:** 19-49.

174. Budagian V, Bulanova E, Paus R, Bulfone-Paus S. IL-15/IL-15 receptor biology: a guided tour through an expanding universe. *Cytokine Growth Factor. Rev.* 2006; **17**(4)**:** 259-80.

175. Sun H, Liu D. Hydrodynamic delivery of interleukin 15 gene promotes resistance to high fat diet-induced obesity, fatty liver and improves glucose homeostasis. *Gene Ther.* 2015; **22**(4)**:** 341-7.

176. Jalah R, Rosati M, Kulkarni V, Patel V, Bergamaschi C, Valentin A *et al.* Efficient systemic expression of bioactive IL-15 in mice upon delivery of optimized DNA expression plasmids. *DNA Cell Biol.* 2007; **26**(12)**:** 827-40.

177. Rosati M, von Gegerfelt A, Roth P, Alicea C, Valentin A, Robert-Guroff M *et al.* DNA vaccines expressing different forms of simian immunodeficiency virus antigens decrease

viremia upon SIVmac251 challenge. *J. Virol.* 2005; **79**(13)**:** 8480-92.

178. Schneider R, Campbell M, Nasioulas G, Felber BK, Pavlakis GN. Inactivation of the human immunodeficiency virus type 1 inhibitory elements allows Rev-independent expression of Gag and Gag/protease and particle formation. *J. Virol.* 1997; **71**(7)**:** 4892-903.

179. Sumithran P, Proietto J. The defence of body weight: a physiological basis for weight regain after weight loss. *Clin. Sci. (Lond.)* 2013; **124**(4)**:** 231-41.

180. Barra NG, Chew MV, Reid S, Ashkar AA. Interleukin-15 Treatment Induces Weight Loss Independent of Lymphocytes. *PLoS One* 2012; **7**(6).

181. Kohl HW. Duration and intensity of exercise in weight loss among overweight women. *Clin. J. Sport Med.* 2009; **19**(2)**:** 151-2.

182. Jakicic JM, Marcus BH, Gallagher KI, Napolitano M, Lang W. Effect of exercise duration and intensity on weight loss in overweight, sedentary women - A randomized trial. *Jama-J Am Med Assoc* 2003; **290**(10)**:** 1323-1330.

183. Chambliss HO. Exercise duration and intensity in a weight-loss program. *Clin. J. Sport Med.* 2005; **15**(2)**:** 113-5.

184. MacLean PS, Higgins JA, Johnson GC, Fleming-Elder BK, Peters JC, Hill JO. Metabolic adjustments with the development, treatment, and recurrence of obesity in obesity-prone rats. *Am. J. Physiol. Regul. Integr. Comp. Physiol.* 2004; **287**(2)**:** R288-97.

185. Almendro V, Fuster G, Busquets S, Ametller E, Figueras M, Argiles JM *et al.* Effects of IL-15 on rat brown adipose tissue: uncoupling proteins and PPARs. *Obesity (Silver Spring)* 2008; **16**(2)**:** 285-9.

186. Lopez-Soriano J, Carbo N, Almendro V, Figueras M, Ribas V, Busquets S *et al.* Rat liver lipogenesis is modulated by interleukin-15. *Int. J. Mol. Med.* 2004; **13**(6)**:** 817-819.

187. Ferre P. The biology of peroxisome proliferator-activated receptors: relationship with lipid metabolism and insulin sensitivity. *Diabetes* 2004; **53 Suppl 1:** S43-50.

188. Berger JP, Akiyama TE, Meinke PT. PPARs: therapeutic targets for metabolic disease. *Trends Pharmacol. Sci.* 2005; **26**(5)**:** 244-51.

189. Grimaldi PA. Regulatory role of peroxisome proliferator-activated receptor delta (PPAR delta) in muscle metabolism. A new target for metabolic syndrome treatment? *Biochimie* 2005; **87**(1)**:** 5-8.

190. Yu S, Matsusue K, Kashireddy P, Cao WQ, Yeldandi V, Yeldandi AV *et al.* Adipocyte-specific gene expression and adipogenic steatosis in the mouse liver due to peroxisome

proliferator-activated receptor gamma1 (PPARgamma1) overexpression. *J. Biol. Chem.* 2003; **278**(1)**:** 498-505.

191. Gavrilova O, Haluzik M, Matsusue K, Cutson JJ, Johnson L, Dietz KR *et al.* Liver peroxisome proliferator-activated receptor gamma contributes to hepatic steatosis, triglyceride clearance, and regulation of body fat mass. *J. Biol. Chem.* 2003; **278**(36)**:** 34268-76.

192. Matsusue K, Haluzik M, Lambert G, Yim SH, Gavrilova O, Ward JM *et al.* Liver-specific disruption of PPARgamma in leptin-deficient mice improves fatty liver but aggravates diabetic phenotypes. *J. Clin. Invest.* 2003; **111**(5)**:** 737-47.

193. Siegel RL, Miller KD, Jemal A. Cancer statistics, 2015. *CA. Cancer J. Clin.* 2015; **65**(1)**:** 5-29.

194. Little AG, Gay EG, Gaspar LE, Stewart AK. National survey of non-small cell lung cancer in the United States: epidemiology, pathology and patterns of care. *Lung Cancer* 2007; **57**(3)**:** 253-60.

195. Azzoli CG, Baker S, Jr., Temin S, Pao W, Aliff T, Brahmer J *et al.* American Society of Clinical Oncology Clinical Practice Guideline update on chemotherapy for stage IV non-small-cell lung cancer. *J. Clin. Oncol.* 2009; **27**(36)**:** 6251-66.

196. Smyth MJ, Cretney E, Kershaw MH, Hayakawa Y. Cytokines in cancer immunity and immunotherapy. *Immunol. Rev.* 2004; **202:** 275-293.

197. Dutcher J. Current status of interleukin-2 therapy for metastatic renal cell carcinoma and metastatic melanoma. *Oncology (Williston Park)* 2002; **16**(11 Suppl 13)**:** 4-10.

198. Kirkwood JM, Strawderman MH, Ernstoff MS, Smith TJ, Borden EC, Blum RH. Interferon alfa-2b adjuvant therapy of high-risk resected cutaneous melanoma: The Eastern Cooperative Oncology Group trial EST 1684. *J. Clin. Oncol.* 1996; **14**(1)**:** 7-17.

199. Waldmann TA. The biology of interleukin-2 and interleukin-15: implications for cancer therapy and vaccine design. *Nat. Rev. Immunol.* 2006; **6**(8)**:** 595-601.

200. Steel JC, Waldmann TA, Morris JC. Interleukin-15 biology and its therapeutic implications in cancer. *Trends Pharmacol. Sci.* 2012; **33**(1)**:** 35-41.

201. Rubinstein MP, Kovar M, Purton JF, Cho JH, Boyman O, Surh CD *et al.* Converting IL-15 to a superagonist by binding to soluble IL-15R{alpha}. *Proc. Natl. Acad. Sci. U. S. A.* 2006; **103**(24)**:** 9166-71.

202. Cheng L, Du X, Wang Z, Ju J, Jia M, Huang Q *et al.* Hyper-IL-15 suppresses metastatic and autochthonous liver cancer by promoting tumour-specific CD8+ T cell responses. *J. Hepatol.* 2014; **61**(6)**:** 1297-303.

203. Steel JC, Ramlogan CA, Yu P, Sakai Y, Forni G, Waldmann TA *et al.* Interleukin-15 and Its Receptor Augment Dendritic Cell Vaccination against the neu Oncogene through the Induction of Antibodies Partially Independent of CD4 Help. *Cancer Res.* 2010; **70**(3)**:** 1072-1081.

204. Chang CM, Lo CH, Shih YM, Chen Y, Wu PY, Tsuneyama K *et al.* Treatment of hepatocellular carcinoma with adeno-associated virus encoding interleukin-15 superagonist. *Hum. Gene. Ther.* 2010; **21**(5)**:** 611-21.

205. Bessard A, Sole V, Bouchaud G, Quemener A, Jacques Y. High antitumor activity of RLI, an interleukin-15 (IL-15)-IL-15 receptor alpha fusion protein, in metastatic melanoma and colorectal cancer. *Mol. Cancer Ther.* 2009; **8**(9)**:** 2736-45.

206. Dubois S, Patel HJ, Zhang M, Waldmann TA, Muller JR. Preassociation of IL-15 with IL-15R alpha-IgG1-Fc enhances its activity on proliferation of NK and CD8(+)/CD44(high) T cells and its antitumor action. *J. Immunol.* 2008; **180**(4)**:** 2099-2106.

207. Stoklasek TA, Schluns KS, Lefrancois L. Combined IL-15/IL-15Ralpha immunotherapy maximizes IL-15 activity in vivo. *J. Immunol.* 2006; **177**(9)**:** 6072-80.

208. Li J, Yao Q, Liu D. Hydrodynamic cell delivery for simultaneous establishment of tumor growth in mouse lung, liver and kidney. *Cancer Biol. Ther.* 2011; **12**(8)**:** 737-41.

209. Johnson DH. Gemcitabine for the treatment of non-small-cell lung cancer. *Oncology (Williston Park)* 2001; **15**(3 Suppl 6)**:** 33-9.

210. Suzuki E, Kapoor V, Jassar AS, Kaiser LR, Albelda SM. Gemcitabine selectively eliminates splenic Gr-1+/CD11b+ myeloid suppressor cells in tumor-bearing animals and enhances antitumor immune activity. *Clin. Cancer Res.* 2005; **11**(18)**:** 6713-21.

211. Gabrilovich DI, Nagaraj S. Myeloid-derived suppressor cells as regulators of the immune system. *Nat. Rev. Immunol.* 2009; **9**(3)**:** 162-174.

212. Yang JC, Sherry RM, Steinberg SM, Topalian SL, Schwartzentruber DJ, Hwu P *et al.* Randomized study of high-dose and low-dose interleukin-2 in patients with metastatic renal cancer. *J. Clin. Oncol.* 2003; **21**(16)**:** 3127-32.

213. Zou W. Immunosuppressive networks in the tumour environment and their therapeutic relevance. *Nat. Rev. Cancer* 2005; **5**(4)**:** 263-74.

214. Aerts JG, Hegmans JP. Tumor-Specific Cytotoxic T Cells Are Crucial for Efficacy of Immunomodulatory Antibodies in Patients with Lung Cancer. *Cancer Res.* 2013; **73**(8)**:** 2381-2388.

215. Ikeda R, Vermeulen LC, Lau E, Jiang Z, Sachidanandam K, Yamada K *et al.* Isolation and characterization of gemcitabine-resistant human non-small cell lung cancer A549 cells. *Int. J. Oncol.* 2011; **38**(2)**:** 513-9.

216. Brahmer J, Reckamp KL, Baas P, Crino L, Eberhardt WE, Poddubskaya E *et al.* Nivolumab versus Docetaxel in Advanced Squamous-Cell Non-Small-Cell Lung Cancer. *N. Engl. J. Med.* 2015; **373**(2)**:** 123-35.

217. Kobayashi H, Dubois S, Sato N, Sabzevari H, Sakai Y, Waldmann TA *et al.* Role of trans-cellular IL-15 presentation in the activation of NK cell-mediated killing, which leads to enhanced tumor immunosurveillance. *Blood* 2005; **105**(2)**:** 721-7.

218. Klebanoff CA, Finkelstein SE, Surman DR, Lichtman MK, Gattinoni L, Theoret MR *et al.* IL-15 enhances the in vivo antitumor activity of tumor-reactive CD8+ T cells. *Proc. Natl. Acad. Sci. U. S. A.* 2004; **101**(7)**:** 1969-74.

219. Yu P, Steel JC, Zhang M, Morris JC, Waldmann TA. Simultaneous blockade of multiple immune system inhibitory checkpoints enhances antitumor activity mediated by interleukin-15 in a murine metastatic colon carcinoma model. *Clin. Cancer Res.* 2010; **16**(24)**:** 6019-28.

220. Yu P, Steel JC, Zhang M, Morris JC, Waitz R, Fasso M *et al.* Simultaneous inhibition of two regulatory T-cell subsets enhanced Interleukin-15 efficacy in a prostate tumor model. *Proc. Natl. Acad. Sci. U. S. A.* 2012; **109**(16)**:** 6187-92.

221. Sneller MC, Kopp WC, Engelke KJ, Yovandich JL, Creekmore SP, Waldmann TA *et al.* IL-15 administered by continuous infusion to rhesus macaques induces massive expansion of CD8+ T effector memory population in peripheral blood. *Blood* 2011; **118**(26)**:** 6845-8.

222. Lugli E, Goldman CK, Roederer M, Waldmann TA. Interleukin-15 Administration to Rhesus Macaques Expands Natural Killer and Memory T Cells and Induces Long-lasting Changes in T-cell Homeostasis. *J. Immunother.* 2009; **32**(9)**:** 958-958.

223. Henningsen J, Rigbolt KTG, Blagoev B, Pedersen BK, Kratchmarova I. Dynamics of the Skeletal Muscle Secretome during Myoblast Differentiation. *Mol. Cell. Proteomics* 2010; **9**(11)**:** 2482-2496.

224. Pedersen BK, Steensberg A, Fischer C, Keller C, Keller P, Plomgaard P *et al.* Searching for the exercise factor: is IL-6 a candidate? *J. Muscle Res. Cell Motil.* 2003; **24**(2-3)**:** 113-119.

225. Riechman SE, Balasekaran G, Roth SM, Ferrell RE. Association of interleukin-15 protein and interleukin-15 receptor genetic variation with resistance exercise training responses. *J Appl Physiol (1985)* 2004; **97**(6)**:** 2214-9.

226. Chertova E, Bergamaschi C, Chertov O, Sowder R, Bear J, Roser JD *et al.* Characterization and favorable in vivo properties of heterodimeric soluble IL-15.IL-15Ralpha cytokine compared to IL-15 monomer. *J. Biol. Chem.* 2013; **288**(25)**:** 18093-103.

227. Tinhofer I, Marschitz I, Henn T, Egle A, Greil R. Expression of functional interleukin-15 receptor and autocrine production of interleukin-15 as mechanisms of tumor propagation in multiple myeloma. *Blood* 2000; **95**(2)**:** 610-8.

228. Huntington ND, Alves NL, Legrand N, Lim A, Strick-Marchand H, Mention JJ *et al.* IL-15 transpresentation promotes both human T-cell reconstitution and T-cell-dependent antibody responses in vivo. *Proc. Natl. Acad. Sci. U. S. A.* 2011; **108**(15)**:** 6217-22.

229. He Y, Wu X, Khan RS, Kastin AJ, Cornelissen-Guillaume GG, Hsuchou H *et al.* IL-15 receptor deletion results in circadian changes of locomotor and metabolic activity. *J. Mol. Neurosci.* 2010; **41**(2)**:** 315-21.

230. O'Connell GC, Pistilli EE. Interleukin-15 directly stimulates pro-oxidative gene expression in skeletal muscle in-vitro via a mechanism that requires interleukin-15 receptor alpha. *Biochem. Biophys. Res. Commun.* 2015; **458**(3)**:** 614-9.

231. Yu YL, Wei CW, Chen YL, Chen MHC, Yiang GT. Immunotherapy of breast cancer by single delivery with rAAV2-mediated interleukin-15 expression. *Int. J. Oncol.* 2010; **36**(2)**:** 365-370.

232. Yiang GT, Harn HJ, Yu YL, Hu SC, Hung YT, Hsieh CJ *et al.* Immunotherapy: rAAV2 expressing interleukin-15 inhibits HeLa cell tumor growth in mice. *J. Biomed. Sci.* 2009; **16**.

233. Stephenson KB, Barra NG, Davies E, Ashkar AA, Lichty BD. Expressing human interleukin-15 from oncolytic vesicular stomatitis virus improves survival in a murine metastatic colon adenocarcinoma model through the enhancement of anti-tumor immunity. *Cancer Gene Ther.* 2012; **19**(4)**:** 238-246.

234. Zhou XK, Li XL, Gou ML, Qiu J, Li J, Yu CJ *et al.* Antitumoral efficacy by systemic delivery of heparin conjugated polyethylenimine-plasmid interleukin-15 complexes in murine models of lung metastasis. *Cancer Sci.* 2011; **102**(7)**:** 1403-1409.

235. Matsumoto K, Kikuchi E, Horinaga M, Takeda T, Miyajima A, Nakagawa K *et al.* Intravesical Interleukin-15 Gene Therapy in an Orthotopic Bladder Cancer Model. *Hum. Gene. Ther.* 2011; **22**(11)**:** 1423-1432.

236. Ugen KE, Kutzler MA, Marrero B, Westover J, Coppola D, Weiner DB *et al.* Regression of subcutaneous B16 melanoma tumors after intratumoral delivery of an IL-15-expressing plasmid followed by in vivo electroporation. *Cancer Gene Ther.* 2006; **13**(10)**:** 969-974.

237. Mellman I, Coukos G, Dranoff G. Cancer immunotherapy comes of age. *Nature* 2011; **480**(7378)**:** 480-9.